[redacted]

410915

WT-1318

OPERATION REDWING—PROJECT 2.64

R

FALLOUT LOCATION and DELINEATION by AERIAL SURVEYS (U)

DELETED VERSION ONLY

R. T. Graveson
M. E. Cassidy
H. D. LeVine

New York Operations Office
Atomic Energy Commission
New York, New York

[redacted]

FOREWORD

This report presents the final results of one of the projects participating in the military-effect programs of Operation Redwing. Overall information about this and the other military-effect projects can be obtained from WT-1344, the "Summary Report of the Commander, Task Unit 3." This technical summary includes: (1) tables listing each detonation with its yield, type, environment, meteorological conditions, etc.; (2) maps showing shot locations; (3) discussions of results by programs; (4) summaries of objectives, procedures, results, etc., for all projects; and (5) a listing of project reports for the military-effect programs.

[redacted]

2

ABSTRACT

The objectives were to: (1) survey the gamma radiation from fallout-contaminated ocean areas by means of aerial detectors and (2) from the aerial detectors make air-absorption measurements so that the data might be related to the dose rates at 3 feet above the sea.

Radiation detectors were mounted in P2V-5 aircraft that surveyed the ocean areas of expected fallout after Shots Cherokee, Zuni, Flathead, Navajo, Mohawk, and Tewa. A control center coordinated all air and surface radiation-survey activities to insure complete coverage of the fallout area. The contamination densities in the delineated areas were related to the percentage of the total yield that produced fission products. Gamma-isodose plots were prepared from data obtained during Shots Zuni, Flathead, Navajo, and Tewa. No fallout could be located following Shot Cherokee and only on atoll islands after Shot Mohawk.

Zuni, a land-surface shot, contaminated 13,400 naut mi^2 of ocean with 48 percent of its fission-product yield.

Navajo, a water-surface shot, contaminated 10,500 naut mi^2 with 50 percent of the fission-product yield. After Flathead, another water-surface shot, the outer boundary could not be determined because of contamination of project aircraft on D + 1 day by airborne radioactive material that resulted in a high background. However, extrapolated values indicate 29 percent of its fission-product yield was present as fallout in the local area. The fallout from the water-surface shots was concentrated primarily in the more remote areas, and a relatively small amount fell close to ground zero.

Tewa, a reef shot, contaminated 43,500 naut mi^2 of ocean with 28 percent of the fission-product yield.

Helicopters and P2V-5 aircraft were used to gather data for air-absorption measurements.

The aerial-survey technique may be used directly for radiological surveys over land. Over the sea, the depth of mixing of the fallout in the water volume must be determined before the survey results may be converted to equivalent land-fallout contours and contamination-density distributions. Data on depth of mixing was obtained from samples of sea water collected by the U.S. Naval Radiological Defense Laboratory and the Scripps Institute of Oceanography. Repeated aerial surveys provided information on the stability of the contaminated volume.

[redacted]

PREFACE

Patrol Squadron ONE, U. S. Navy, operated the aircraft used for the aerial surveys. The author gratefully acknowledges the diligence and high professional competence which contributed so much to the project's operations.

Commander Kelly, USN, was the Air Officer on the staff of Commander, Task Group 7.3. His efforts were responsible for the fulfillment of the project's aircraft requirements.

Members of the Health and Safety Laboratory, U.S. Atomic Energy Commission, who participated in the field operations, and whose contributions are gratefully acknowledged are I. Whitney, G. Hamada, S. Tarras and T. French of the Analytical Branch, H. Sadowski and F. Wilson of the Instruments Branch and K. O'Brien of the Radiation Branch.

[redacted]

4

CONTENTS

[redacted]

5

FIGURES

6

TABLES

[redacted]

7

[redacted]

Chapter 1
INTRODUCTION

1.1 OBJECTIVES

The objectives were to: (1) survey the gamma radiation from fallout-contaminated ocean areas using an airborne detector and (2) make air-absorption measurements so that the data from the airborne detector might be related to the dose rates at 3 feet above the sea.

1.2 BACKGROUND

During Operation Ivy, the USAEC Health and Safety Laboratory (HASL) carried out a program of aerial surveys of the islands outside the Eniwetok Proving Ground (Reference 1). No major fallout occurred on any of these land surfaces. Traces of contamination were clearly discernible from the air, indicating the feasibility of aerial surveys. However, with the meager basic data then available, it was not possible to determine whether the contamination from a multimegaton shot, namely, Shot Mike, was primarily deposited as local fallout or remained in the upper levels of the atmosphere.

A similar program of aerial surveys was organized for Operation Castle (Reference 2). It was expanded to include monitoring installations at certain selected islands outside the Eniwetok Proving Ground. Shot 1 deposited appreciable fallout on the monitoring installation at Rongerik. Although heavy fallout was thus documented from a multimegaton shot, no estimate of the total quantities of contamination in local fallout could be formed. Succeeding shots in this series deposited little contamination on any of the islands.

Just before Shot 5 during Operation Castle, it was found that fallout material remained suspended in the sea. Radiation detectors were hurriedly mounted in aircraft, and the ocean was surveyed following Shots 5 and 6. The work was necessarily limited by the lack of special radiation detectors, sufficient personnel, and aircraft. Because only one aircraft was available, the survey was confined to the area between 20 and 100 miles from ground zero. However, the rough estimates based on this survey data indicate that each of these shots contaminated about 4,000 mi^2 with somewhat less than half of their total fission yield (Reference 3).

The experience during Operation Castle indicated special problems that would arise in aerial surveys, particularly in surveys over the ocean. Navigational correlation would be difficult to achieve over the open sea on long flights. One aircraft could not cover the widespread areas contaminated after megaton-range shots. Isodose data could not be reduced in the aircraft, although required immediately during the flight period to control the aircraft's flight pattern. Barometric altimeters are not accurate enough to provide the close altitude control necessary for relating readings of radiation to an equivalent surface level. And lastly, the radiation detector would need special characteristics for the aerial-survey operations. The detector would need a fast speed of response, shielding to minimize the contribution of aircraft contamination to the readings, and independence from the aircraft supply of power for any critical section of the detector. The voltage from the aircraft generators varies over wide limits, and regulation must be added separately. Also, it would be highly desirable for the detector to have a logarith-

[redacted]

mic response, ... that a wide range of radiation intensity ...ld be recorded without a change of scales.

The Top Hat aerial radiation detector was developed by HASL to overcome these problems. Units were installed in three AD-5N aircraft and field-tested at the Nevada Test Site (NTS) during Operation Teapot.

The AD-5N aircraft used during Operation Teapot were transferred to an aircraft carrier for surveys following the undersea test during Operation Wigwam (Reference 4). A wide range of radiation intensities were encountered in this operation. The first pass over surface zero was shortly after H + 11 minutes, and measurements were made which extrapolated to approximately 400 r/hr at the surface. At the other extreme, surveys were made at D + 4 days to delineate the edges of the contaminated area, where the dose rates were approximately 0.1 mr/hr.

The Top Hat system was modified for Operation Redwing, and additional units were constructed. No changes were made in the basic detecting elements; however, the hermetic sealing was improved in anticipation of the humidity at the Eniwetok Proving Ground.

1.3 THEORY

The heat resulting from an atomic explosion vaporizes the products of the explosion and the bomb casing. Soil and water in the vicinity of ground zero are also vaporized and picked up by the updraft produced by the rise of the ball of incandescent gases. On cooling, the material in the fireball condenses into particles that include the radioisotopes resulting from the fission process and from neutron activation of inert materials. The energy released in the explosion will influence not only the quantity of particulate material but also its altitude distribution in the vicinity of ground zero. The portion of the yield related to the fission process is represented by the amount of radioactive contamination carried by the particles. Once the particles are formed, they fall and, influenced by the winds, will reach the surface displaced from ground zero. The radioactive fallout from megaton shots may contaminate thousands of square miles of surface.

The shot conditions influence the form and quantity of the fallout. When a shot is exploded on land, a large amount of soil is picked up and much of it is vaporized by the intense heat. This material condenses in a wide range of particle sizes. Some of the radioactive products are condensed around large particles that were picked up in the updraft but not vaporized. These larger particles fall rapidly and reach the surface relatively close to ground zero.

When a shot takes place at the surface of deep water, vaporized water can carry some of the activity away from the site. The large particulate fallout encountered in the land shot will be missing, and this will be reflected in the distribution of fallout on the surface.

An air shot is one in which the fireball does not touch the surface, so that compared with surface shots relatively little foreign material is vaporized. Because there are no available particulates on which the fission products can condense, most of the active material remains in the upper atmosphere and little fallout is likely to be detected in the vicinity of the shot site.

1.3.1 Fallout Contamination of a Water Volume. When the contamination falls into the sea, dispersion and dilution carry much of the material below the surface (Reference 3). The intervening water acts as a shield between the surface and much of the gamma activity. Thus, the radiation dose rates measured above the surface are reduced many orders of magnitude; however, sensitive detectors can be used to delineate the area of contamination. Also, if samples are taken at various depths, the quantity of radioactivity present can be integrated to the maximum depth of mixing, and in this manner, it is possible to secure isodose distributions of the fallout as they would appear on an equivalent land surface.

The location of detector and source volume on a coordinate system is shown in Figure 1.1. Because of the absorption of the gamma rays by the water, radiation detected above the surface comes from the top 10 to 20 cm of the sea. The following equation describes the variation of dose rate, I_ν, above such a contaminated volume (Appendix A, Equation A.10).

$$I_\nu = \frac{0.3549}{2} C_\nu L(h, \theta)\ R/hr \qquad (1.1)$$

Where: C = curies per cubic meter

$L(h, \theta)$ = a polynomial, dependent on the altitude of the aircraft, h; and half angle, θ which subtends the diameter at the surface contamination.

The gamma rays from the fission products are assumed to have an effective gamma energy of 0.5 Mev when 1 to 6 days old (Reference 5). This reference states quantitatively that gamma curies and beta curies are nearly equivalent in this period.

Estimates based on this assumption indicate that contamination with a beta activity of 4.43×10^6(dis/min)/liter at the surface should produce a 1 mr/hr gamma flux at 3 feet from the surface, when the diameter of the contamination is large enough to appear infinite (θ = 90 deg).

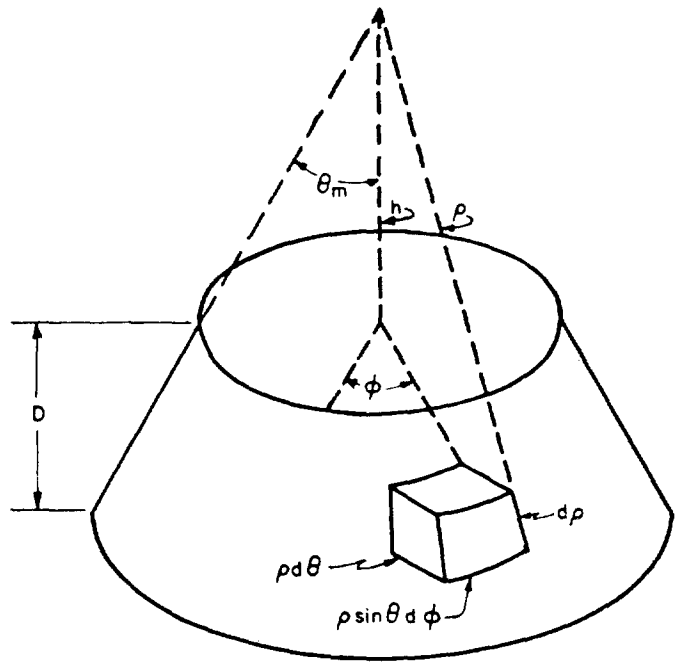

Figure 1.1 Coordinate system of gamma radiation from a water volume.

Fallout of 0.404 megacurie per naut mi^2 deposited in the sea, uniformly mixed to a depth of 60 meters (Reference 3 and Section 3.4.2), would produce a 1 mr/hr gamma field at 3 feet above the surface.

The gamma dose rate at any altitude f_a, related to the 3-foot value is expressed by the ratio of the polynomials L(h, 90 deg). The altitude absorption $1/f_a$ is plotted in Figure 1.2.

1.3.2 Fallout Contamination of a Land Surface. When fallout is deposited on land, the contaminated area appears as a large plane source. At any point in the radiation field, the gamma intensity will include contribution from a circle whose radius is determined by the absorption of the gamma photons in air. The dose rate (I_p) above such a plane is given by the following equation (Appendix A, Equation A.15).

$$I_p = 3.4427\ C_p J(h, \theta) \times R/hr$$

Where: C = curies per square meter

$J(h, \theta)$ = a polynomial similar in construction to that in Section 1.3.1.

With the same assumptions as for the water case (Eo = 0.5 Mev and the ratio of beta and gamma curies equal to 1), 2.1×10^7(dis/min)/ft^2 of beta activity will result in a 1 mr/hr gamma field at 3 feet from the surface, when the source diameter is proportional to θ = 90 deg. A

gamma field 1,000 mr/hr will correspond to a contamination of 0.356 megacurie per naut mi^2.

The altitude absorption factor, over land, is shown in Figure 1.2.

1.3.3 Radioactive Decay. Mixed fission products have been assumed to have a radioactive decay proportional to $t^{-1.2}$ (Reference 6), to reduce the aerial-survey measurements to a common time, t is the time since the detonation.

Large amounts of Np^{239} may be found in the fallout from thermonuclear shots. It is possible to calculate the expected increase in the total activity, over that resulting solely from fission

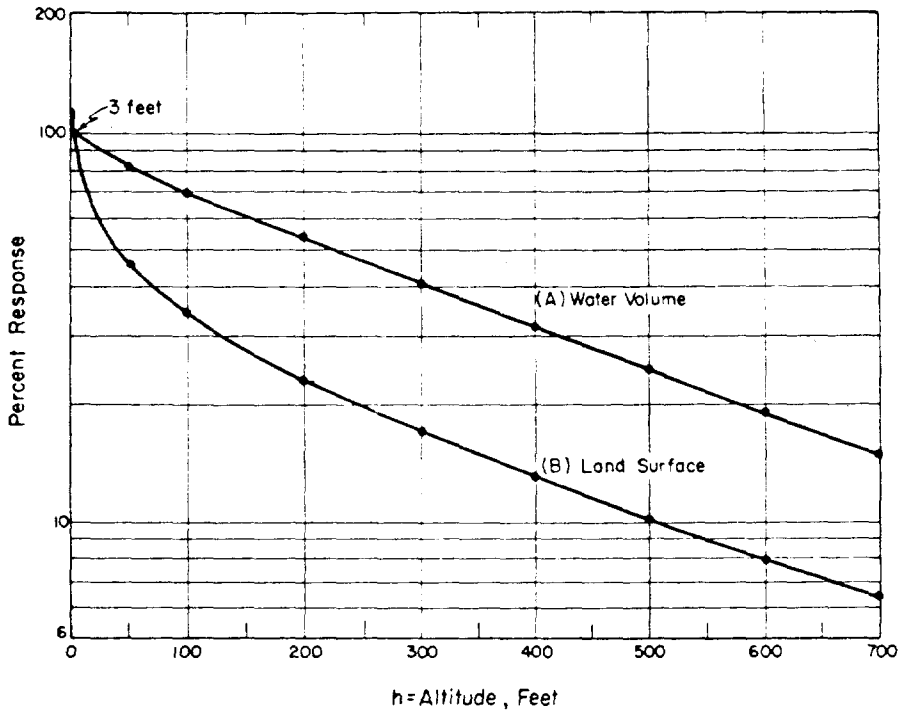

Figure 1.2 Radiation attenuation referred to h = 3 feet.

products, from the capture-to-fission ratio of the device. The decay characteristics of the fallout activity will be modified by the Np^{239} contribution. The Np^{239} can be present in amounts up to 50 percent of the total activity, 1 to 3 days after the shot, based on a mixed fission product activity described in Reference 7.

Because of the low energy of the neptunium gamma emission which is predominately 120 kev, the Np^{239} adds relatively small contribution to the gamma dose rate when compared to the average fission-product gamma energy. In water the mean free-path length of the lower-energy gamma ray is less than that for the mixed fission product gamma; hence, a lesser volume at the surface of the ocean contributes to the dose rate measured above the surface. This is inversely proportional to the total absorption coefficients of water, at 120 and 500 kev, and reduces the neptunium gamma contribution to 60.6 percent. In addition, the lower-energy gamma flux deposits less energy per unit volume of air, and therefore contributes less to the dose rate. This is an additional reduction to 18½ percent of the fission product dose rate (Reference 8). The aerial-survey detector response is down to 75 percent at 120 kev energy (Figure 2.5). Because of these factors, even with the neptunium gamma ray contribution to the total activity at 50 percent, the dose rate response in the Top Hat detector will be increased about 4 percent. The relative attenuation, in air, for these two gamma energies, approximately 65 percent, reduces the neptunium gamma contribution to less than 2½ percent of the fission product dose rate measured at an aircraft at 300 feet flight altitude.

It is possible that other isotopes may be formed, depending on the type and location of the test. Primary among these is Na^{24} produced by neutron activation of the sodium in sea water. This isotope has a 14.8-hour half life and emits two gamma photons, 1.38 and 2.76 Mev. Refer-

ence 6 may be ..d to deduce the dose-rate contribution f.. an amount, in curies, equal to that for the mixed fission products. The dose-rate measurement at 300 feet is more sensitive to this isotope by a factor of 3.6 because of its increased roentgen conversion from curies, and the larger volume of water contributing to the surface radiation flux.

1.3.4 Distribution of Fallout. To estimate the distribution of fallout, the equation relating gamma dose rate above the surface to contamination density in a volume of sea water may be used in conjunction with the isodose distribution charts and depth of mixing measurements. The contamination density in a thin layer at the surface may be estimated from the average gamma dose rate in the various isodose defined areas. Summation of the estimated contamination would

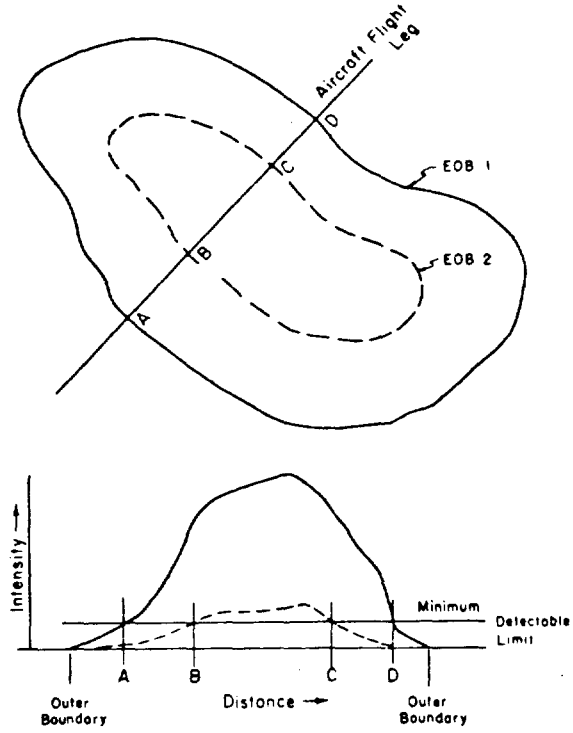

Figure 1.3 Determination of estimated outer boundary.

yield an estimate of the megacuries of surface radioactivity in the fallout area. This may be correlated with the depth of mixing and the total fallout activity computed.

If the fallout is deposited in the sea, the equation in Section 1.3.1 indicates that a contamination density of 1 megacurie per naut mi^2 would produce a gamma dose rate of 2.5 mr/hr at 3 feet from the surface. The same contamination density, on land, would produce 2,800 mr/hr (Section 1.3.2). For rough estimates, 1 mr/hr at 3 feet over water is equivalent to a 1,000:1 increase in activity per naut mi^2 when compared to 1 mr/hr on land.

The calculations for land and water are summarized as follows: on land, 1 mr/hr at 3 feet is equivalent to 2.1×10^7 (dis/min)/ft^2 or 3.56×10^{-4} megacuries/naut mi^2; on water, 1 mr/hr at 3 feet is equivalent to 4.43×10^6 (dis/min)/liter or 4.04×10^{-1} megacuries/naut mi^2 where depth of mixing is 60 meters.

When the fission product falls into the sea, the outer boundary of the contaminated area will be indicated by gamma-radiation readings that are only slightly above the background gamma dose rate. Figure 1.3 illustrates the radiation profile across a contaminated area. The estimated outer boundary (EOB) from a shot with a high-fission yield is indicated at A and D. A shot with the same total energy yield, but producing a smaller quantity of fission products, will have an EOB at B and C. Both shots may have the same actual outer boundary, yet the minimum detectable limit of radiation of the instrumentation will result in a low estimate for the area. For material-balance calculations, the quantity of radioactivity outside the EOB will be small in relation to the quantity located in the higher-intensity areas.

[redacted]

12

Chapter 2
PROCEDURE

2.1 SHOT PARTICIPATION

Prior to the operation, aerial surveys were scheduled to follow Shots Cherokee, Zuni, Flathead, Navajo, Apache (secondary participation), and Tewa. Because Shot Cherokee was delayed, Program 2 requested that the project add Shot Lacrosse to its schedule in order to give the aerial survey an opportunity to obtain operational experience. However, this survey was cancelled, because flight clearance below 1,000 feet in the region of Eniwetok Atoll could not be obtained.

A change in the Apache scheduling introduced a conflict with the project's participation during Navajo. The new schedule called for dual capability involving both Eniwetok and Bikini Atolls. Participation in Apache was therefore, canceled.

Because of the long waiting period between Flathead and Navajo, the project requested secondary participation in Shot Mohawk.

Preshot surveys were flown before the Navajo and Tewa shots, based on a Program 2 request, to define the background status resulting from the flow of contaminated lagoon water over the reef at Bikini.

Helicopter missions, for altitude absorption data, were originally scheduled after Shots Seminole, Mohawk, and Navajo. The mission for the latter was subsequently canceled at the request of the project, because of a shortage of personnel. During June and July, it was necessary to assign two technicians to Kwajelein to service the aerial-survey equipment; therefore, they were no longer available for on-site operations.

The project operations are summarized in Table 2.1.

2.2 OPERATIONS

Many projects in Program 2 studied different phases of fallout. Project 2.64 developed isodose plots of the contaminated area by aerial surveys. The operations were primarily to secure aerial survey data; subsidiary measurements were performed in support of this objective to correlate this data. Altitude absorption studies were required to verify the correction factors used in relating the aerial survey to a reference plane 3 feet above the surface.

2.2.1 Aerial Surveys. Four P2V-5 aircraft were assigned for the project operations, and were administratively attached to the Security Squadron, Patrol Squadron 1. Three of the aircraft were supplied from outside the squadron, and the fourth came from its assigned strength. The squadron provided all maintenance and operational control. This control was shifted to the Program 2 Control Center on the USS Estes, AGC-12, during the aerial-survey flights. The Air Operations Officer, Task Group 7.3, assumed primary radio guard during this period.

The plan of the project air control in the Program 2 Control Center is shown in Figure 2.1. The communication routing is shown in Figure 2.2. The telemeter operator logged all incoming radiation readings, which were immediately recorded on a time-based continuous plot. Navigational information was received from the radio operator on Channel C (6693 kc). The Project 2.64 Operations Officer correlated the navigational and radiation data on the rough flight-control chart. The plotter transferred this information to the tactical isodose plot, under the supervision of the 2.64 Project Officer, who used the flight and isodose charts to determine the next area of search for each aircraft. The operations officer laid out the required navigational ref-

erences for the designated flight legs and transferred this information to the working flight log. The Task Group 2.3 Air Operations Officer reviewed the legs for flight safety, and the information was relayed to the appropriate aircraft by the radio operator.

D-day flights used one aircraft, with a second aircraft on standby. The flights were limited to the upwind areas until active fallout had ceased. Surface ship reports, received by the Proj-

TABLE 2.1 SUMMARY OF PROJECT OPERATIONS

Shot	Date	Time	Location	Aerial Survey	Altitude Absorption
Cherokee	21 May	0551M	Bikini	D-day D+1	
Zuni	28 May	0566M	Bikini	D-day D+1 D+2 D+3	
Seminole	6 June	1255M	Eniwetok		D-day
Flathead	12 June	0626M	Bikini	D-day D+1 D+2	
Mohawk	3 July	0606M	Eniwetok	D+1	D+2
Navajo	11 July	0556M	Bikini	D−3* D−2* D-day D+1 D+2 D+3	
Tewa	21 July	0546M	Bikini	D−1* D-day D+1 D+2 D+3 D+4	

* Preshot surveys of lagoon water outside the Bikini Atoll.

ect 2.63 representatives in the Control Center, indicated when fallout had stopped in the close-in downwind sector. The aircraft was then controlled through the area to limits described by the ship reports. The D-day flights delineated the upwind boundary and obtained some intensity readings in the radioactive area immediately downwind of ground zero.

Two aircraft were used on D + 1. One delineated the close-in radioactive area and confirmed the upwind boundary located on the previous day. The second aircraft flew an extensive search pattern to locate the edges of the contaminated area.

The D + 2 survey re-examined the overall contaminated area. One aircraft was usually sufficient. However, the Tewa pattern was so large that two aircraft were needed. Flights on subsequent days used one aircraft and tracked the area until the dose rates became too low for adequate delineation.

Survey data which delineated the outer boundary and points of interest in the fallout pattern were plotted in the control center to guide the Project 2.62 surface ships with their oceanographic surveys.

During the period prior to the next shot, each aircraft was scheduled to spend a day on Site Fred for instrument calibration and service. Two technicians calibrated each radiation detector at Kwajalein prior to and immediately following each survey flight and returned the Top Hat detectors to Site Elmer between shots, where a complete routine battery change and recalibration was performed.

[redacted]

14

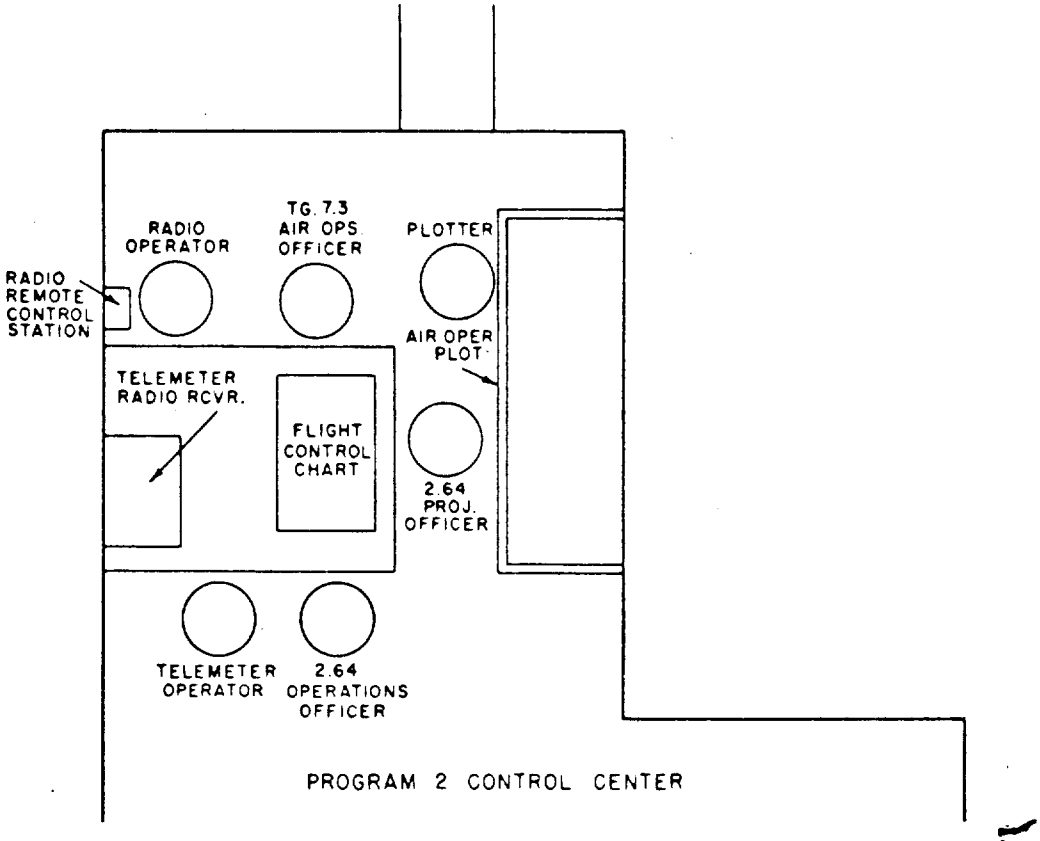

Figure 2.1 Project 2.64 air control.

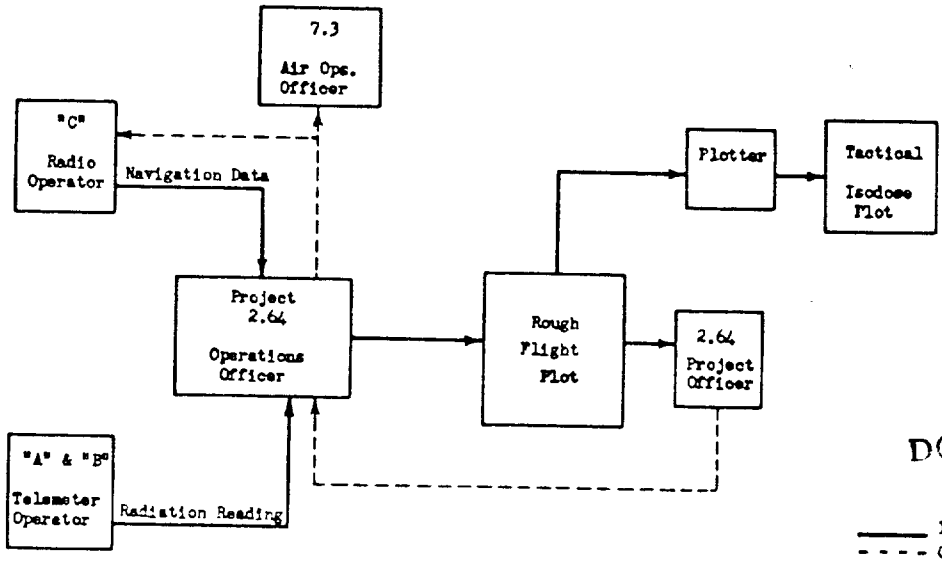

Figure 2.2 Communication routing, Project 2.64 air control.

[redacted]

15

2.2.2 Altitude Absorption. Because considerations of aircraft safety limit the minimum altitude at which aircraft can fly over water, automatic gamma monitors were mounted over the sides of two ships of Project 2.10, to measure the gamma-radiation field at 35 feet above the sea surface. This was to provide low-altitude readings simultaneous with aircraft passes in the same area at higher altitudes.

Survey aircraft made altitude-calibration passes over islands of the Eniwetok Atoll after Shot Mohawk. After Shot Tewa, the P2V-5 dropped a smoke light in the open sea to be used as a navigational reference and made altitude passes in the vicinity. These data are examined for the variation of radiation reading between different flight altitudes and given in Section 3.2.

Helicopter missions, after Shots Seminole and Mohawk, obtained data similar to the altitude-correction-calibration data collected by the survey aircraft. Because the helicopters could not safely hover at low altitudes, complete information could not be obtained. It had been planned to obtain gamma-energy spectra at various altitudes above a contaminated surface. The Top Hat dose-rate response was to be compared to the gamma-energy spectra to determine whether the assumption of air-equipment response was valid. However, instrumentation difficulties and the limitations in hovering altitudes resulted in fragmentary data. The survey using a scintameter obtained dose-rate readings at altitudes between 25 and 1,000 feet.

2.3 INSTRUMENTATION

The major instrumentation consisted of aerial radiation detectors. Scintillation survey meters and ship-mounted gamma monitors were used for measurements relating to altitude-correction factors. A spectrometer was used to obtain the distribution of the gamma energies at survey altitudes. The instruments are described in Appendix B.

2.3.1 Aerial Survey. Each of the project aircraft had the following equipment: (1) Top Hat aerial radiation detector, HASL TH-10-B (Appendix B); (2) detector control assembly, HASL TC-14-A; (3) strip-chart recorder, Esterline Angus Co., AW; (4) telemeter assembly, HASL TT-3-X; (5) power supply, HASL TB-6-A; and (6) radio transmitter, U.S. Navy ART-13. The permanent components were installed by the Overhaul and Repair Department, U.S. Naval Air Station, Alameda, California, at the air station prior to Operation Redwing. The removable components were installed by project personnel after the squadron deployed to the EPG.

The location of the assemblies is indicated in Figure 2.3. The radiation detector was mounted aft to avoid the major areas of aircraft contamination, namely, the engines, oil-cooler air intakes, leading edges of the wings, propellers, and front of the radome. The cabin intake vents were sealed to prevent contamination of the interior ductwork. The control assembly and the operator were placed forward, next to the navigator. This facilitated close correlation between the navigational and radiation reports. The remainder of the equipment was located on an available-space basis.

The relationship of the various sections, both in the aircraft and in the Program 2 Control Center, is shown in Figure 2.4. The radiation detector and its associated control assembly drives a strip-chart recorder to provide a permanent, continuous record of the radiation intensities as measured in the aircraft. This detector is nearly air-equivalent from 80 to 1,400 kev, Figure 2.5. An annular radiation shield is built into the detector to reduce the effect of aircraft contamination. The angular response due to this shield is shown in Figure 2.6.

The aircraft's radio altimeter (U.S. Navy APN-1) supplies an altitude indication to the altitude compensator, which modifies the radiation detector so that its output is a current that is proportional to the radiation which would be measured at 3 feet above the surface. As the altitude changes, the compensator corrects the resulting radiation change and keeps the ground-level reading constant.

The telemetering system did not perform satisfactorily. The radiation readings on the aircraft radiation-detector strip-chart recorder were, therefore, transmitted by voice over the navigational net. At the control center, the radiation readings were logged and immediately plotted.

2.3.2 Altitu. bsorption. The automatic gamma mon. s, HASL TN-4-C, were mounted on the YAG-39 and YAG-40. Each instrument was mounted at the end of a boom that was also used to suspend the depth probe of Project 2.62. The boom extended 35 feet from the side of the ship and was set at an approximate mean height of 35 feet above the sea. An Esterline-Angus strip-chart recorder was installed in the shielded control room on the ship, to continuously record the gamma dose rate. The installation of the monitors and recorders was accomplished by Project 2.10.

Scintameter survey meters, HASL TH-3-B and TH-7-A, were used for helicopter operations. Gamma dose rate was measured at various altitudes over contaminated water and land surfaces.

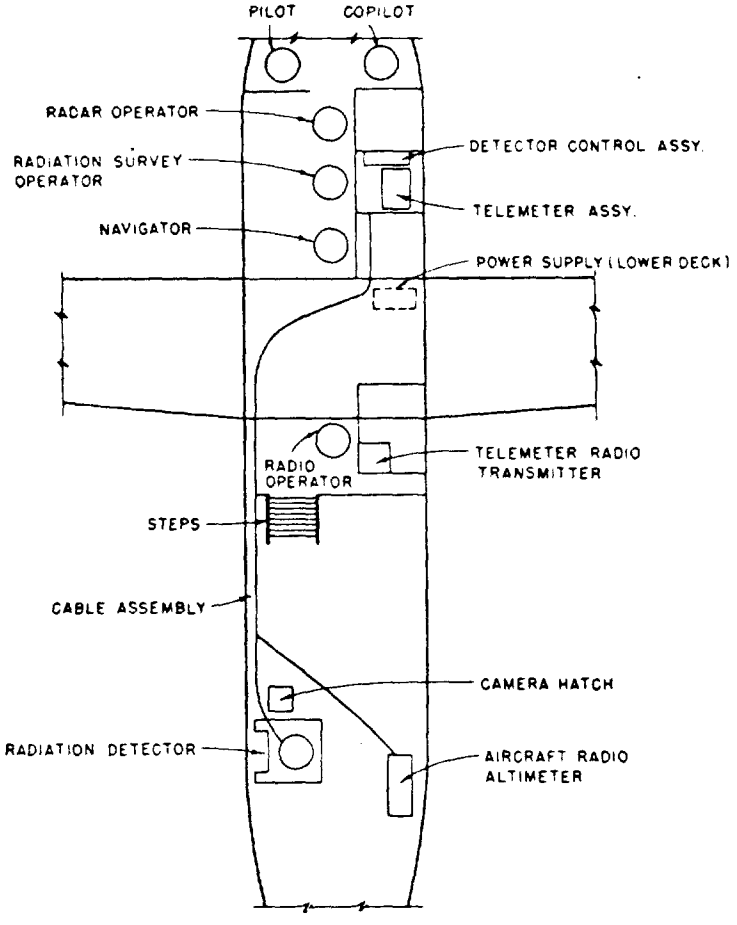

Figure 2.3 Radiation-survey-equipment mounting locations in P2V-5 aircraft.

A gamma spectrometer, HASL TM-10-A, which consists of a scintillation head, pulse-height analyzer, and a recorder, was loaded into the same helicopter. The 28-volt power in the helicopter was converted to 115 volts, 60 cps, by a separate inverter to supply the spectrometer. The count rate at various energy levels was observed on a meter as the base line automatically swept through an energy scan from 50 kev to 3 Mev.

The survey aircraft had the same instrumentation as described in the previous section, plus a scintameter survey meter, TH-3-B.

2.4 REQUIRED DATA

The project operations were directed mainly toward obtaining isodose plots of the gamma

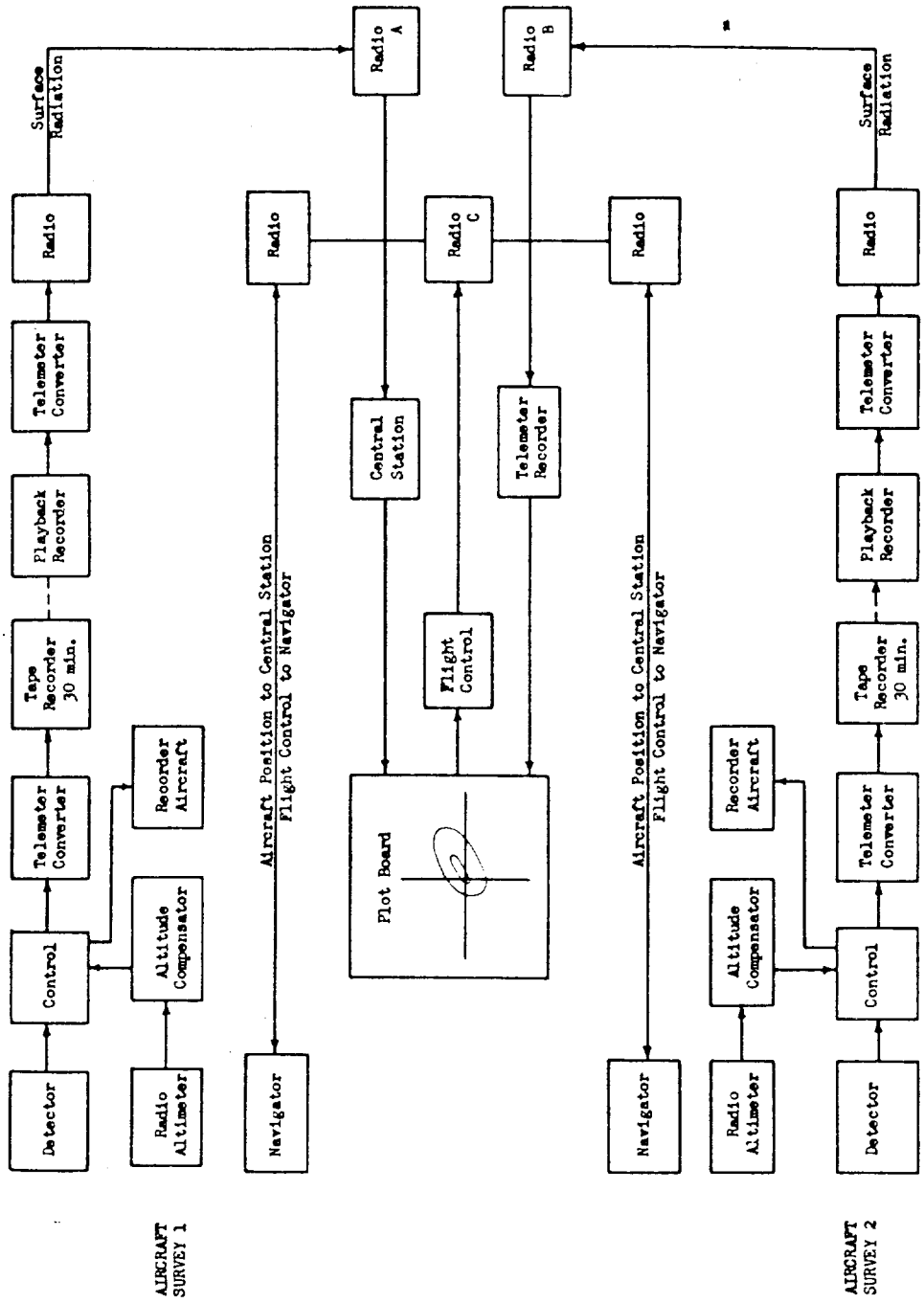

Figure 2.4 Aerial-survey system.

[redacted]

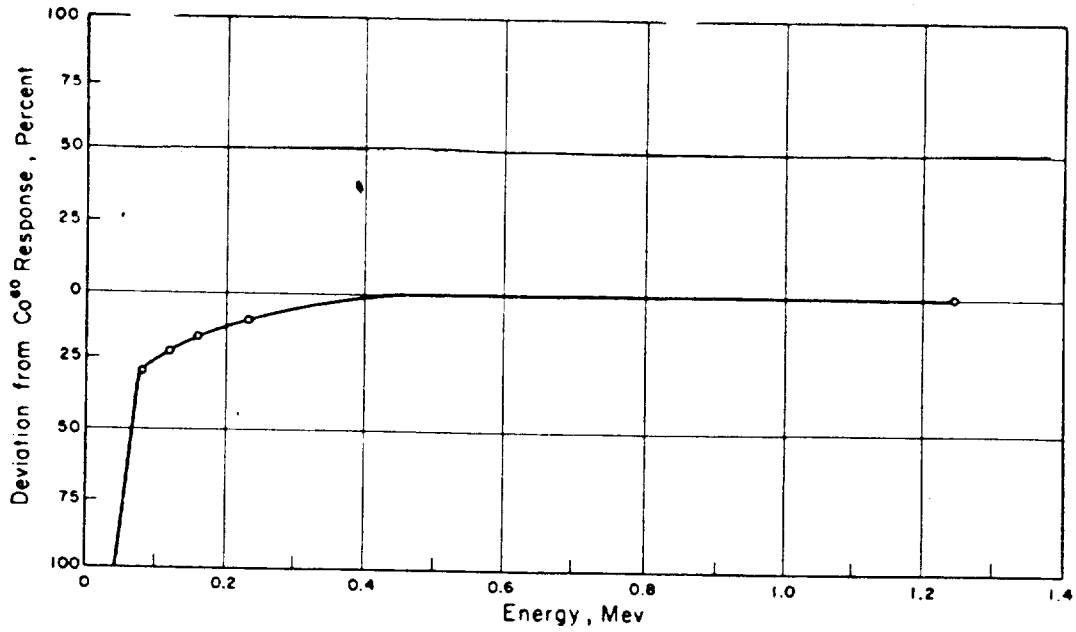

Figure 2.5 Energy dependence of dose rate response, Top Hat plastic phosphor, $1\frac{1}{8}$-inch diameter by $\frac{3}{8}$ inch long.

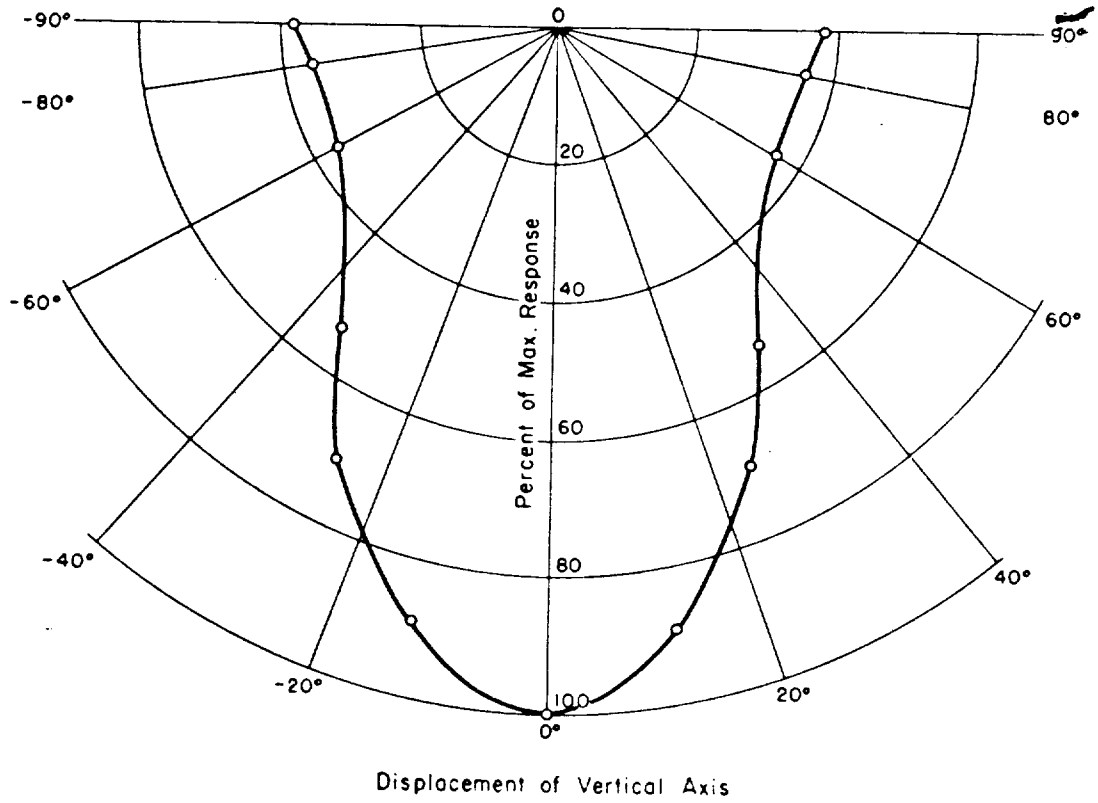

Figure 2.6 Angular response of Top Hat radiation detector; measured with 1-mg radium source.

dose rates resu[illegible]ng from fallout in the sea. Only those s[illegible]diary measurements which were directly applica[illegible] to an understanding of the aerial-surve[illegible]echnique were undertaken.

2.4.1 Distribution of Contamination in the Sea. The gamma isodose plots may be directly related to the surface layer of contamination in the sea. To obtain these plots, gamma dose rate was recorded in the aircraft as it was flown on a search pattern. The aircraft flew between designated points at constant speed. The plot of the flight leg was then marked with time divisions. The recorder chart is calibrated in time, so the gamma reading can be related to the position of the aircraft. Readings were plotted on the flight chart, and points of equal dose rate connected to develop the isodose chart. The values of these isodoses were then corrected to H + 24 hours and to 3 feet above the surface.

2.4.2 Altitude Absorption. To refer the aircraft readings to 3 feet above the surface, verification of the attenuation resulting from air absorption was required. Survey aircraft and helicopter passes at varying altitudes were made over fixed locations to obtain the gamma dose rate as a function of altitude.

2.4.3 Stability of Contaminated Area. Variations in the density of surface contamination during an aerial survey can modify the estimates of the location on an isodose line, because various points along this isodose must necessarily be determined at different times. The surface stability is directly influenced both by surface ocean currents that horizontally translate the contamination, and by mixing which removes contamination from the surface. The gamma-intensity measurements made by aerial surveys cannot view the gamma activity of contamination more than a few feet below the surface of the sea. A measure of the stability of a contaminated area may be achieved by comparing the aerial-survey results over a period of several days. The change in position of the isodose lines provides information on the horizontal translation of the surface contamination. The area enclosed by a given isodose pattern is proportional to the amount of surface contamination.

Data on the vertical-mixing function may be obtained directly by the analysis of samples taken from varied depths at a specific location. The analysis is included as Appendix D.

[redacted]

Chapter 3
RESULTS

3.1 INSTRUMENTATION PERFORMANCE

The bulk of the radiation-detection equipment performed satisfactorily throughout the operation. The limit of detectability was determined by the background dose rate on, or close to, the detector. Because the source of radiation to be measured, namely the surface of the sea, was located considerable distance from the radiation detectors, contamination on or close to the detector units would contribute a relatively large portion of the total reading.

The aerial-survey dose-rate measurements were continuously recorded and stored on a strip-chart recorder. The strip charts were correlated with the navigational logs to develop preliminary isodose plots. The results of the surveys are presented in this compiled form. The altitude absorption measurements are presented as gamma dose rate versus altitude and have been fitted to an appropriate, derived curve.

3.1.1 Aerial Surveys. The records of 37 pre- and post-flight calibrations of the Top Hat detectors have been summarized in Figure 3.1. Thirty-two calibrations were within plus or minus 1 percent of the desired curve. This is within the reading accuracy of the recorder. A 1-percent instrument stability corresponds to a 10-percent radiation variation because of the logarithmic character of the scale. All calibrations were within a maximum limit of ± 25 percent of the desired response.

As mentioned previously, the automatic telemetering system failed to provide reliable transmission of the aircraft data to the control center on the USS Estes, AGC-12. Voice relay of the recorder readings over the navigational net, Channel C, was substituted. The ship's radio receivers did not provide clear, long-range communication with aircraft operating at an altitude of 300 feet. A radio receiver, U.S. Army R-390, was obtained from Task Unit 3 and tuned to the aircraft frequency, Channel C. The R-390 had a lower noise level, and the aircraft transmissions could be clearly detected at a greater distance. When an aircraft exceeded the reliable-communication range, messages were relayed through a second aircraft.

3.1.2 Altitude Absorption. The automatic gamma monitors mounted on the YAG-39 and YAG-40 were calibrated for each shot participation prior to departure from Site Elmer. Examination of the calibration records shows close conformity to the desired radiation response.

A plastic bag was used to protect each monitor. However, the bag became contaminated during fallout, and the readings of sea activity were completely masked. The readings could not be used to provide a surface measurement for aircraft-altitude calibration.

The scintameter survey meter was calibrated just prior to each helicopter mission. Long-term stability was not required for this application.

When used in a helicopter, the gamma spectrometer required alternating current power which was supplied by inverters fed from the 28-volt supply in the helicopter. During Shot Seminole, the vibrator-type inverters failed. Rotary converters were obtained, and a dry run scheduled prior to Shot Mohawk. The energy response was checked against sources containing known radioisotopes, and the performance was satisfactory. The mission was flown on Mohawk D + 2. On arrival at the station, the recorder failed because of the heavy vibration encountered during the hovering of the helicopter. Visual observation of the meter was used to obtain general energy distributions at 500 and 800 feet. The pilot was unwilling to risk hovering at lower altitudes.

3.2 ALTITUDE ABSORPTION MEASUREMENTS

Data on radiation versus altitude, over land, are summarized in Table 3.1. Scintameter survey meters were used for the measurements during helicopter missions. A Top Hat radiation detector and a scintameter were used in the P2V-5 aircraft.

The differences in the absolute values of the readings in the P2V-5 are due to the difference

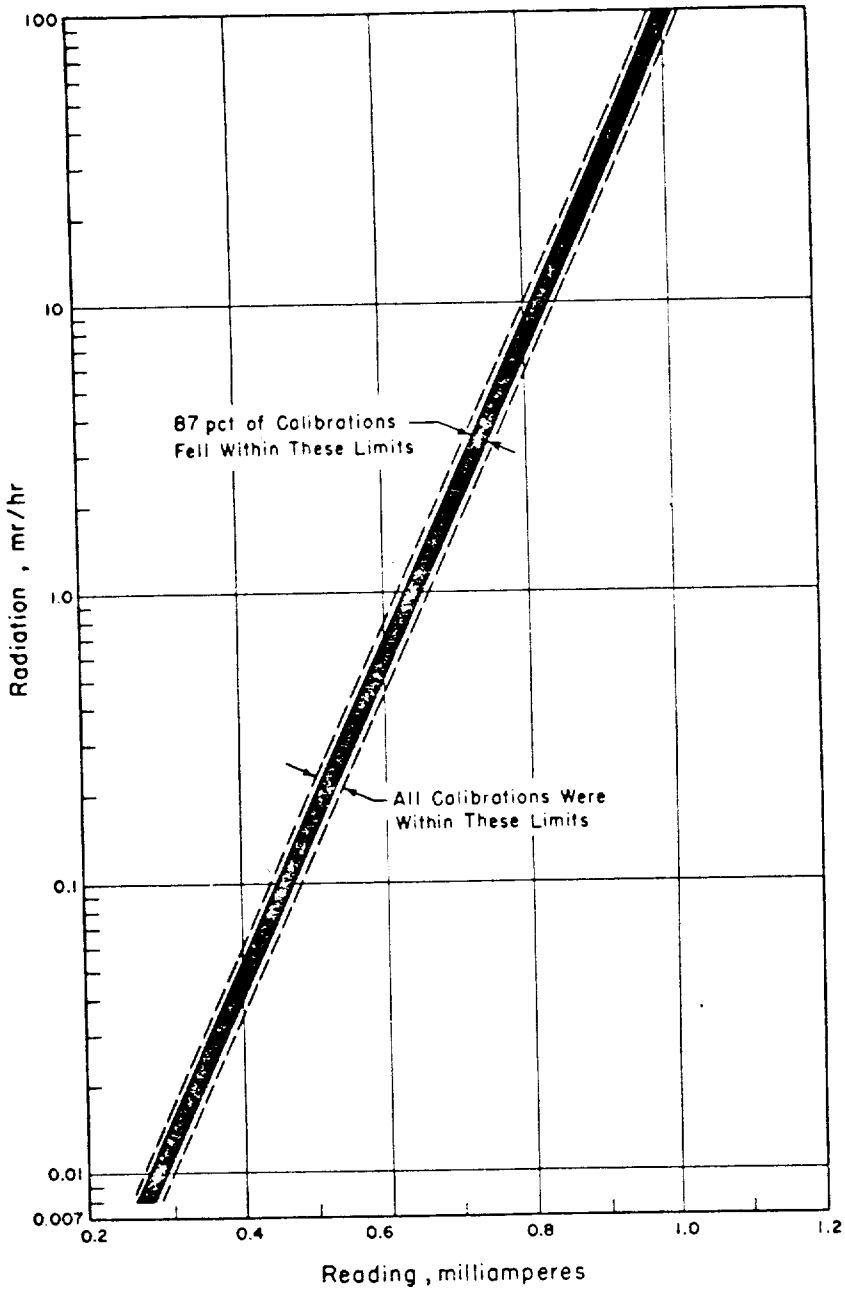

Figure 3.1 Summary of 37 pre- and postflight calibrations of Top Hat radiation detectors.

in the energy response of the two types of detectors. The scintameter, TH-3, uses a sodium iodide phosphor, which is more sensitive to soft gamma radiation. The Top Hat detector uses a plastic phosphor and has a response that is nearly energy-independent. The response of the two types of instruments is summarized in Figure B.2. Because fresh fission products have a

[redacted]

22

TABLE 3.1 ALTITUDE RADIATION DATA OVER LAND (ENIWETOK ATOLL)

Altitude	mr/hr*	mr/hr†	mr/hr‡	mr/hr§	mr/hr¶	mr/hr**
ft						
1,000				1.0, 1.1††		
800			130	1.5		
600			180	1.8		
500	0.7				18	5.7
400				2.8		
300	1.0	1.2			30	8.5
200	1.9	1.9	500	4.1	42	12.5
100			950		70, 55††	18.0
75			1,200			
50	2.5	2.3	1,700	11.0		

* Mohawk + 2, over Tilda, scintameter TH-3, S/N 25 in helicopter.
† Mohawk + 2, over Tilda, scintameter, TH-3, S/N 2 in helicopter.
‡ Mohawk + 2, over Sally, scintameter, TH-7, S/N 3 in helicopter.
§ Seminole D-day, over Janet, scintameter TH-3 in helicopter.
¶ Mohawk + 1, over Janet, scintameter, TH-3, in P2V-5.
** Mohawk + 1, over Janet, Top Hat radiation detector in P2V-5.
†† Values from repeat runs.

gamma-emission energy that is considerably softer than the radium used in instrument calibration, the sodium iodide detector should read high on an actual survey.

The data in Table 3.1 were normalized to the theoretical curve, and are shown in Figures 3.2 and 3.3.

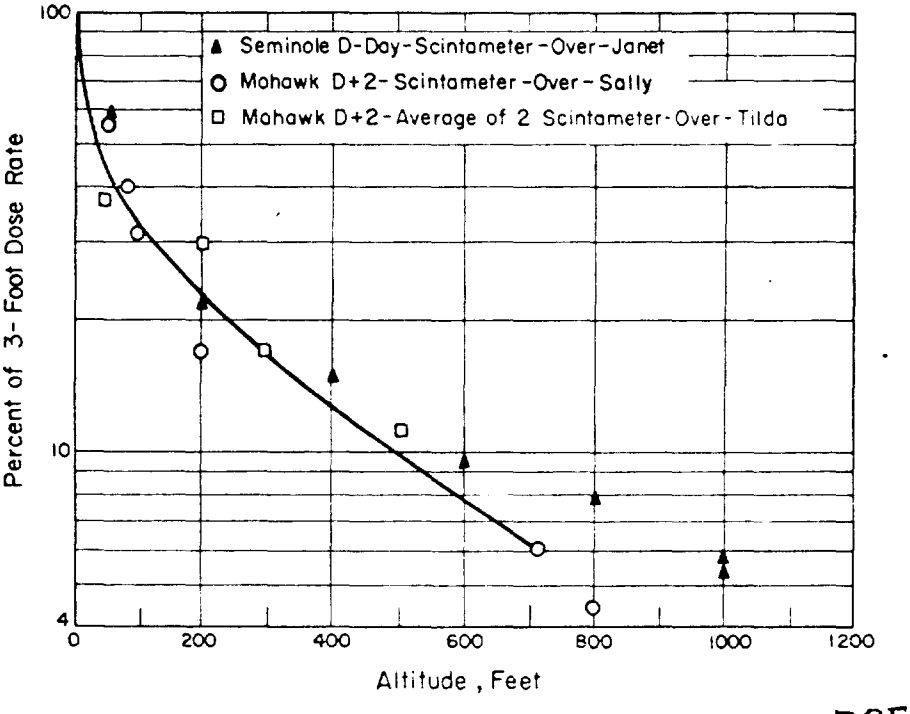

Figure 3.2 Radiation attenuation over land (Helicopter).

Table 3.2 summarized the data obtained over water, and these are plotted in Figure 3.4.

Additional data of this type have been derived from measurements made in previous operations. This information is presented in Appendix C. The curves in Figures C.1 and C.2 show a similar correspondence to the theoretical curves.

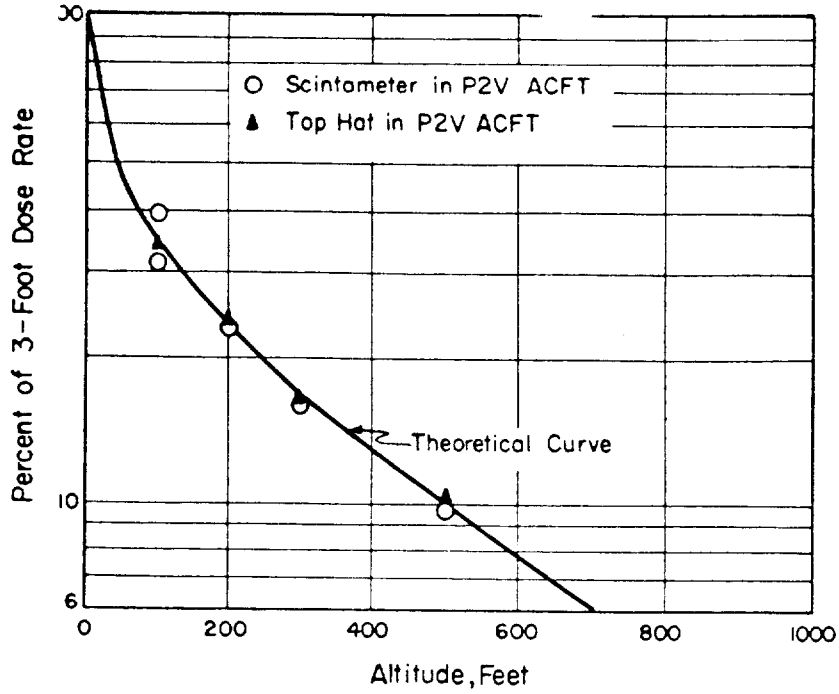

Figure 3.3 Radiation attenuation over land (P2V-5 aircraft).

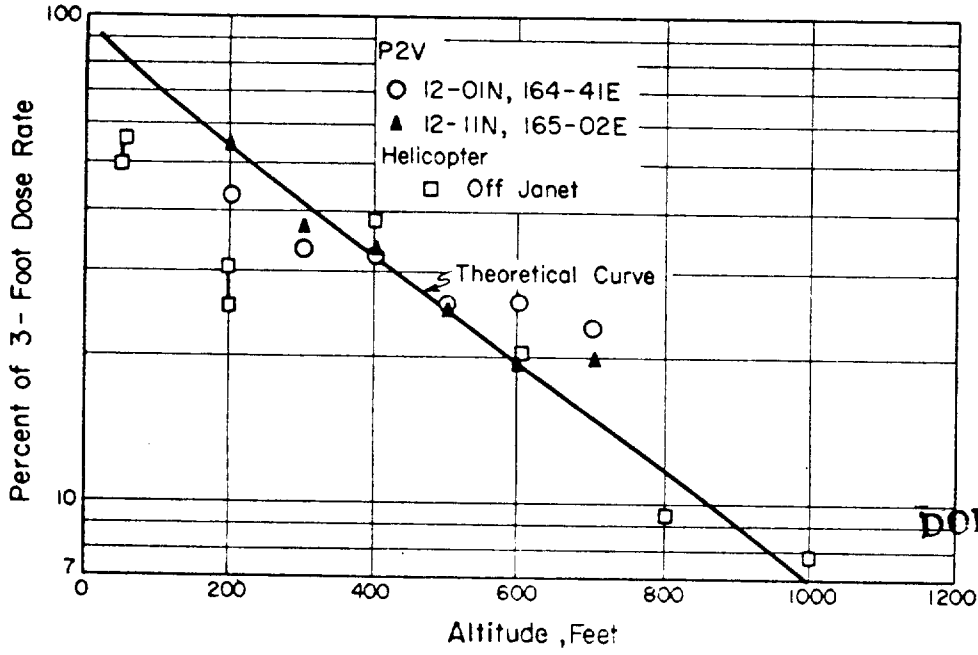

Figure 3.4 Radiation attenuation over water.

[redacted]

As discussed in Section 3.1.2, the distribution of gamma energies was estimated from the visual observations of a meter on the gamma spectrometer. Observations at 500 and 800 feet above Site Sally on Mohawk D + 2 showed a general response where the predominant portion of the energy spectrum fell between 350 and 600 kev.

3.3 DISTRIBUTION OF FALLOUT

The isodose charts contained in this section have been referred to H + 24 hours and gamma dose rate at 3 feet above the surface. The decay correction is based on $t^{-1.2}$. The flight altitude was 300 feet for all surveys, so the altitude correction is based on a factor of 2.5.

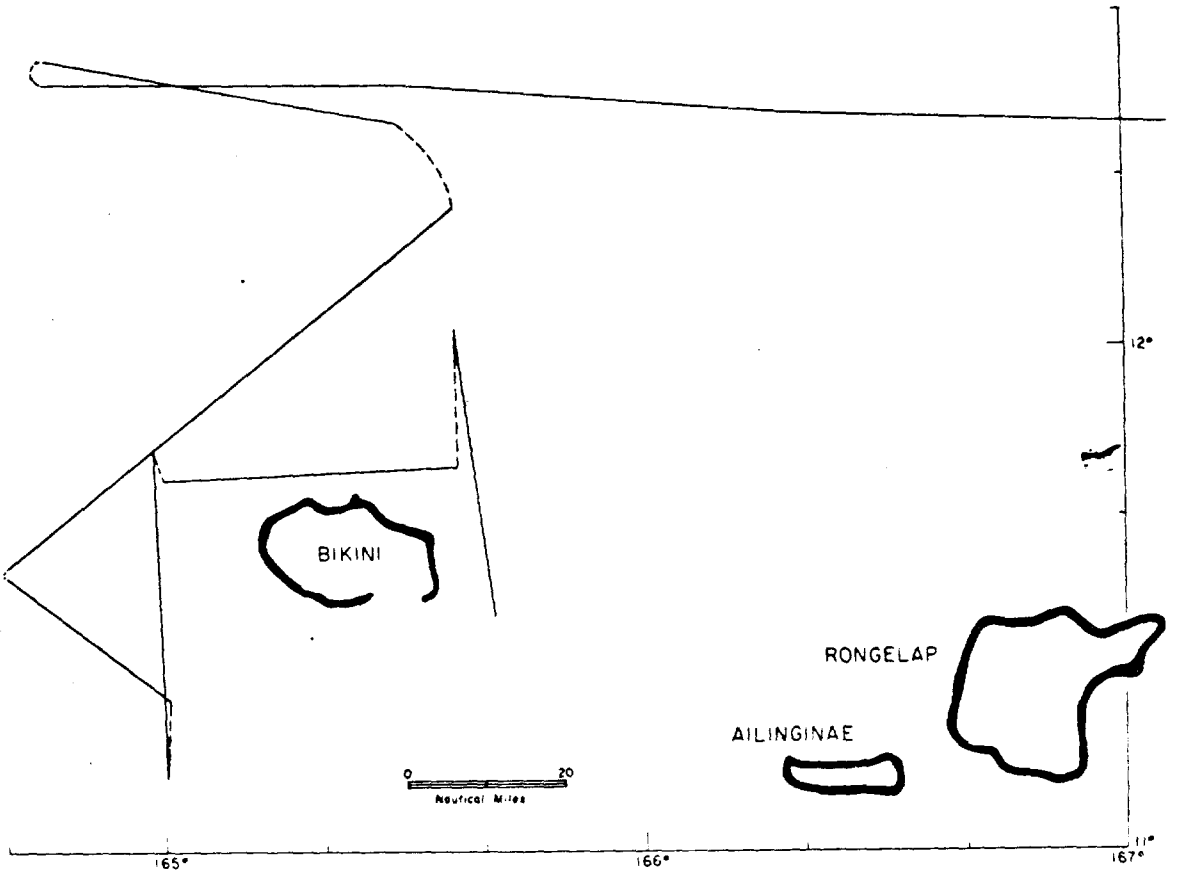

Figure 3.5 Flight pattern, Shot Cherokee D-day.

The EOB is based on a minimum detectable limit by the detector of 0.01 mr/hr. This converts to 0.025 mr/hr at the surface. Where there are no flight legs in a position to close an isodose plot, dotted lines indicate the estimated position. The estimates are based on previous days' results wherever possible. Contamination enclosed within an isodose bounded area is calculated on the basis of the average gamma intensity between consecutive isodose lines, and a contamination density of 0.4 megacurie/naut mi^2 for 1 mr/hr of gamma dose rate (Section 1.3.1).

3.3.1 Shot Cherokee. The D-day flight encountered no radiation intensities above the detectable limit. The flight pattern is included to show the area searched (Figure 3.5). The D + 1 flight was used for instrument check, because no contamination was found on the previous day.

3.3.2 Shot Zuni. The D-day flight examined the region in the vicinity of the atoll (Figure 3.6). Because there was not enough data to develop isodose plots, radiation profiles have been plotted along the flight legs.

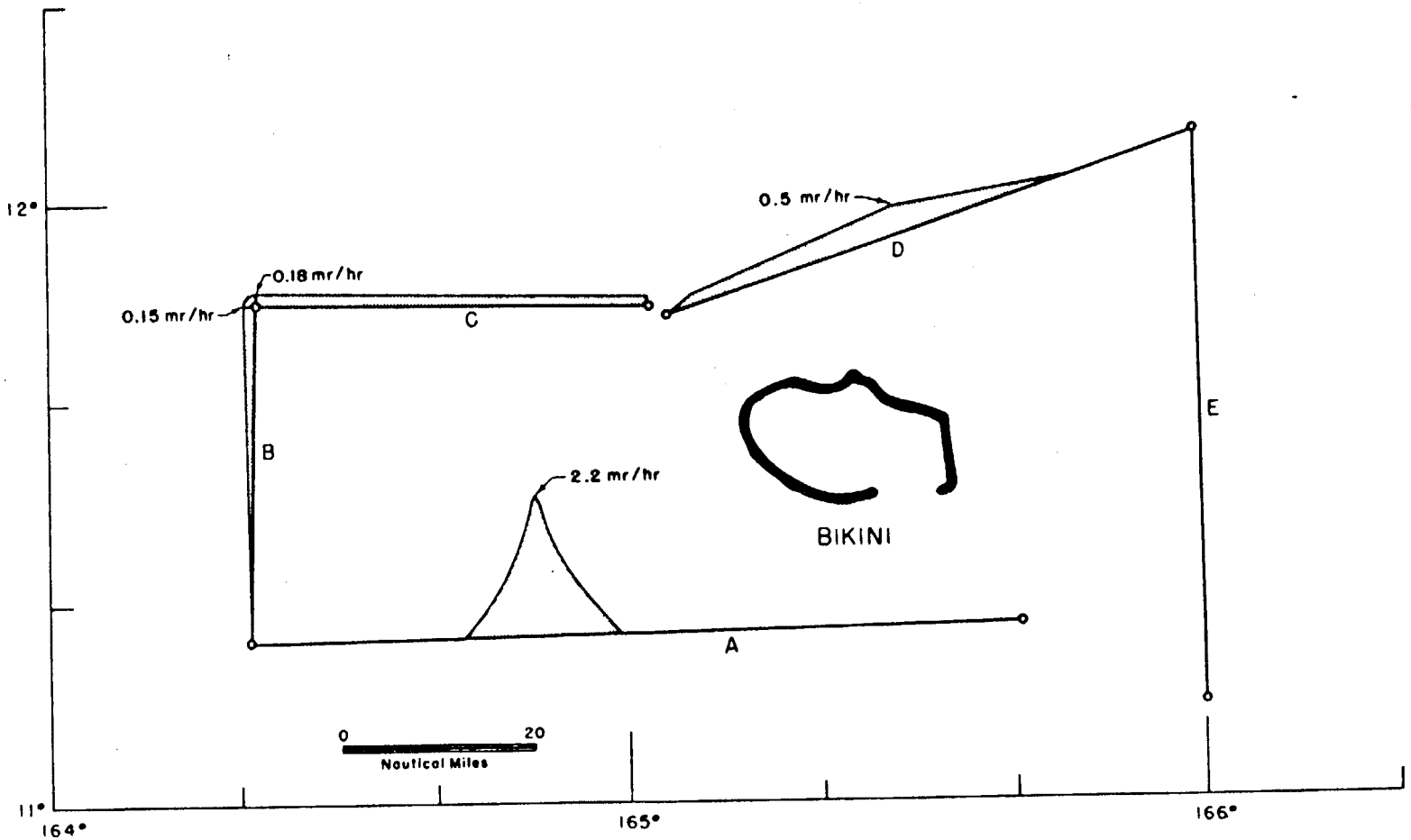

Figure 3.6 Flight pattern, Shot Zuni, D-day. All readings referred to H + 24 hours and 3 feet above surface.

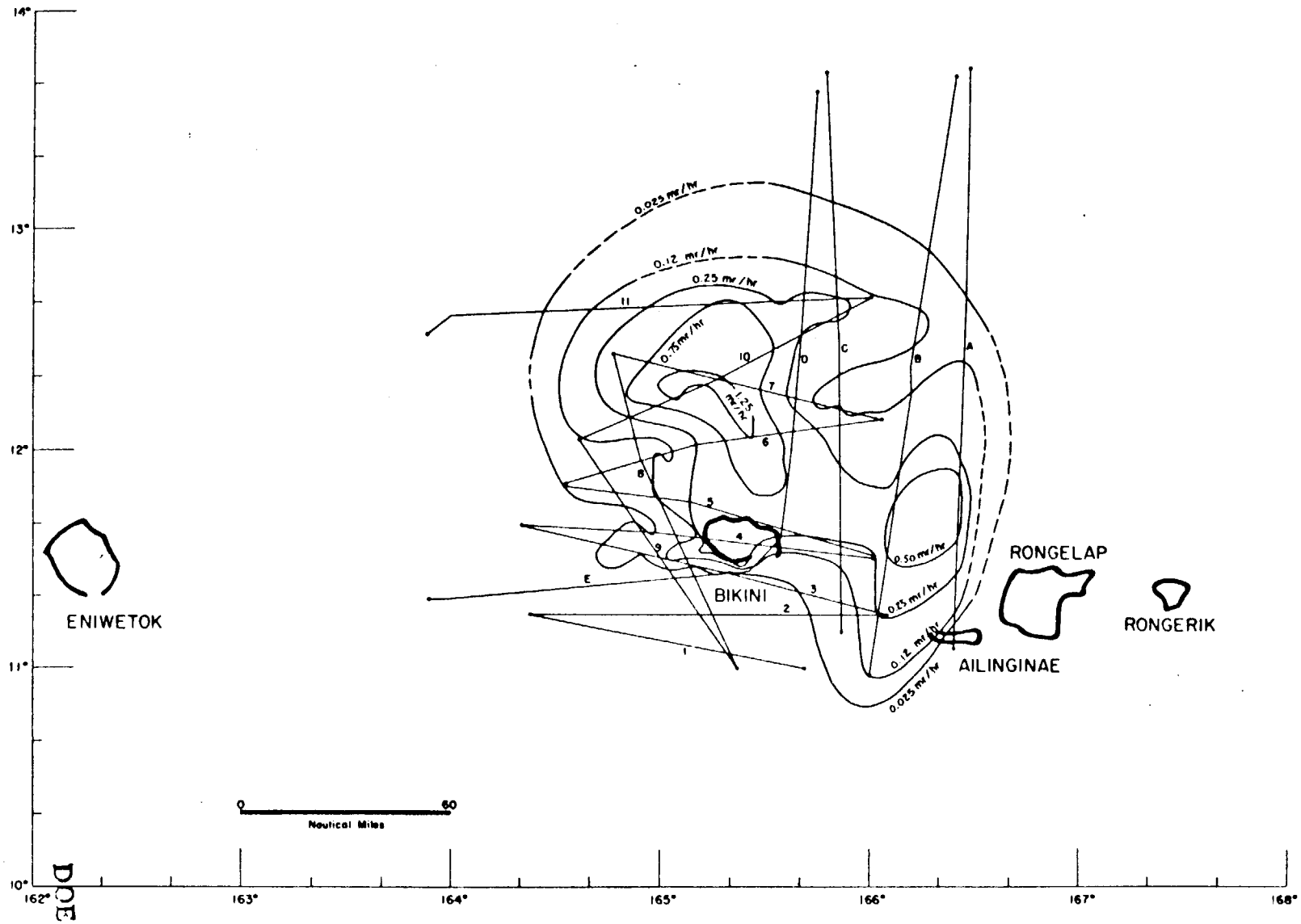

Figure 3.7 Flight pattern, Shot Zuni, D+1 day. All data readings referred to H+24 hours and 3 feet above surface. Numbers show legs flown by Aircraft 1, letters show legs flown by Aircraft 2.

The D + 1 fli[illegible] located the EOB and delineated the co[illegible]inated areas (Figure 3.7). A contaminated patch was suspected to be northeast of Bikini, based on the control center plots. During the data reduction, a navigational reporting error was discovered which changed the relatively isolated patch from the northeast to a position almost due east of Bikini.

TABLE 3.2 ALTITUDE RADIATION DATA OVER WATER

Altitude	mr/hr*	mr/hr†	mr/hr‡
ft			
1,000			0.41
800			0.52
700	0.12	0.225	
600	0.135	0.225	1.1
500	0.135	0.29	
400	0.175	0.38	2.1
300	0.175	0.42	
200	0.225	0.62	1.4, 1.7§
50			2.6, 3.0§

* Tewa + 3, 12-01 N, 164-41 E, Top Hat detector in P2V-5.
† Tewa + 3, 12-11 N, 165-02 E, Top Hat detector in P2V-5.
‡ Seminole D-day, off Janet, scintameter, TH-3, in helicopter.
§ Values from repeat runs.

The D + 2 flights (Figure 3.8) investigated the northeast sector without discovering contamination. The eastern contamination was not suspected until the data-reduction period, so no further examination was scheduled in that sector.

The D + 3 flights (Figure 3.9) reconfirmed the hot area. No further flights were scheduled,

TABLE 3.3 SUMMARY OF FALLOUT DISTRIBUTION, ZUNI

Isodose	Area	Difference Area	Average	Contamination
mr/hr	mi^2	mi^2	mr/hr	mc
D+1				
1.25	165	165	1.25	83
0.25	4,677	4,512	0.59	1,065
0.125	8,433	3,756	0.18	270
0.025	13,683	5,250	0.06	126
				1,544 mc at H + 24 hours
D+3				
0.75	757	757	1.25	379
0.25	6,775	6,018	0.50	1,204

as low intensities were encountered on this day.

The fallout distribution is summarized in Table 3.3.

3.3.3 Shot Flathead. The D-day flight discovered relatively high dose rate just west of Bikini (Figure 3.10). The position immediately adjacent to the reef indicated that this could be lagoon water passing over the reef, rather than fallout. This area was not completely mixed,

[redacted]

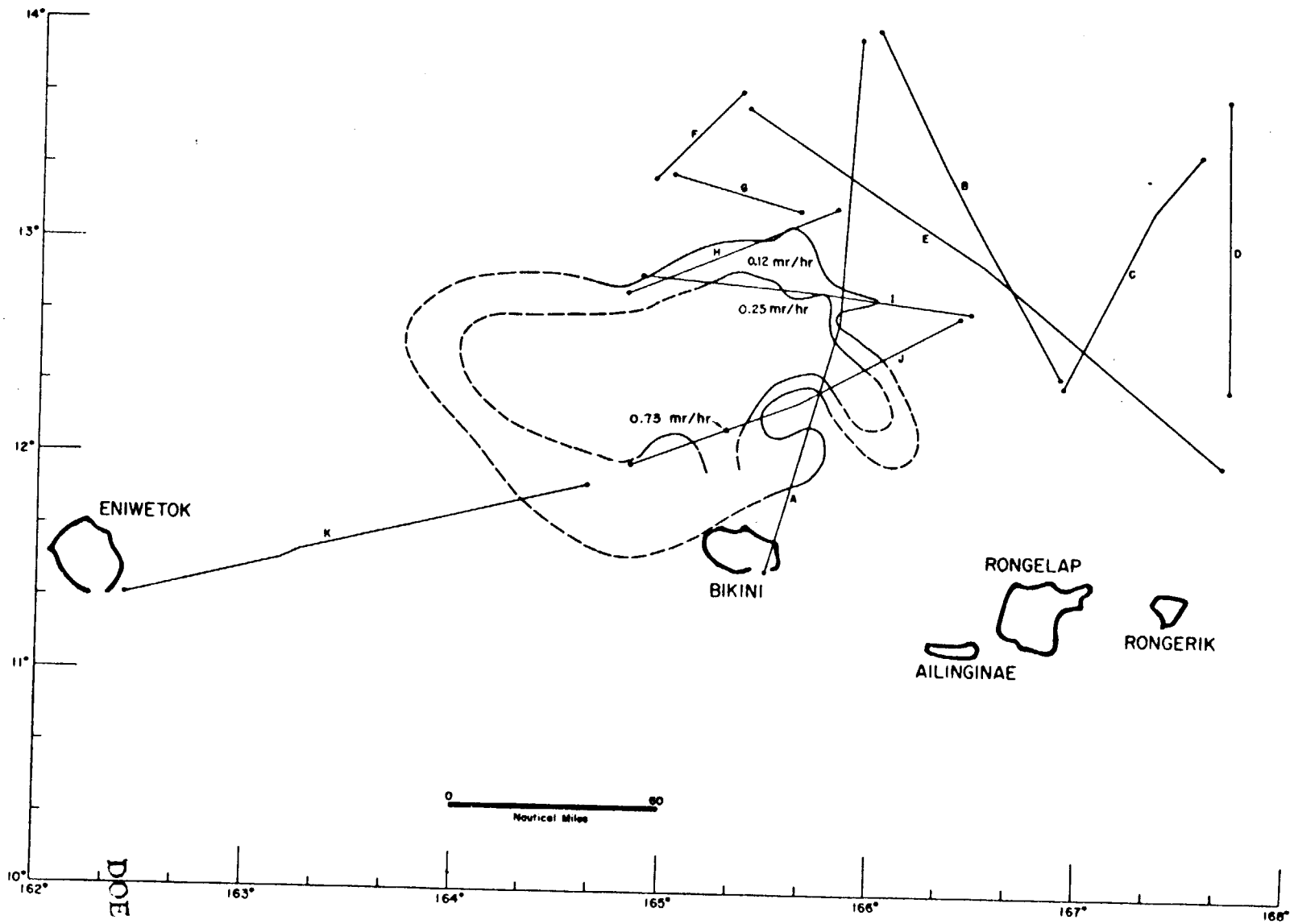

Figure 3.8 Flight pattern, Shot Zuni, D+2 days. Letters indicate flight legs. All data readings referred to H+24 hours and 3 feet above surface.

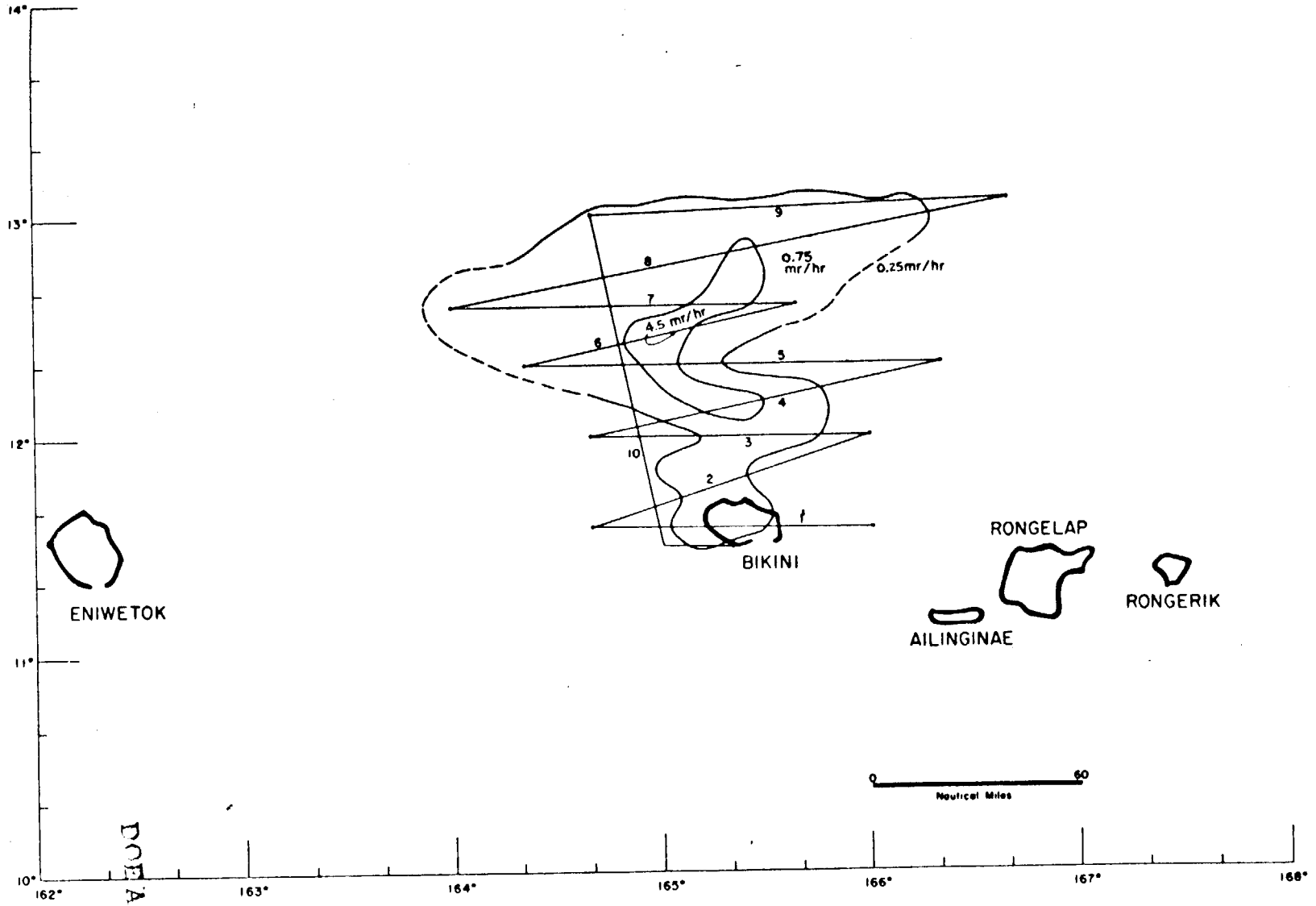

Figure 3.9 Flight pattern, Shot Zuni, D+3 days. Numbers indicate flight legs. All data readings referred to H+24 hours and 3 feet above surface.

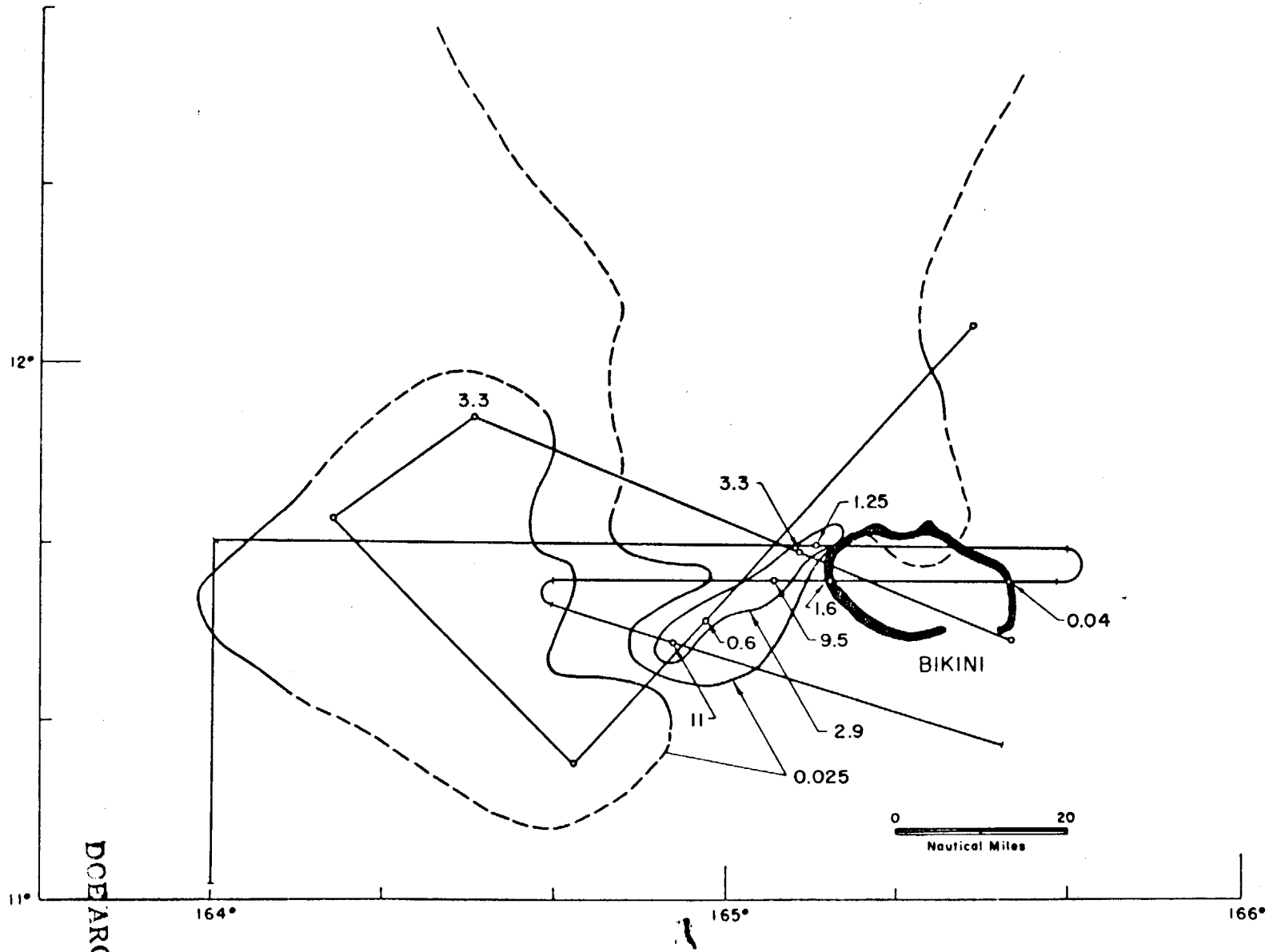

Figure 3.10 Flight patterns, Shot Flathead, D-day. Numbers shown are readings in mr/hr.

as the D + 1 su y does not indicate comparable dose rat The aircraft encountered active fallout and became contaminated. A replacement aircraft was flown to the survey area. This also became contaminated. At no time was the level in the aircraft allowed to exceed 20 mr/hr.

Both aircraft on the D + 1 flights (Figure 3.11) were also lightly contaminated. Active fallout was encountered 100 miles northwest of Bikini at H + 30 hours. The northwest sector was closed, as far as aerial surveys on D + 1 were concerned. As indicated on the chart, it was not possible to close the isodose plot at that time.

The project had four aircraft to choose from for the D + 2 flight, all reading a background of approximately 0.1 mr/hr inside the detector shielding. The survey for this day could not detect any surface contamination reading above a minimum detectable limit of 0.25 mr/hr at 3 feet from the surface. Table 3.4 summarizes the fallout distribution.

TABLE 3.4 SUMMARY OF FALLOUT DISTRIBUTION, FLATHEAD

Isodose	Area	Difference Area	Average	Contamination
mr/hr	mi^2	mi^2	mr/hr	mc
D+1				
0.2	383	383	0.368	56
0.1	908	525	0.148	31
0.05	3,350	2,442	0.074	73
0.025	11,000*	7,650*	0.037	115
				275 mc at H+24 hours

* Based on estimated position of isodose line.

The EOB is roughly estimated and may not be representative of the actual extent of the contamination.

3.3.4 Shot Mohawk. A survey of the islands of Eniwetok Atoll was flown on D+1. The island readings are shown in Figure 3.12. The readings are referred to 3 feet above the surface of the islands by a factor of 5.8 for the 300-foot flight altitude (Figure 1.2). Sites Fred and Elmer were excluded from the survey pattern, because a 300-foot flight altitude would have interfered with the air traffic in the vicinity. The open-sea aerial survey could find no detectable contamination in the area searched (Figure 3.13).

3.3.5 Shot Navajo. A background survey was made on D−1 day to determine if the hot intensities, reported by Project 2.62, adjacent to the reef after Shot Flathead, could have come from contaminated water crossing the reef. This flight (Figure 3.14) subsequently became a D−3 survey because of postponement of the shot. The next flight (Figure 3.15) became the D−2 survey, again because of a postponement. The aircraft flight, on the day which would have resulted in a D−1 survey, was not completed because of malfunction.

The background surveys were coordinated with a Project 2.62 ship survey. Because the shape and position of the contaminated area varied from day to day, it is possible that the variation may have been a function of the surface winds. An outline of the area, based on the ship data has been included as Figure 3.16. The agreement between these plots appears good, in view of the 12-hour displacement between the ship and aerial survey.

The D-day survey (Figure 3.17) located the estimated upwind boundary. On D+1, the flights covered an area of 10,000 mi^2 but did not close the 0.025 mr/hr isodose line in the northwest sector (Figure 3.18). The D+2 chart (Figure 3.19) shows that this isodose extended farther than estimated on the previous days. The narrow 1.25 mr/hr line extending to the west of the atoll had disappeared. Reef readings have been included in this chart.

The summary of the fallout distribution (Table 3.5) indicates considerable instability in the contaminated area during the aerial-survey operations. As experienced after the previous water

ings in mr/hr.

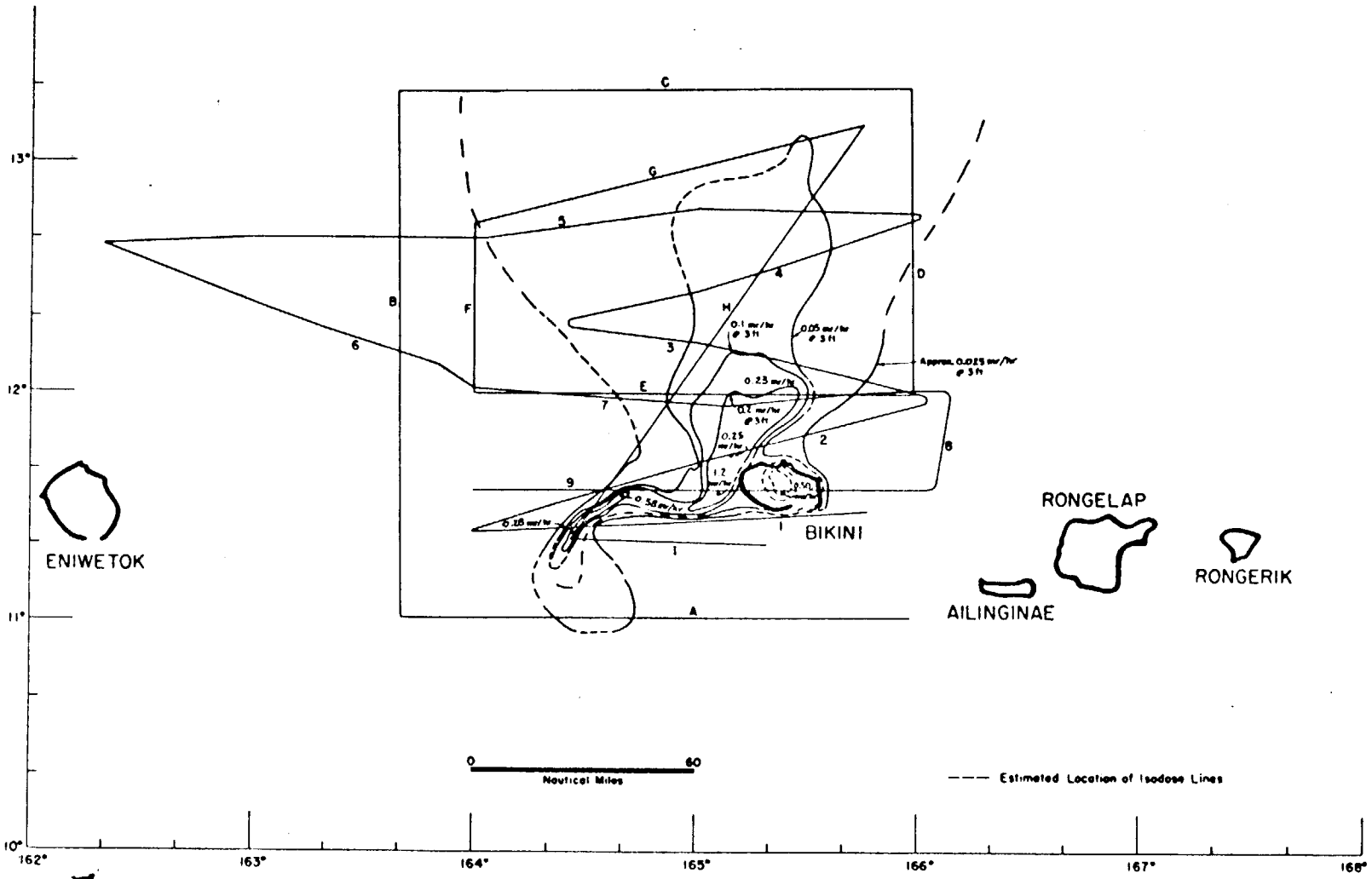

Figure 3.11 Flight pattern, Shot Flathead, D+1 day (H+24 to H+35 hours). Numbers show legs flown by Aircraft 1; letters show legs flown by Aircraft 2. Isodose values referred to: H+24 hours and 3 feet above surface. Airborne contamination encountered H+28 to H+30 hours.

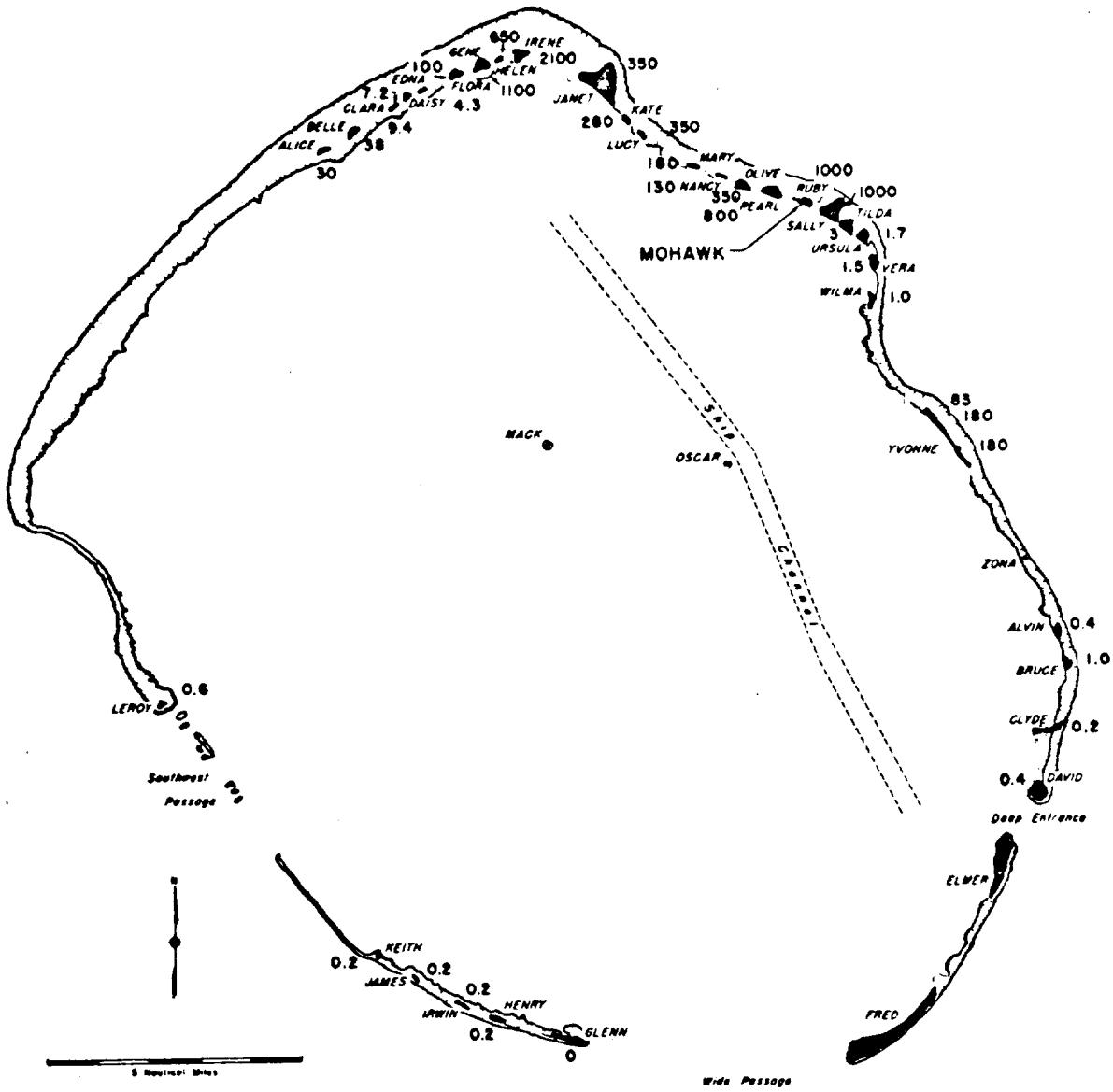

Aarsanbiru	Vera	Chinieero	Alvin	Igurin	Glenn	Ribaion	James
Aitsu	Olive	Chinimi	Clyde	Japtan	David	Rigili	Leroy
Aniyaanii	Bruce	Cochita	Daisy	Kirinian	Lucy	Rojoa	Ursula
Aomon	Sally	Coral Heads	Mack, Oscar	"M"	Zona	Ruchi	Clara
Bijiri	Tilda	Eberiru	Ruby	Mui	Henry	Rujoru	Pearl
Bogairikk	Helen	Elugelab	Flora	Muzin	Kate	Runit	Yvonne
Bogallua	Alice	Engebi	Janet	Parry	Elmer	Sandildefonso	Edna
Bogombogo	Belle	Eniwetok	Fred	Piiraai	Wilma	Teiteiripucchi	Gene
Bogon	Irene	Giriinien	Keith	Pokon	Irwin	Yeiri	Nancy
Bokonaarappu	Mary						

Figure 3.12 Atoll readings, Shot Mohawk, D + 1 day. All readings referred to mr/hr at 3 feet from the surface and to the time of the survey. Sites Elmer and Fred not surveyed.

[redacted]

34

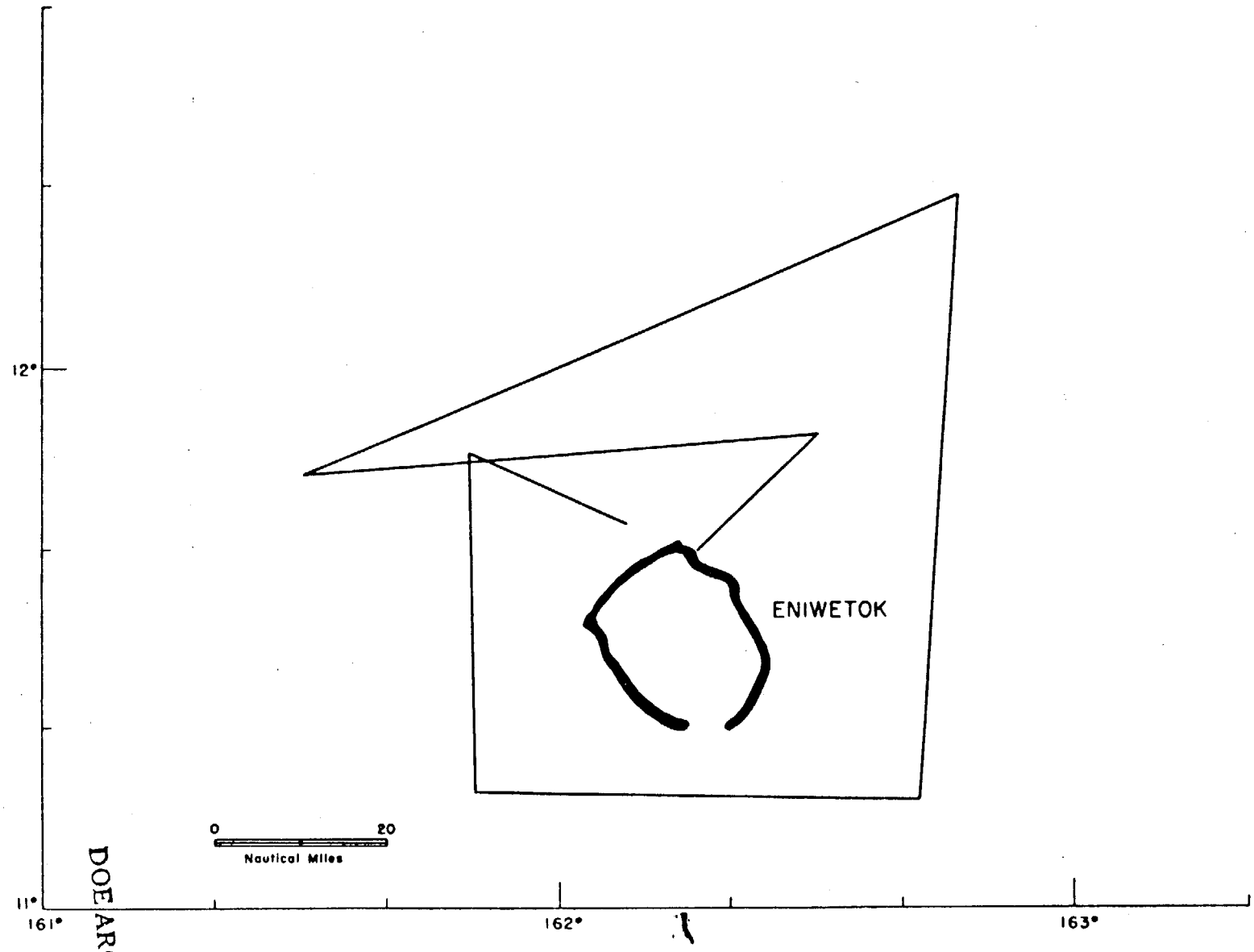

Figure 3.13 Flight pattern, Shot Mohawk, D + 1 day.

Figure 3.13 Flight pattern, Shot Mohawk, D + 1 day.

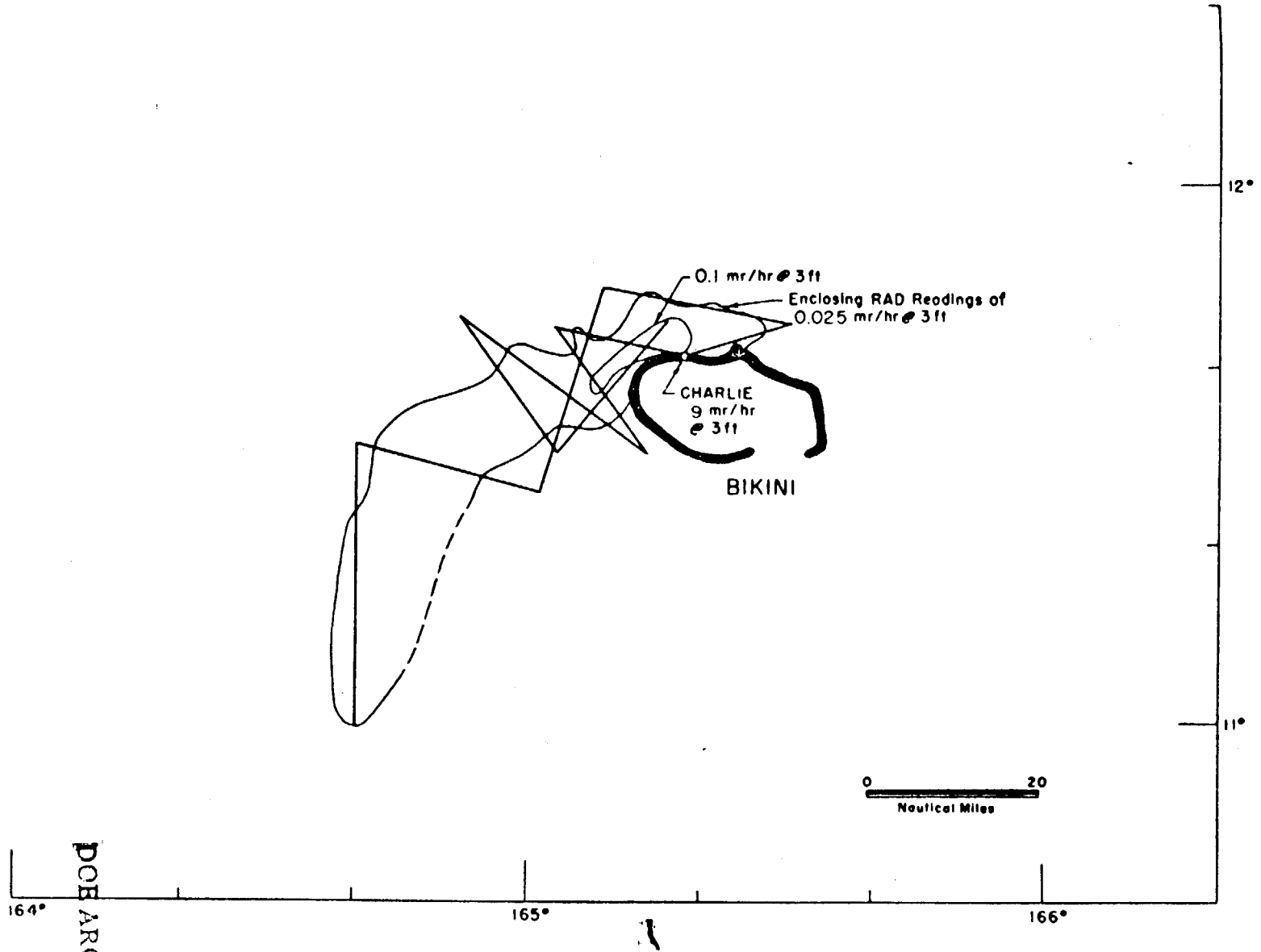

Figure 3.14 Special aerial survey, Shot Navajo, D−3 days.

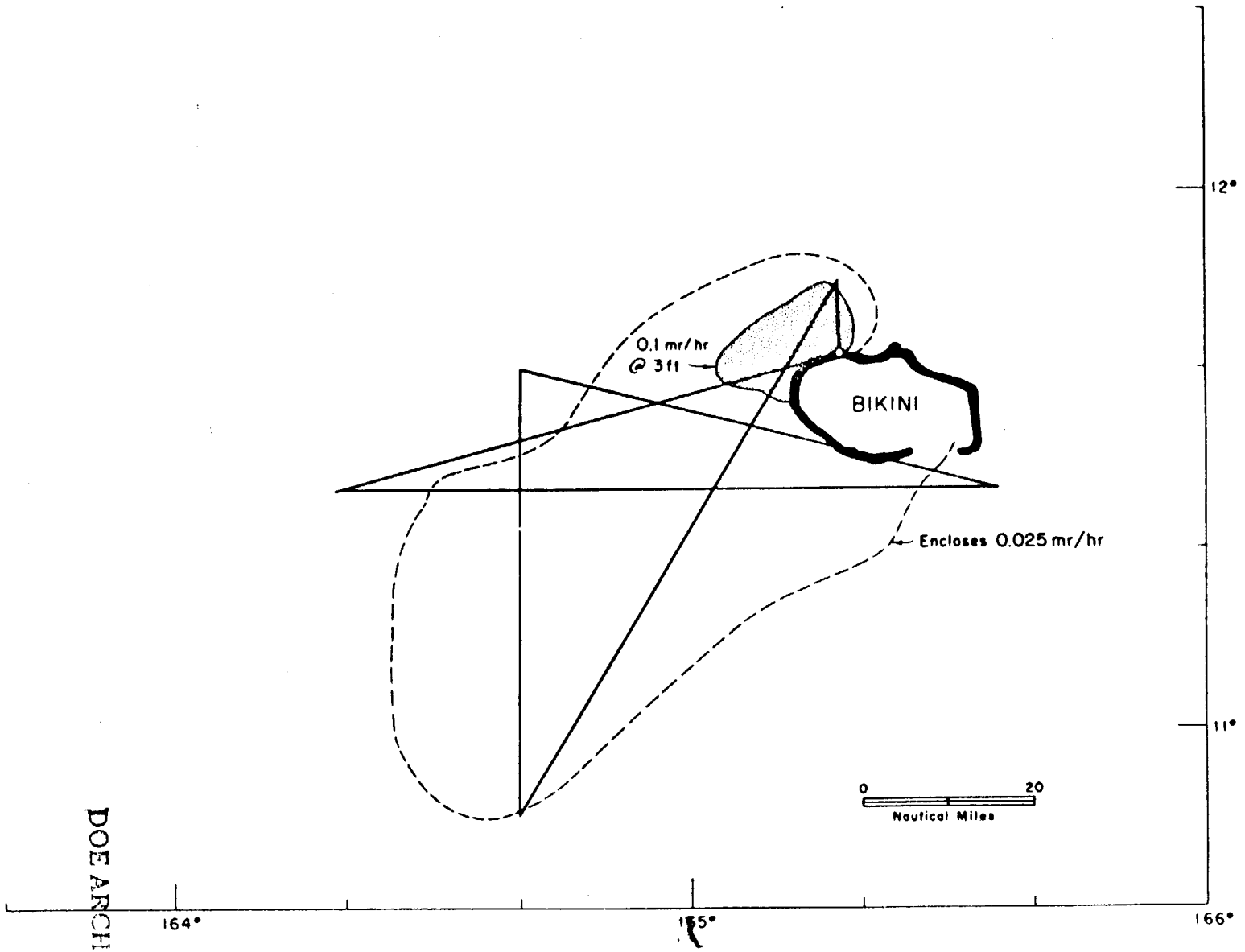

Figure 3.15 Aerial survey ("flush" flight pattern) Shot Navajo D−2 days. All readings referred to 3 feet above the surface and time of survey.

Figure 3.15 Aerial survey ([illegible] readings referred to 3 feet above the surface and time of survey.

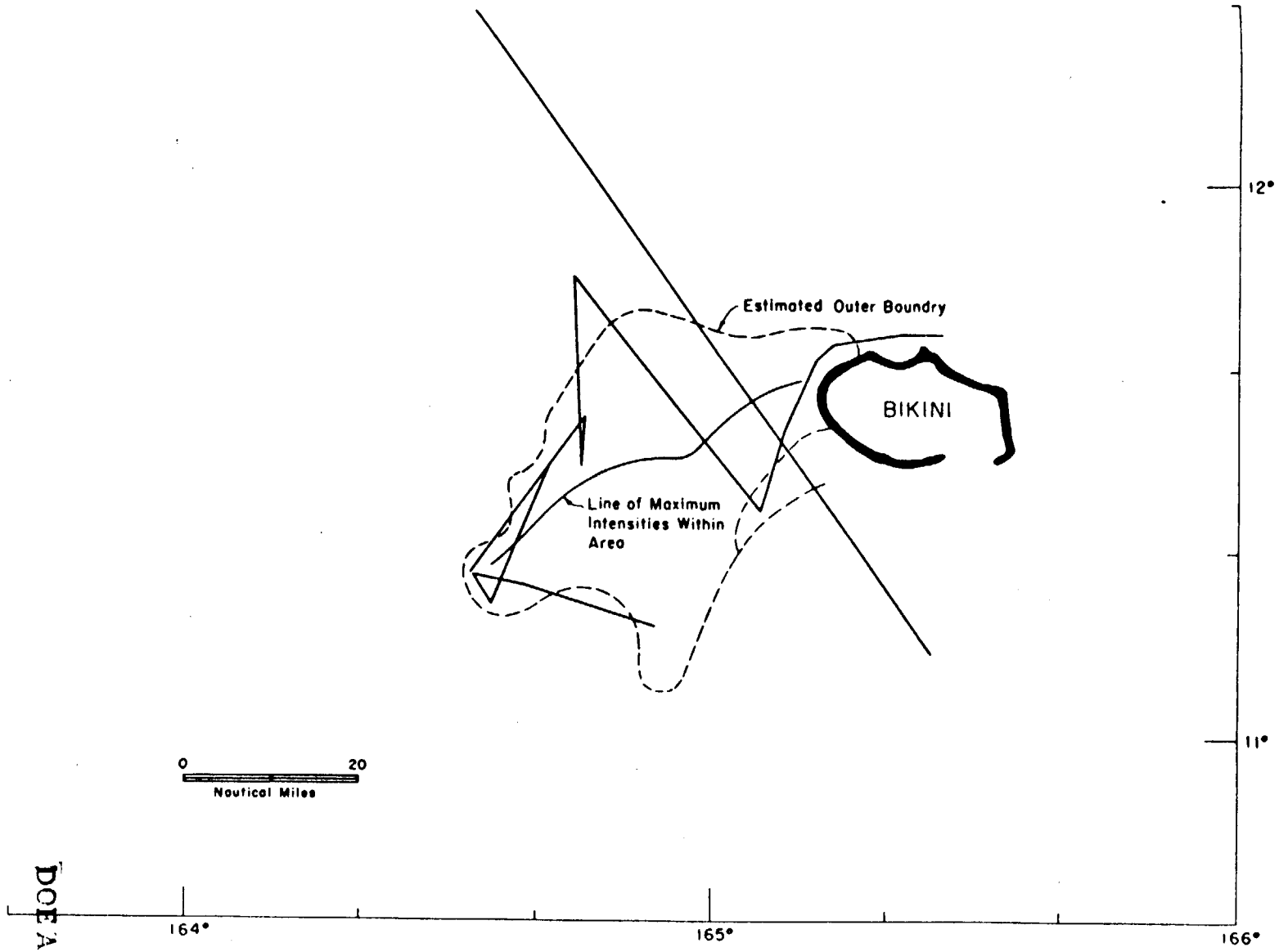

Figure 3.16 Ship pattern derived from data received from Project 2.62. Shot Navajo, D−2 days.

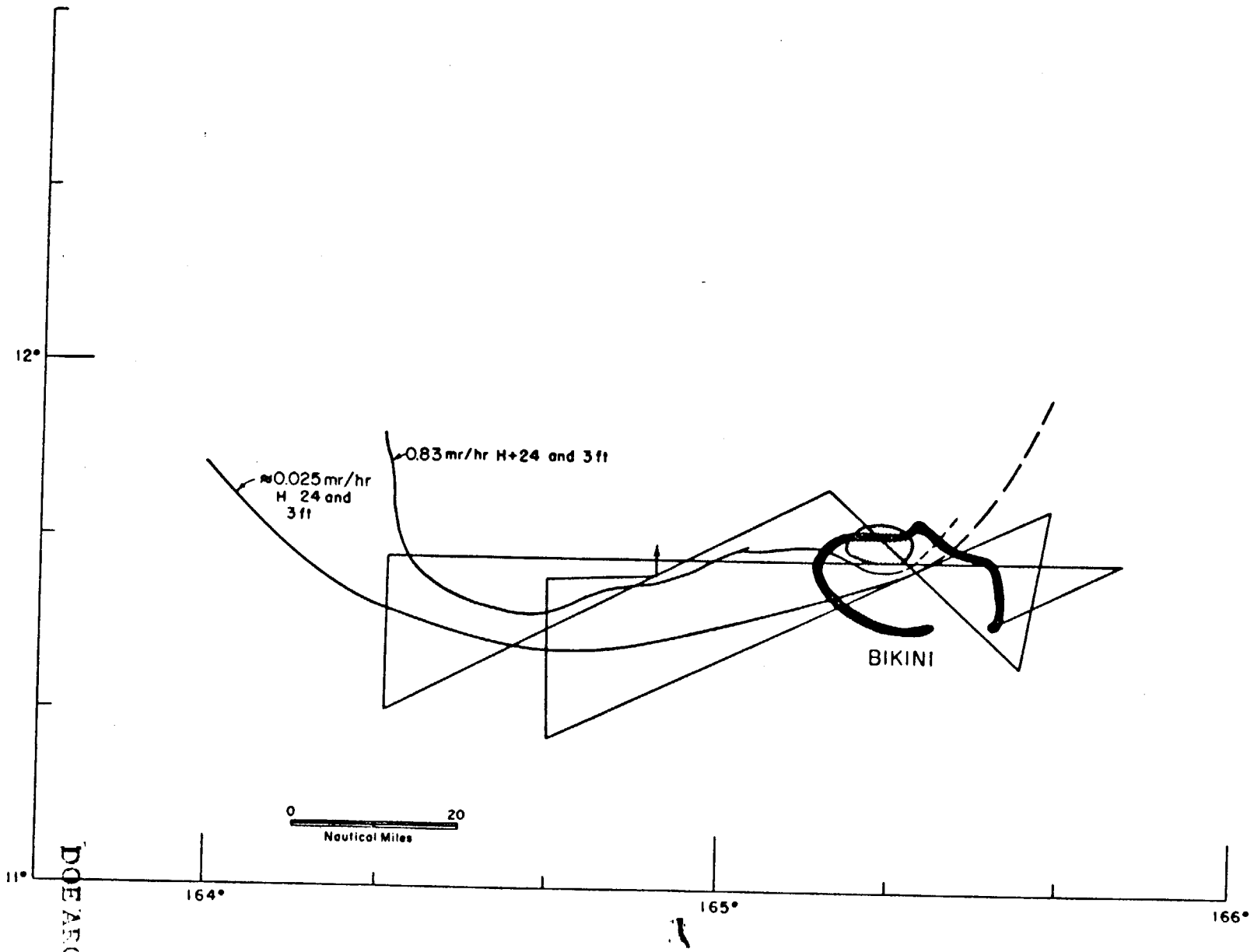

Figure 3.17 Flight pattern, Shot Navajo, D-day.

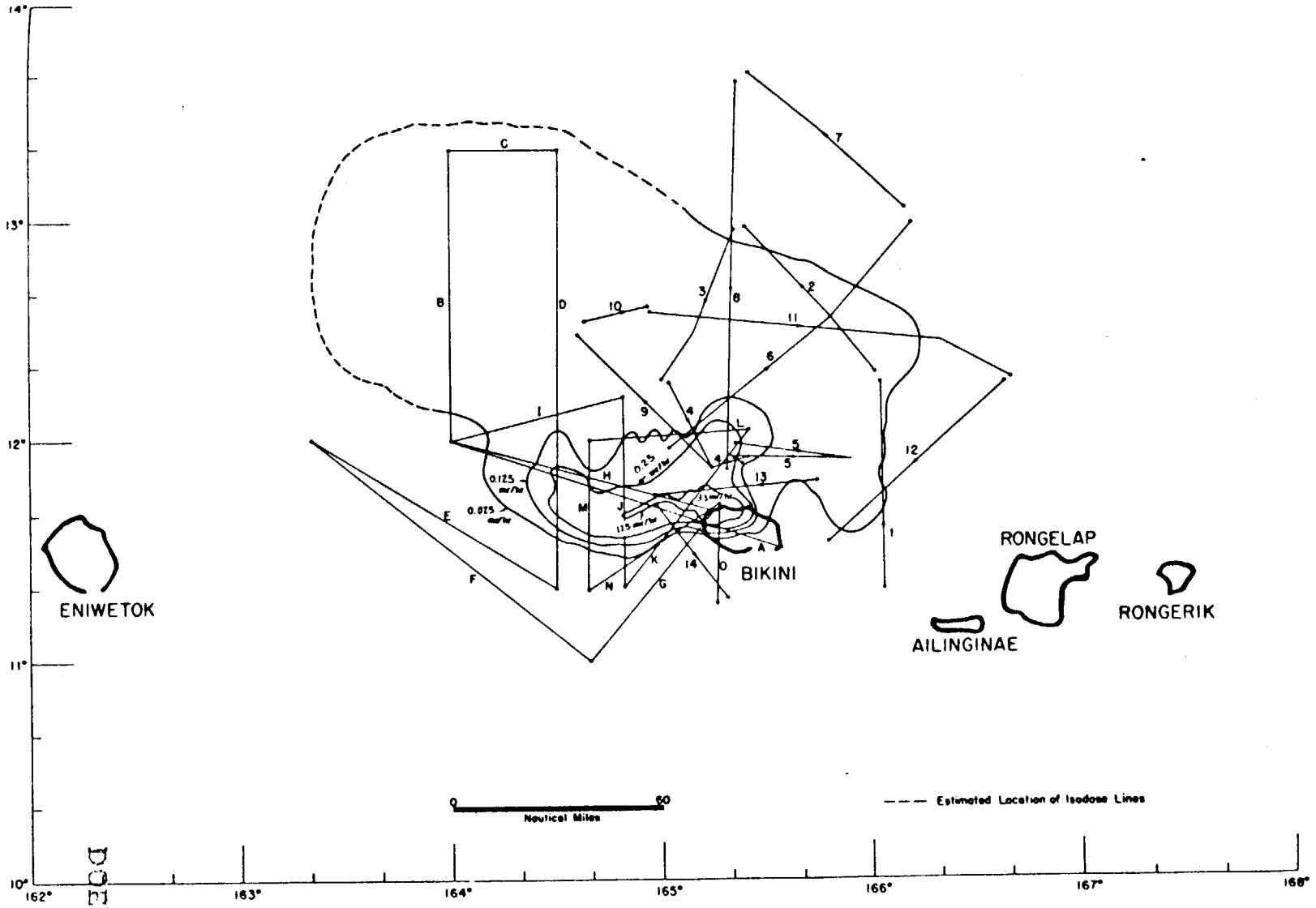

Figure 3.18 Flight pattern, Shot Navajo; D + 1 day. All data readings refer to H + 24 hours and 3 feet above surface. Numbers show legs flown by Aircraft 1, letters show legs flown by Aircraft 2.

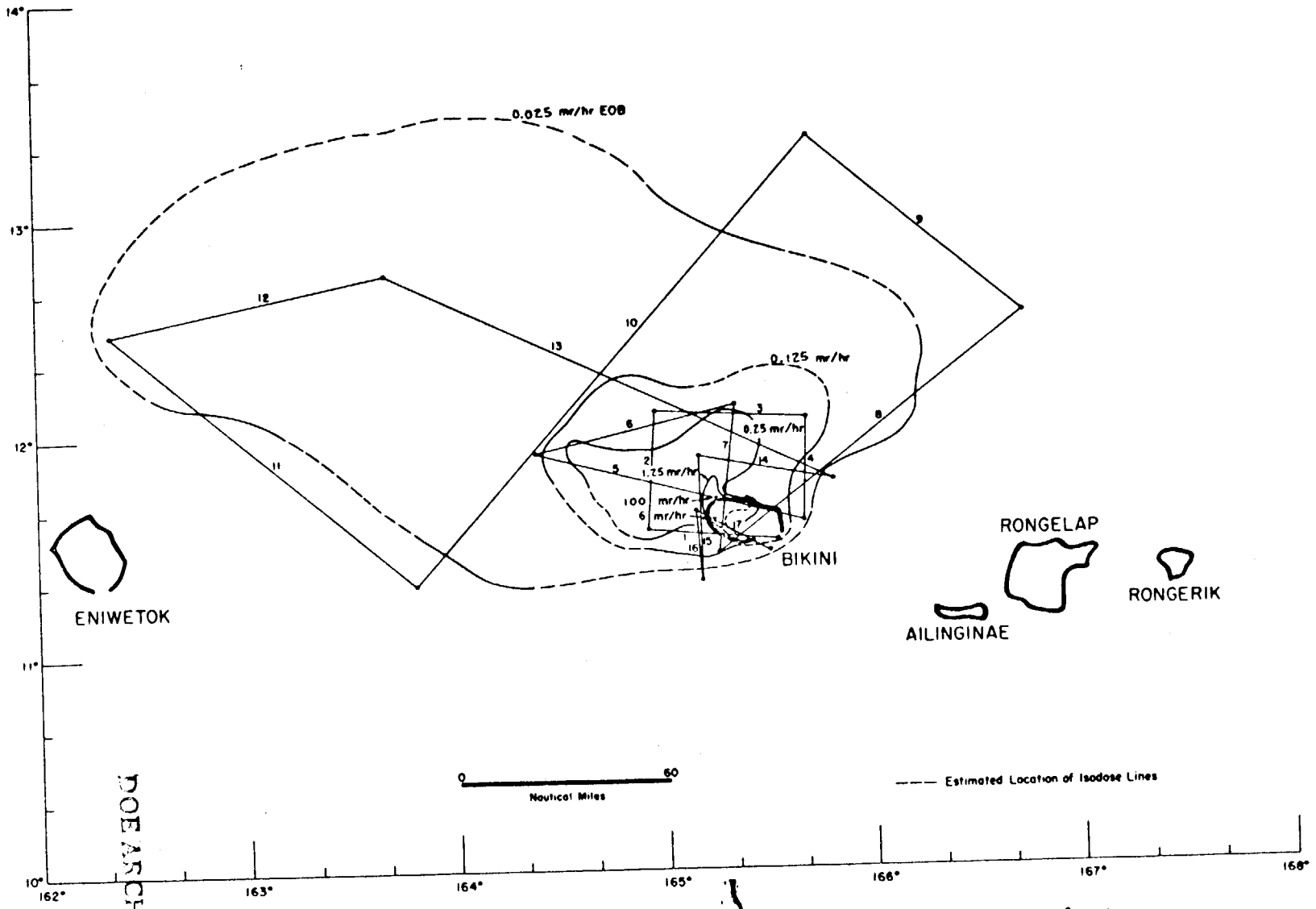

Figure 3.19 Flight pattern, Shot Navajo, D + 2 days. All data readings refer to H + 24 hours and 3 feet above surface. Numbers show legs flown by aircraft.

shot, Flathead, ı. .h of the fallout remains airborne. Thus, .allout and mixing in the sea could be expected to persist well into D + 1.

3.3.6 Shot Tewa. A D−1 survey (Figure 3.20) defined the background status to the west of the atoll, prior to the shot. The D-day flight (Figure 3.21) located the upwind boundary. The

TABLE 3.5 SUMMARY OF FALLOUT DISTRIBUTION, NAVAJO

Isodose	Area	Difference Area	Average	Contamination
mr/hr	mi^2	mi^2	mr hr	mc
D + 1				
1.25	158	158	1.35	85
0.25	958	800	0.75	240
0.125	1,788	830	0.18	60
0.025	10,490*	8,702	0.06	209
				594 mc at H + 24 hours
D + 2				
1.25	90	90	1.35	49
0.25	1,267	1,177	0.75	353
0.125	3,263	1,996	0.18	144
0.025	20,930*	17,667	0.06	424
				970 mc at H + 24 hours

* Based on estimate of isodose position.

D + 1 survey (Figure 3.22) discovered a contaminated area extending over 200 miles west of Bikini. The outside boundary could not be closed on this survey, because of the far-out sector contained active fallout from Shot Huron. The D + 2 survey (Figure 3.23) extended the estimated position of the EOB. The isodose was still not completely closed. The aircraft was not allowed to lose radio contact, so the survey covered only the area out to 275 miles from Bikini.

The 0.25 mr/hr isodose extended into the far northwest sector on D + 1. By D + 2, the position had shrunk to approximately a third of the enclosed area. The predicted pattern shows that this far-out material could not be expected to arrive before H + 19 hours. Thus, it is probable that the readings in the area on D + 1 were due to material that was not completely mixed. By D + 2, some 30 hours had elapsed, and mixing was probably complete.

The D + 3 and D + 4 surveys, Figures 3.24 and 3.25, delineated the hot area, permitting an examination of the shape and position of these inner areas from D + 1 through D + 4. Table 3.6 summarizes the fallout areas throughout the shot participation.

Figure 3.19 Flight pattern, [illegible]. Numbers show legs flown by [illegible] H + 24 hours and 3 feet above surface.

3.4 SAMPLES OF CONTAMINATED SEA WATER

Duplicate samples of sea water were furnished to this project by the U.S. Naval Radiological Defense Laboratory (NRDL) and by Scripps Institution of Oceanography (SIO) from their sea-sampling programs. After the close of Operation Redwing, these samples were analyzed for beta activity in the particulate and salt fractions at the HASL.

3.4.1 Gamma Radiation as a Function of Beta Activity. The analysis of each sample, the gamma intensity estimated at each sampling location, and the comparison of these results are contained in Appendix D. A straight averaging of the beta activity and the estimated gamma intensity yields a figure of 4×10^6 (dis/min)/liter per mr/hr. The wide variability of the comparison for each sample obviates definite conclusions. However, much of the data falls within ± 50 percent of the theoretical calculation of 4.43×10^6 (dis/min)/liter of beta activity per mr/hr of gamma activity 3 feet above the surface. Thus, these results may be considered indicative of validity of the assumption.

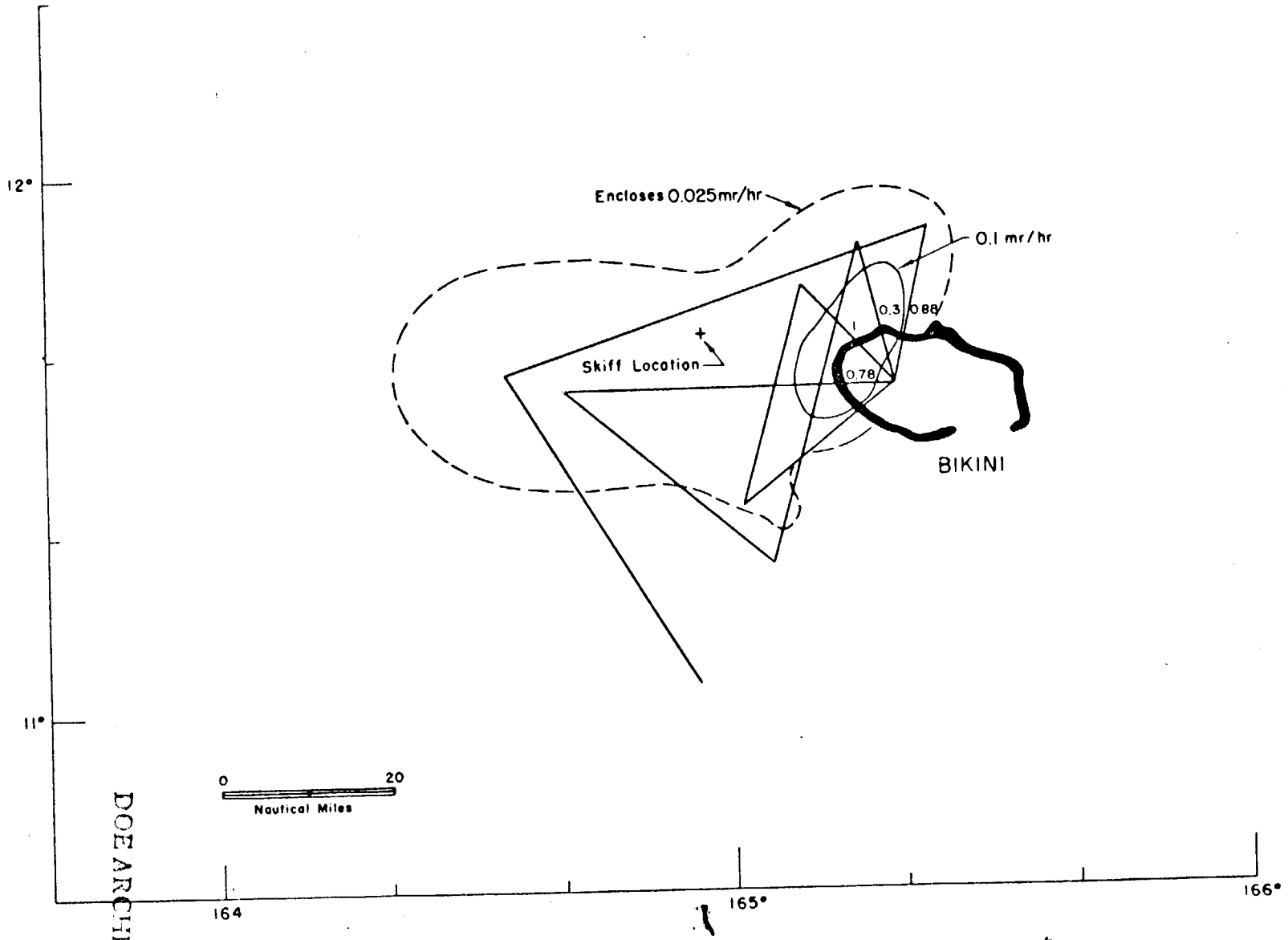

Figure 3.20 Flight pattern, Shot Tewa, D−1 day. All readings in mr/hr at 3 feet at time of survey.

3 feet at time of survey.

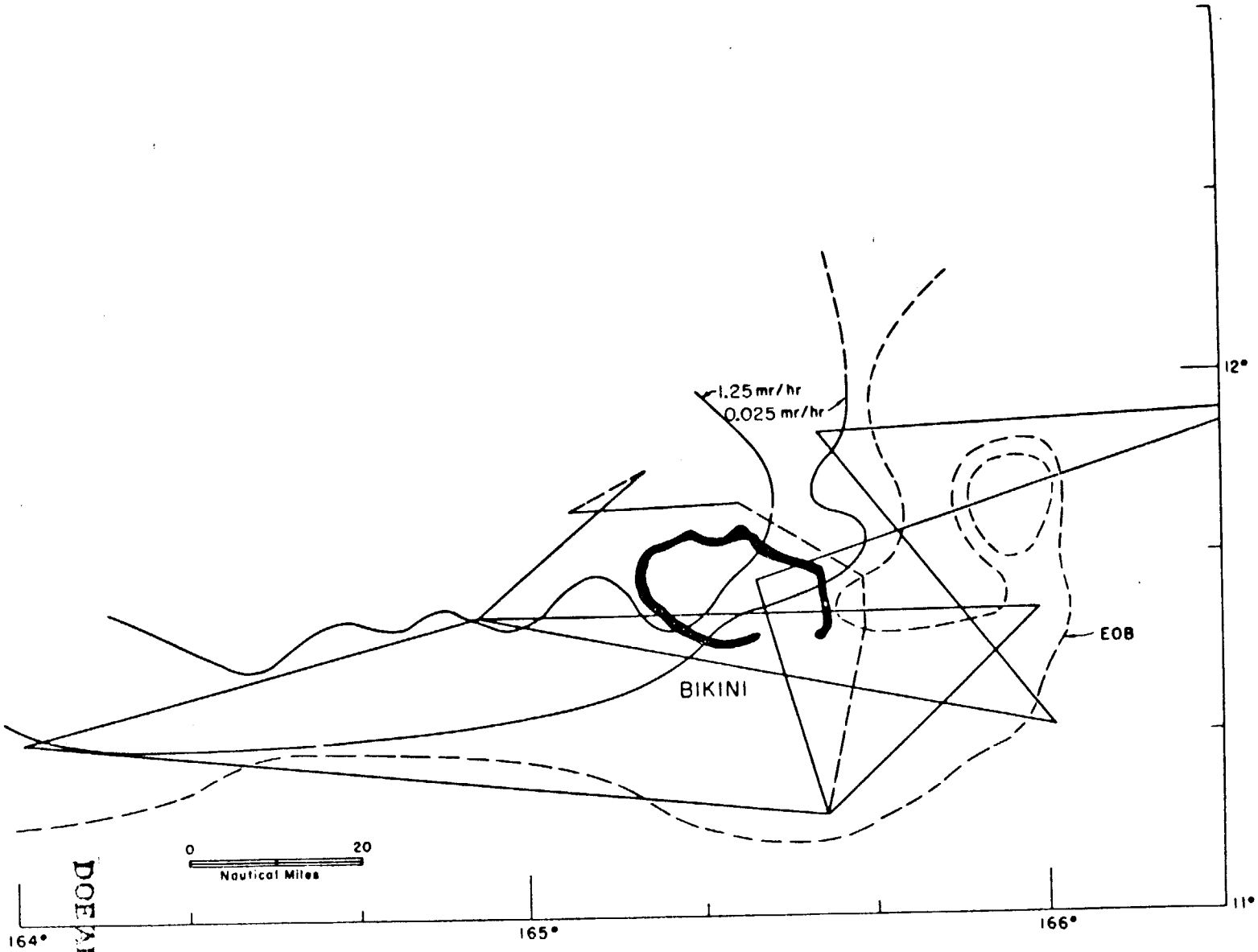

Figure 3.21 Flight pattern, Shot Tewa, D-day. All readings referred to H + 24 hours and 3 feet above surface.

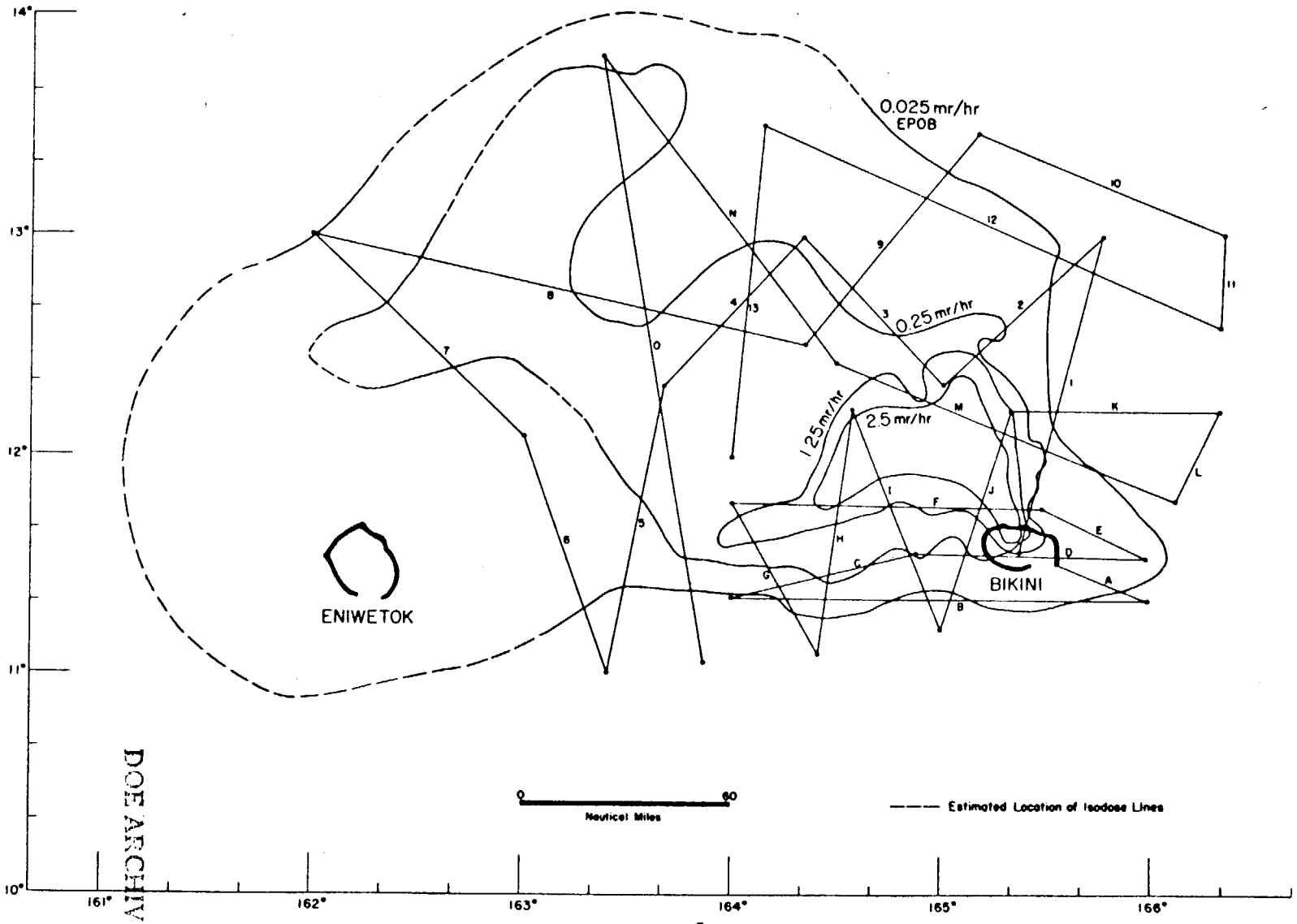

Figure 3.22 Flight pattern, Shot Tewa, D+1 day. All data readings refer to H+24 hours and 3 feet above surface. Numbers show legs flown by Aircraft 1; letters show legs flown by Aircraft 2.

H + 24 hours and 3 feet above surface. Numbers show legs flown by Aircraft 1; letters show legs flown by Aircraft 2.

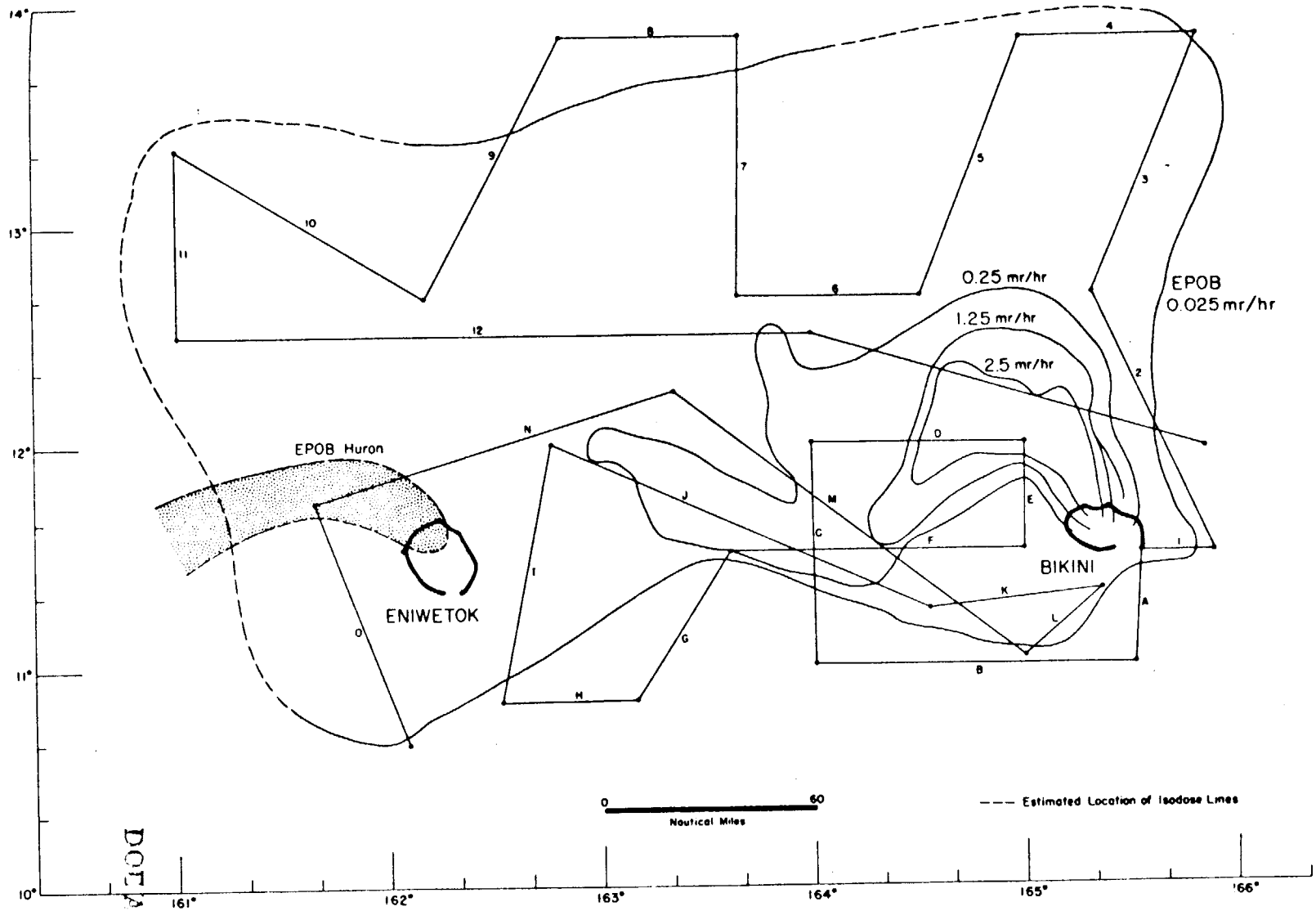

Figure 3.23 Flight pattern, Shot Tewa, D + 2 days. All data readings refer to H + 24 hours and 3 feet above surface. Numbers show legs flown by Aircraft 1; letters show legs flown by Aircraft 2.

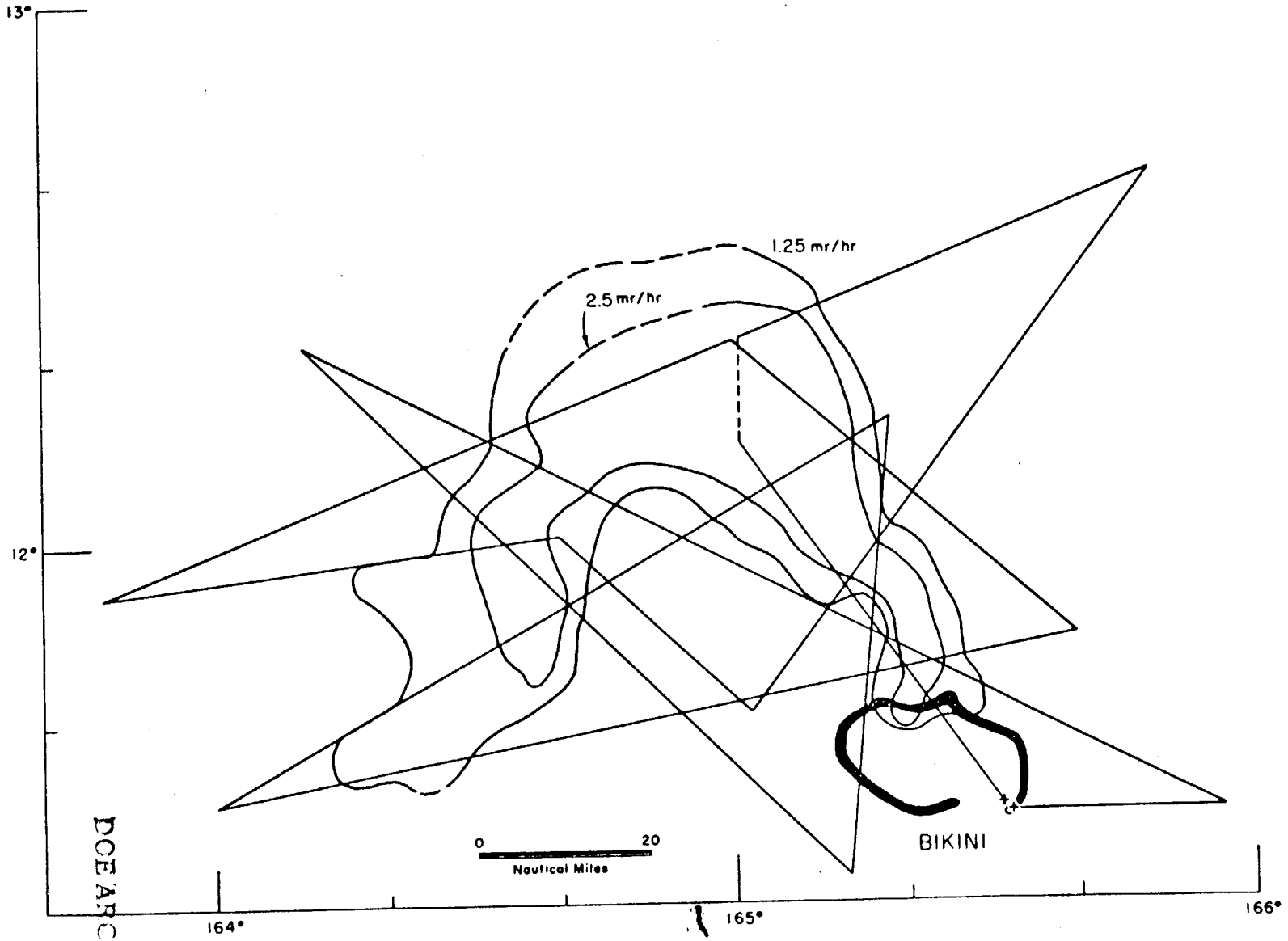

Figure 3.24 Flight pattern, Shot Tewa, D + 3 days. All readings referred to H + 24 hours and 3 feet above surface.

Figure 3.24 Flight pattern, Shot Tewa, D + [illegible]
H + 24 hours and 3 feet above surface.

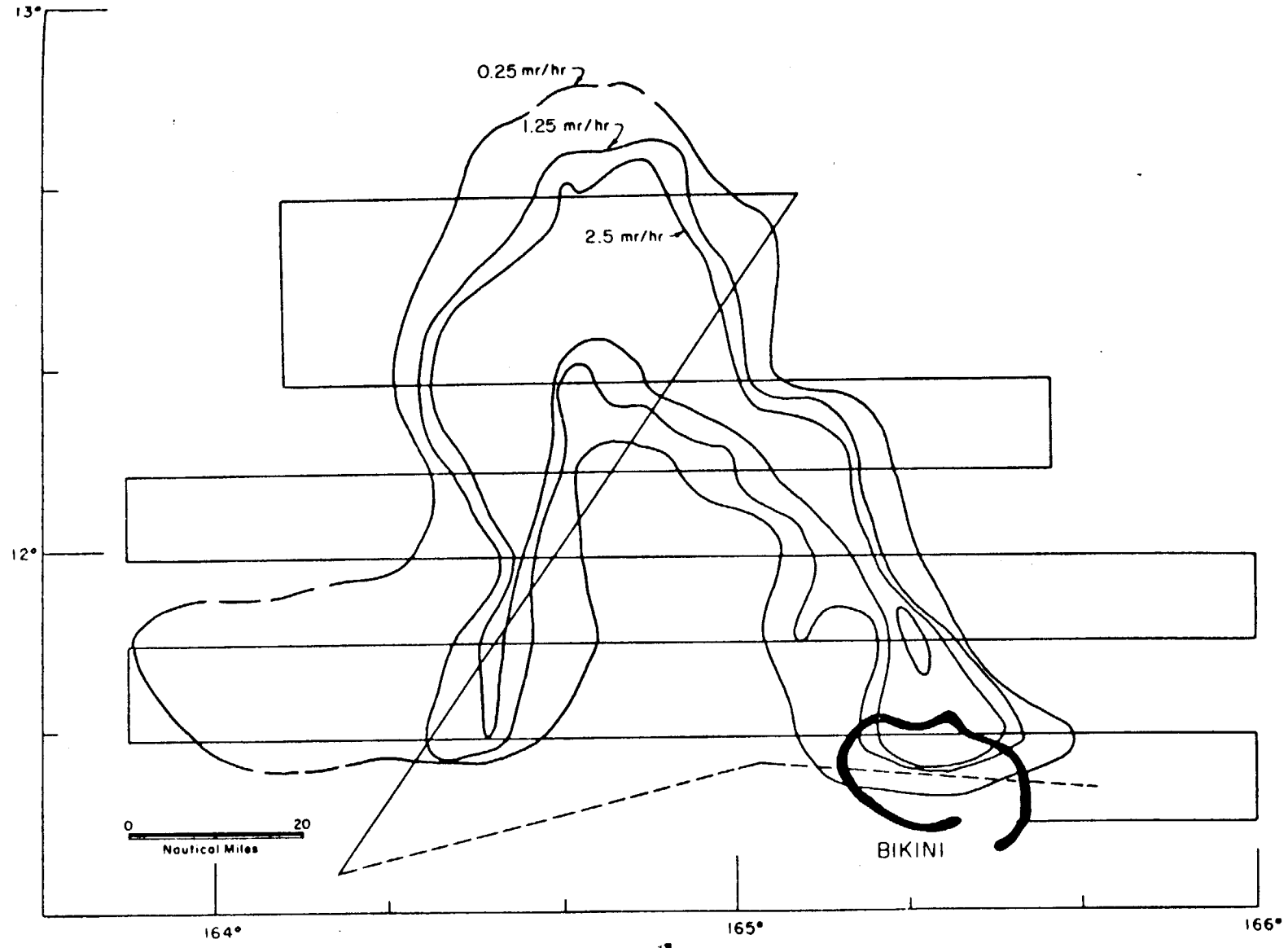

Figure 3.25 Flight pattern, Shot Tewa, D + 4 days. All readings referred to H + 24 hours and 3 feet above surface.

48

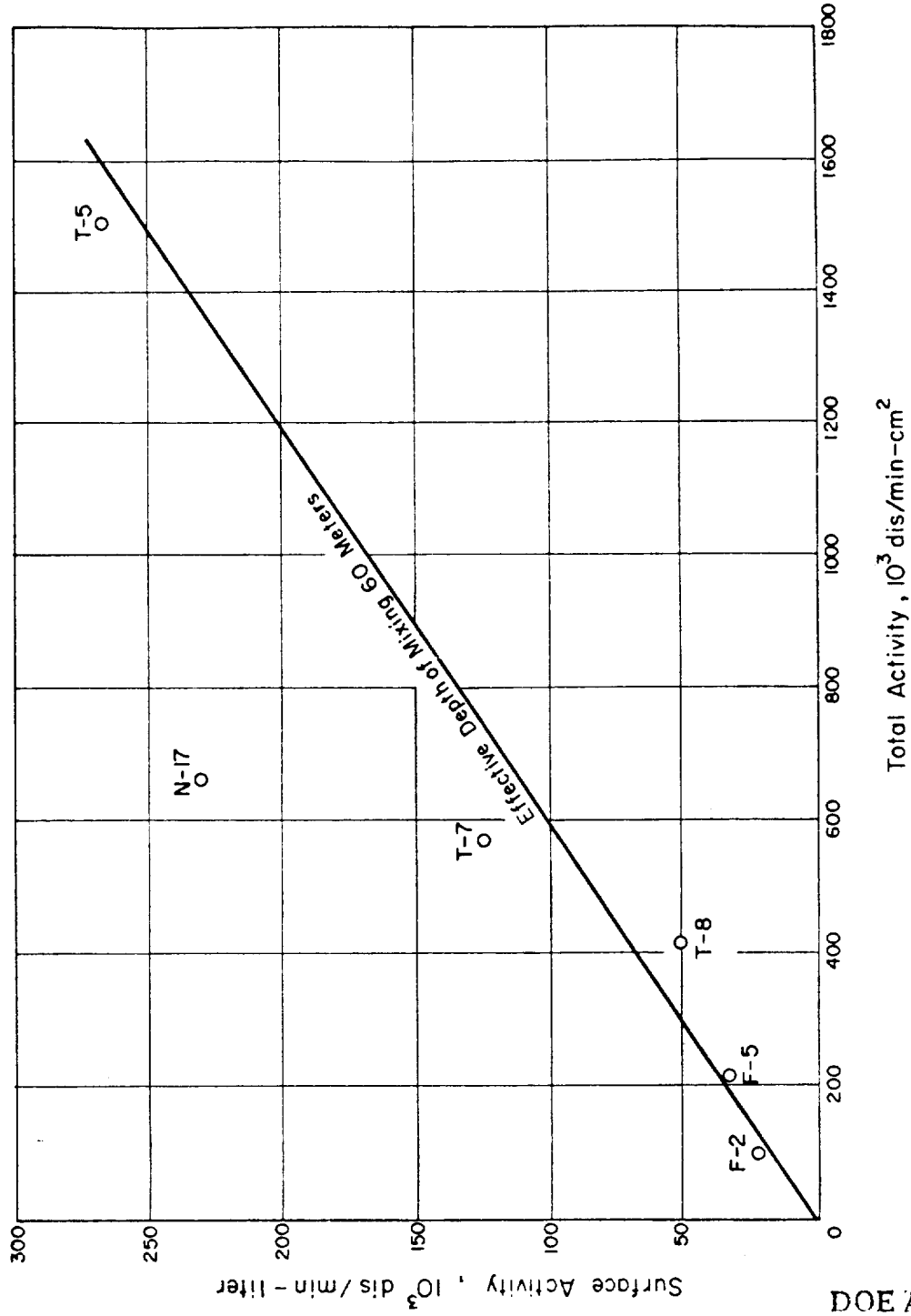

Figure 3.26 Effective depth of mixing for fallout in the sea.

TABLE 3.6 SUMMARY OF FALLOUT DISTRIBUTION, TEWA

Isodose	Area	Difference Area	Average	Contamination
mr/hr	mi^2	mi^2	mr/hr	mc
D+1				
2.5	1,230	1,230	5	2,460
1.25	2,390	1,160	1.84	858
D+2				
2.5	1,150	1,150	5	2,300
1.25	2,340	1,190	1.84	880
0.25	6,750	4,410	0.75	1,323
0.025	43,505	39,095	0.125	1,955
				6,458 mc at H+24 hours
D+3				
2.5	982	982	5	1,964
1.25	2,035	1,053	1.84	779
D+4				
2.5	1,070	1,070	5	2,140
1.25	1,695	625	1.84	462
0.25	3,580	2,955	0.75	887

TABLE 3.7 SUMMARY OF DEPTH SAMPLES OF SEA WATER

Shot	Station	Sample Time	Distance*	Surface	Total
		H+hours	naut mi	10^3(dis/min)/liter	10^3(dis/min)/cm^2
Flathead	F-2	29.5	32	20	93
Flathead	F-5	49.5	39	32	205
Navajo	N-17	90	—	230	658
Tewa	T-5	41	31	266	1,514
Tewa	T-7	52	54	124	563
Tewa	T-8	59	13	51	412

* Distance from surface zero.

3.4.2 Depth of Mixing. The analyses of samples from various depths are included in Appendix D. The summary of these results (Table 3.7) show beta activity of the surface samples, and the integrated area under the curve for depth versus beta activity of sample. This area is representative of the total activity contained under a square centimeter of ocean surface.

The surface and total activity are plotted in Figure 3.26. This figure indicates an effective depth of mixing of 60 meters for fallout deposited in the sea around Bikini Atoll. A more thorough discussion of the mixing function may be found in Reference 9.

Chapter 4
DISCUSSION

The accuracy of the dose-rate measurements depends on the navigation, instrumentation, and correction factors that refer the aircraft readings to the 3-foot references plane. The isodose plots most closely represent the actual fallout distribution in the region where the flight legs are close together. Less information is available in the far-out areas, because of the greater distances between the legs of the flight patterns. The position of isodose lines are estimated between the measured equal dose-rate points.

4.1 OPERATIONAL PERFORMANCE

The records of the Top Hat aerial survey meters indicate that their calibrations remained stable throughout the surveys. Complete and frequent calibrations were made to insure optimum operation of the equipment. Only one breakdown, an interconnecting cable break on Zuni D-day, occurred during the entire operation.

The failure of the automatic telemetering link between the aircraft and the control center created the requirement for more intensive clerical effort in the data-collection period. Voice transmission of the data provided immediate information for the tactical isodose plot and the flight-control chart, but the aircraft positions and radiation records had to be reviewed during the development of the survey plots.

The airborne radioactivity encountered after Shot Flathead limited the contaminated-area survey. The EOB of the fallout could not be detected after the aircraft became contaminated; however, high-value isodose data were obtained, and a partial plot was developed.

4.2 DATA RELIABILITY

Errors in delineation of areas enclosed by isodose lines depend on variations during the survey and on the estimates of isodose positions between measured points. Navigational accuracy, variations in the individual radiation detectors, and the accuracy of determining the aircraft altitude contribute to the accuracy of the primary measurements.

Determinations of surface dose rate and contamination are dependent on the primary measurements and the accuracy of the theoretical calculations.

4.2.1 Isodose Determinations. Navigation was based on Loran fixes at the end, and at points during each flight leg. Each transit along a flight leg was flown at constant speed and course heading. The aircraft positions are estimated to be within a 3-mile error circle at any time.

The radiation response of the Top Hat detectors was assumed to be represented by the calibration curve (Figure 3.1). Reproducibility of all instruments was within 10 percent for over 87 percent of the calibrations, and no instrument exceeded 25 percent at any time. The change in radiation intensity at the edges of the highly contaminated sections is rapid. A 20-percent error in the reading will not displace the 0.25 to 1 mr/hr isodose contour by over a mile. This is well within navigational accuracy.

The aircraft are assumed to have been within 5 percent of their reported altitude, based on the specified accuracy of the APN-1 radio altimeter. This altimeter indicates the altitude between surface and aircraft directly and is not dependent on atmospheric pressure. Altimeter error does not appear directly in the results, rather the error is modified by the slope of the altitude

correction factor. The altitude error at the 300-foot level has a maximum value of 15 feet based on the APN-1 specification. The altitude correction-factor error will be less than 4 percent.

The absolute value assigned to an isodose depends on the calibration of the radiation detector and altimeter, and on the altitude-correction factor. The major assumption of an average gamma-emission energy of 500 kev in evaluating the altitude absorption derivation is supported by the gamma-spectrometer results (Section 3.1.2), and the ratio of the radiation readings of an energy-dependent detector and the Top Hat detector during a survey over the Eniwetok Atoll (Section 3.2).

Examination of the radiation dose-rate relations between various altitudes over land and water during Operation Redwing (Section 3.2), during previous operations (Appendix C), and during Operation Plumbbob (Reference 12) indicate the validity of the assumptions and the accuracy of the calculated altitude-correction values.

4.2.2 Contamination-Density Determinations. As indicated in Section 1.3.4, fallout on a land surface is expected to produce, at 3 feet from the surface, a gamma dose rate about 1,100 times higher than the dose rate resulting from the same fallout density in the sea. Agreement of data with the theoretical derivation primarily depends on the accuracy of three factors: (1) the depth of vertical mixing, because material below the surface of the sea will not contribute to the gamma field, (2) the average gamma-emission energy, which determines the thickness of the surface layer that does contribute to the gamma field, and (3) the air absorption, which determines the surface area viewed by the radiation detector. The equivalent depth of mixing was estimated as 60 meters (Section 3.4.2). This is in essential agreement with measurements made during Operation Castle.

The experimental work was based on only a few stations and did not necessarily represent the conditions throughout the fallout area. However, variation in mixing will introduce variations in the area enclosed by an isodose contour; this is discussed in Section 4.3.1. The average gamma energy and the altitude absorption characteristics assumptions are supported by several measurements as discussed in Section 4.2.1.

There is one direct comparison of the land and water equivalence based on the fallout following Tewa (Figure 3.23). The isodose pattern encloses Parry Island, Eniwetok Atoll. This island is located between the 25 and 250 mr/hr land-equivalent isodose lines (0.025 and 0.25 mr/hr water isodose). Radsafe measurements indicate a gamma dose rate between 100 and 125 mr/hr on Parry at 24 hours following Shot Tewa.

The contamination density calculations are based on the factors discussed above, and on the relationship between beta and gamma curies. A direct comparison of the conversion between gamma dose rate and beta specific activity is discussed in Appendix D. The measurements are not conclusive. However, the general trend of this data does agree with the theoretical calculations (Section 1.3.1).

4.3 DISTRIBUTION OF CONTAMINATION IN THE SEA

The fallout estimates based on the aerial-survey charts show a definite relation to the fission yield. However, the distribution of this material is not related to the total energy yield, because the conditions of the shot — water, land, or air — affect the fallout. Meteorological conditions also play a major part in determining the area of contamination.

4.3.1 Stability of Contaminated Area. Fallout deposited in the sea is acted upon by the ocean currents, producing a horizontal translation of the location of the material, and a vertical displacement based on the mixing of the material in the sea volume. To obtain a measure of the stability over a period covered by the aerial surveys, measurements were repeated from day to day. All gamma radiation measurements were referred to 3 feet from the surface and to H + 24 hours so that a common comparison could be made for any particular isodose area. The horizontal translation is clearly indicated by the positional shift of the isodose pattern. The vertical mixing is indicated by the amount of area enclosed within the described pattern.

The mixing of radioactive material in the ocean will ease the amount of gamma flux which may be measured in the aircraft. If the survey is made soon after fallout ceases, this mixing will not be complete. On D+1, Shot Tewa, the 0.25 mr/hr contour extended nearly 200 miles west and northwest of Bikini. The survey on D+2 placed the end of this isodose pattern closer to ground zero. The aerial flight surveyed the fallout area approximately 6 hours after the fallout, and mixing was apparently not completely uniform to the thermocline. By the next day some 30 hours had elapsed, much of the material had been removed from the surface, and it is expected that the mixing was more nearly uniform, as represented by the data described in Appendix D.

The area enclosed by a particular contour appears to be stable for a relatively long period of time. The 2.5 mr/hr isodose after Shot Tewa was followed for several days. While the effect

TABLE 4.1 FALLOUT SUMMARY

Shot	Total Yield	Shot Site	Area*	Fission Yield		Fallout		
	Mt		mi²	Mt	mc†	mc‡	pct‡	pct§
Tewa	5.0	Reef	43,500			6,458	24	28
Navajo	[redacted]	Water	10,490			970	36, 58	50
Zuni	3.5	Land	13,400			1,540	46	48
Cherokee	[redacted]	Air	None			None	—	—
Flathead¶	[redacted]	Water	11,000			275	15	29

DELETED

* Area out to 0.1 mr/hr at H+24 hours and 3 feet above surface.

† [redacted]

‡ Based on material located within the surveyed area, Tables 3.3 through 3.6.

§ Based on extrapolated values, Figures 4.1 and 4.2.

¶ Flathead survey limited by aircraft contamination. Results based on estimated position of boundary.

of surface displacement is clearly visible, the enclosed area is approximately the same each day within the limits of measurement error.

The indications are that the survey results, properly related to mixing in the ocean volume, may be used for estimates of fallout density. The oceanographic surveys of Project 2.62 (SIO) provide more detailed study of the mixing function.

4.3.2 Estimates of Total Fallout. The fallout distribution from the aerial-survey estimates are plotted in Figures 4.1 and 4.2. The percentage of the total fission yield is displayed against the particular boundary isodose contour. These curves can then be extrapolated to the zero mr gamma contour and the estimate made of the total amount of fallout in the local area. The conclusions must be applied judiciously, because the estimates are not between measured values, but an extrapolation beyond the survey area.

The estimates are summarized in Table 4.1. The megacurie summaries represent the material within the EOB of the surveys, and the percentage fallout is based on the percentage of the total yield found within the surveyed area and on the values extrapolated in Figures 4.1 and 4.2. Natural radiation background and the residual background from previous shots vary from place to place. Because small fluctuation in the radiation detector readings are an indication of the boundary of the fallout, variations in background will affect the outer boundary estimates (Section 1.3.4). While this does not vary the position of the isodose lines, it does affect the position of the EOB and the estimates contained in the fallout summations.

Of the isotopes produced by neutron activation, two are primarily important in contributing to the gamma activity: Np^{239} and Na^{24}. The Np^{239} contribution to aerial-survey measurements is small, because of the low energy of its gamma photon (Section 1.3.3).

The Na^{24} emits high-energy gamma photons and can increase the gamma dose rate measured by aerial survey appreciably in the period from 5 to 100 hours (Section 1.3.3). Measurable

[redacted]

54

DELETED

DOE ARCHIVES

[redacted]

55

Chapter 5
CONCLUSIONS and RECOMMENDATIONS

5.1 CONCLUSIONS

The gamma radiation field over fallout-contaminated ocean was successfully surveyed by aerial detectors after Shots Zuni, Navajo, and Tewa. No fallout was found in the sea following Shots Cherokee and Mohawk.

Contamination on the aircraft determined the minimum detectable dose rate over the sea. Airborne radioactive material was encountered by the survey aircraft on D+1 day after Shot Flathead. These isodose plots therefore were limited to the relatively hot close-in fallout area.

5.1.1 Altitude Absorption. The field measurements of gamma dose rate at various altitudes over contaminated land and water areas agree with the relationships developed by theoretical calculations.

A 500-kev average gamma-emission energy was assumed, and this is substantiated by the ratio of readings of an energy-dependent detector compared to the readings of an energy-independent detector.

5.1.2 Fallout Distribution. A land-equivalent isodose plot may be inferred from the surveys over the sea. For example, a fallout density of 0.36 megacurie/naut mi^2, on a land surface, will result in 1 r/hr at 3 feet from the surface. The same fallout density in the sea, after mixing, will result in 0.88 mr/hr at 3 feet from the surface (Section 1.3.4). However, the location of the isodose contours must be corrected to the location of the ocean surface at the time of fallout. The repeat surveys on subsequent days after the shot indicate the distortion of the contours, and the direction and magnitude of the ocean currents at the surface. The 0.1 r/hr gamma dose rate at Parry Island 24 hours after Shot Tewa agreed with its location between the 0.025 and 0.25 r/hr land-equivalent isodose contours determined from the aerial survey over the sea.

The land-equivalent conversion is based on uniform mixing of the fallout in the sea to a depth of 60 meters. Samples of sea water from various depths provided the data on which this estimate was based. While only a few stations could be sampled, the reproducibility of the areas enclosed by the isodose contours from aerial surveys on succeeding days indicate that the mixing becomes stabilized for a reasonable number of days after a shot.

5.1.3 Material-Balance Estimates. The conversion from fission-product contamination density to gamma dose rate could not be conclusively validated from the data available. However, estimates were made based on the calculated factors. The measurements show no detectable fallout from the air burst, Shot Cherokee.

The two water-surface shots, Flathead and Navajo, deposited [redacted] percent, respectively, of their fission-product yield as fallout in the local area

Shot Zuni was fired on a land site, and its fallout accounted for [redacted] of its fission-product yield. It is possible that the soil picked up in the fireball provides relatively heavy particles which, on condensation, fall to the surface faster than the products resulting from a water shot.

The fallout from Shot Tewa, fired on a reef site, was approximately 30 percent of the total yield.

5.2 RECOMMENDATIONS

Operationally, D-day aerial surveys provide little information because of the necessity of avoiding active fallout. Even light contamination on an aircraft hinders surveys on later days when the intensity from the sea is reduced by radioactive decay. Unless the aircraft can be decontaminated, aerial surveys should not be made on D-day.

With regard to instrumentation, a linear-scale radiation detector would provide more accurate and more readable recordings over water, where most of the gamma dose rates are slightly above the natural background of the sea and the aircraft. The logarithmic scale is essential for surveys over land, where a wide range of intensities must be measured.

[redacted]

57

Appendix A
DERIVATION of ALTITUDE ABSORPTION of GAMMA RADIATION

Keran O'Brien, Radiation Branch, Health and Safety Laboratory

The equation giving the dose rate above a hole in an infinite half-space that subtends an angle θ^0, when the half-space is uniformly contaminated with a gamma emitter, is described in Reference 10 and is:

$$I_\nu = \frac{E}{2\sigma Y} \Lambda(h, \theta^0) \quad (A.1)$$

Where: E is the gamma energy emitted per cubic centimeter by the contaminant
σ is the density of the absorbing medium
h is the height of the detector, in meters, and
$Y = \frac{\mu_t}{\mu_e}$, the ratio of the total attenuation coefficient to the energy absorption coefficient of the medium, corresponding to the source energy

For Λ:

$$\Lambda(h, \theta^0) = \frac{1}{u}\{tuEi(-tu) + e^{-tu} B(tu)\} \quad (A.2)$$

$t = \mu_t h$, $u = \sec \theta^0$, and B(tu) is a polynomial

The dose rate above a plane, similarly contaminated, can be obtained by the partial derivative of Equation A.1 to obtain an infinitesimal thickness of slab:

$$\frac{\partial I_\nu}{\partial h} dh = I_p \quad (A.3)$$

This is:

$$I_p = \frac{E}{2\sigma Y} \mu_t \, dh \, M(tu) \quad (A.4)$$

$$\text{with } M(tu) = -E_i(-tu) + e^{-tu}[B(tu) - B'(tu) - 1] \quad (A.5)$$

Where: $B' = \frac{dB}{d(tu)}$

The clearing on the surface also subtends on angle θ.

For the case of radiation from water or land contaminated with fission products, seen by an aircraft-mounted detector, a finite diameter of contamination on the surface is described by a half-angle sensitivity, θ.

CASE I. Water contamination from Equation A.1.

$$L(h, \theta) = \Lambda(h, \theta^0) - \Lambda(h, \theta) \quad (A.6)$$

and

$$\frac{E}{2\sigma Y} = \frac{E_0 j}{2\sigma Y} \quad (A.7)$$

where j is the disintegration per second per cubic centimeter and E_0 is the average source energy.

$$I_\nu = \frac{E_0 j}{2\sigma Y} L(h, \theta) \quad (A.8)$$

The constants may be converted to appropriate units to relate contamination density to gamma dose rate by:

$$K = \frac{cq\mu_e (3{,}600)}{W\mu_t} E_0 \quad (A.9)$$

Where: $c = 3.7 \times 10^{10}$ (photons/sec)/m^3
$q = 4.8 \times 10^{-10}$esu
$\mu_e = 3.54 \times 10^{-5} cm^{-1}$ (for water)
$W = 3.25 \times 10^{-5}$ Mev (32.5 ev)
3,600 sec/hr
10^6 cm^3/m^3, and
E_0 is assumed to be 0.5 Mev

Then:

$$I_\nu = \frac{0.3549}{2} C_\nu L(h, \theta^0) R/hr \quad (A.10)$$

where C_ν = curies per cubic meter.

CASE II. Land Contamination:

$$J(h, \theta) = M(h, \theta^0) - M(h, \theta) \quad (A.11)$$

and

$$\frac{\mu_t E dh}{2\sigma Y} = \frac{\mu_e E_0 K}{2\sigma} \quad (A.12)$$

where k represents disintegrations per second per square centimeter.

This reduces Equation A.4 to:

$$I_p = \frac{\mu_e E_0 k}{2\sigma} J(h, \theta^0) \quad (A.13)$$

With the constants converted to appropriate units as in Case I, and 10^4 cm^2/m^2.

$$K = \frac{cq\mu_e (3{,}600)k}{W} E_0 \quad (A.14)$$

$$I_p = 3.4427 \, C_p J(h, \theta^0) R/hr \quad (A.15)$$

where C_p = curies per square meter.

Appendix B
DETAILS of MAJOR INSTRUMENTS

B.1 AERIAL RADIATION DETECTOR, HASL TH-10-B

The Top Hat aerial radiation detector is a scintillation detector utilizing plastic phosphors. The phosphors are coupled to photomultiplier tubes, and the integrated current output is amplified by a dc amplifier. The amplifier has a logarithmic response and covers a 4-decade range of radiation intensity. By switching between two photomultipliers which have different-size phosphors, two ranges of 4-decades each are achieved: Range A, 0.01 to 100 mr/hr, and Range B, 10 mr/hr to 100 r/hr.

The A phosphor is 3 inches in diameter and 3 inches high, and the B phosphor is $1\frac{1}{8}$ inches in diameter and $\frac{3}{8}$ inch high. The output of each range varies from 0 to 1 ma and drives a strip-chart recorder, Esterline Angus Co., AW. The radiation calibration of a typical unit is shown in Figure B.1. Both phosphors are collimated by an annular lead shield, which was added to reduce the effect of aircraft contamination.

For a more detailed description of the instrument, see Reference 11.

B.2 ALTITUDE COMPENSATOR

The surface radiation reading, R_3 is related to the aircraft reading, $R_{a/c}$, by a constant, f_a, which depends on the height above the surface. Thus, $R_3 = R_{a/c} \times f_a$. However, the circuit current is related to the logarithm of $R_{a/c}$, and the altitude, h, is proportional to the logarithm of f_a. The indicated multiplication can be performed by the addition of the logarithms:

$$R_3 = I_{a/c} + kh \quad (200 < h < 1{,}000)$$

Where: I is a current measured in milliamperes
k is a circuit constant

The altitude-compenstion circuit electrically adds an altitude signal, derived from the aircraft radio altimeter, APN-1, to the output of the detector circuit. The aircraft radiation reading is continuously modified for changes in flight altitude, and the surface readings remain proportional to the gamma intensity at 3 feet above the surface.

B.3 TELEMETER, HASL TT-3-X

The telemeter is connected in series with the strip-chart recorder and converts its drive current, 0 to 1 ma direct current, to an alternating-current wave form suitable for transmission through audio circuits. The output of the telemeter is a 1,000-cps tone, gated on and off within a 1-second cycle. The ratio of on to off time within the 1-second time interval is proportional to the input dc signal. These bursts of 1,000 cps may be coupled directly into the microphone input of a radio transmitter or stored on an audio tape recorder.

A high-fidelity transmitter, U.S. Navy ART-13, was used in the P2V-5 aircraft. It has an output power rating of 100 watts. Continuous operation is not possible because of heat dissipation limitations. Also, the transmitted signal blocks the receivers in the aircraft. Therefore, the telemeter output, the gated 1,000-cps tone, is recorded on a tape recorder running at $3\frac{3}{4}$-in/sec. The tape is then manually shifted to a playback recorder, which runs at 30-in/sec. The recording reel, containing up to 30 minutes of data, is played back through the radio transmitter in less than 4 minutes.

An electronically regulated power supply, HASL TB-6-A, supplies all the voltages to the telemeter and the detector control assembly. The regulators compensate for the varying 28-volt input power from the aircraft generators.

The telemeter central station is connected to the earphone output jack of a receiver, which is tuned to the transmitter frequency. The input to the central station has a noise filter, designed to reject 54 decibels of radio noise above the signal level. This is followed by a conventional ratemeter which converts the bursts of 1,000-cps tone to a deflection of the pen on a strip-chart recorder.

B.4 AUTOMATIC GAMMA MONITOR, HASL TN-4-C

The automatic gamma monitor is based on a detector similar to the Top Hat aerial radiation detector. A plastic phosphor is optically coupled to a photomultiplier, whose output is converted in a dc amplifier to a logarithmic response. The unit reproduces a radiation range from 1 mr/hr to 10 r/hr on a single scale. The output is continuously recorded on an Esterline Angus strip-chart recorder. The monitor operates on 115-volt, 60-cps current and is completely sealed in an immersionproof case.

B.5 SCINTAMETER SURVEY METERS

The scintameters are portable survey meters that are powered by dry batteries and are completely self-contained.

[redacted]

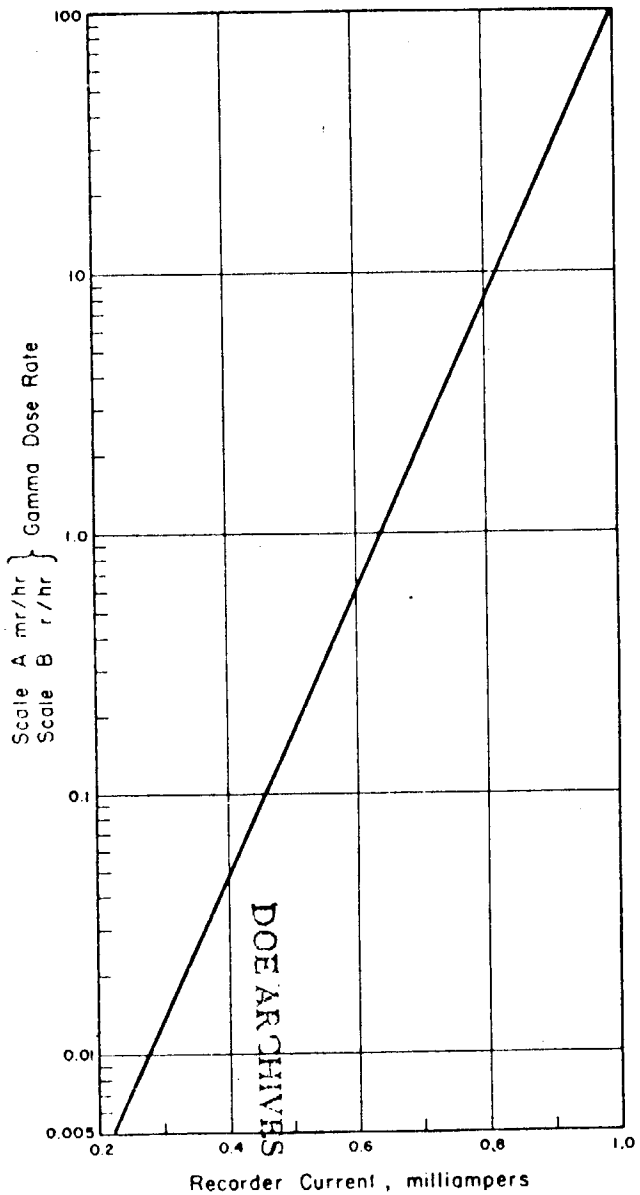

Figure B.1 Radium gamma-radiation calibration, Top Hat detector, HASL TH-10-A.

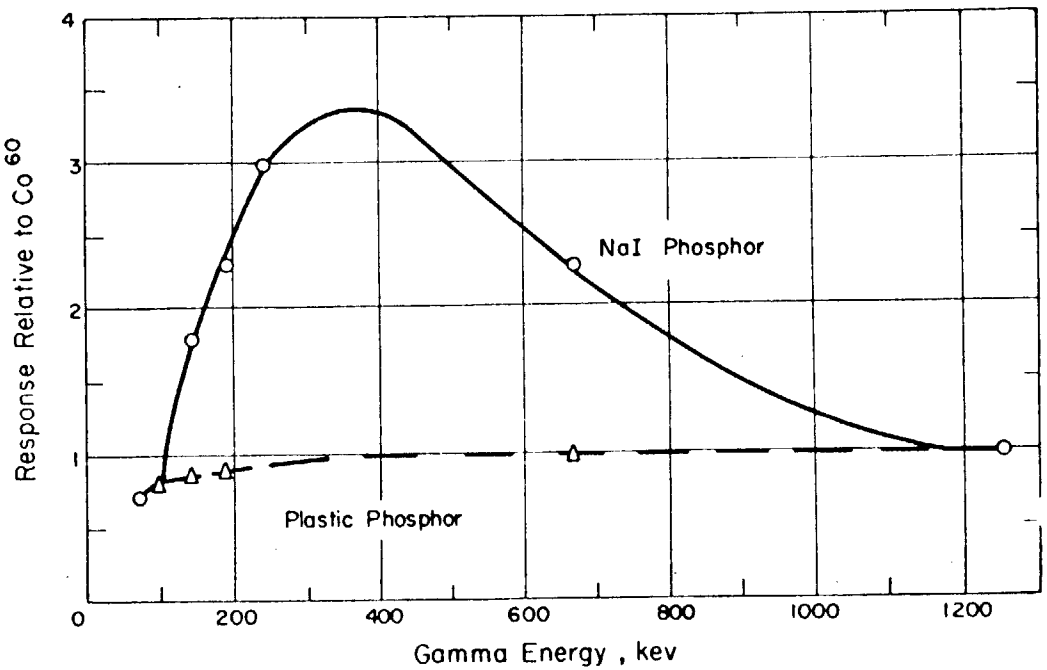

Figure B.2 Energy dependence of dose-rate response, plastic and sodium iodide detectors.

The TH-7-A uses the same phosphor and circuit as the Top Hat radiation detector meter and has a nearly air-equivalent energy response. The unit has a logarithmic scale, calibrated from 1 mr/hr to 10 r/hr.

The standard high-sensitivity scintameter, TH-3-B uses a sodium iodide detector that has an energy-dependent dose-rate response (Figure B.2). It has a logarithmic scale, calibrated from 0.01 to 100 mr/hr.

B.6 GAMMA SPECTROMETER, HASL TM-10-A

The gamma spectrometer is a single-channel, automatic-sweep pulse-height analyzer. Its detector is a crystal of sodium iodide, thallium iodide activated, 4 inches in diameter and 4 inches high. The circuits are designed to handle high pulse rates, and the rate-meter section is calibrated in seven ranges from 100 to 100,000 counts/sec. The base line may be selected as 3, 1.5, or 0.75 Mev full scale and swept automatically from 1 minute to 4 hours for the full-energy scan. Data is displayed on a Mosely Autograf 2, X-Y recorder.

The unit operates on 115-volt, 60-cps current. For helicopter use, external inverters must be supplied to invert the 28-volt current of the aircraft.

Appendix C
ALTITUDE ABSORPTION MEASUREMENTS DURING PREVIOUS OPERATIONS

Aerial dose-rate measurements above contaminated areas have been abstracted from records of previous weapon tests. These data include surveys over land contaminated with old and with fresh fission products, and surveys over water containing fresh fission products.

Table C.1 contains data collected over land contaminated with old fission products, at the Nevada Test Site, between operations and prior to Operation Castle. During Operations Teapot and Plumbbob, careful measurements were made 3 feet from the surface, in conjunction with simultaneous aerial measurements. Data abstracted from these surveys (Reference 12) are included in Table C.2.

Fresh fission products in water volume were examined during Operation Wigwam (Reference 4), and the altitude absorption measurements are contained in Table C.3.

All data have been normalized to the theoretical curve, except the Plumbbob gamma dose rates that have been related to the surface measurement. Figures C.1 and C.2 are altitude plots for land and water, respectively. The agreement with the calculated attenuation curve is within the limits of error imposed by altitude measurement and instrument calibration. A single surface reading, i.e., 3-foot dose rate over land, usually deviates markedly from the value predicted from the readings at higher altitudes. This is a function of the nonhomogeneous contamination on the small areas viewed close to the surface and the unevenness of the surface. The NTS (Table C.1, No. 1) and Plumbbob (Table C.2, Nos. 2 and 3) data are based on careful surface measurements, made by survey over an extended area and averaged; and the 3-foot value agrees with the predicted values. Measurements over water are difficult to obtain, because a ship will distort the radiation field. Data below 50 feet from sea surface are not available.

TABLE C.1 ALTITUDE ABSORPTION MEASUREMENTS OVER LAND, OLD FISSION PRODUCTS

Altitude	Absorption of Radiation				
	1*	2†		3‡	
ft	pct	mr/hr	pct	mr/hr	pct
3	100	4.3	57,128	4.3	50
50	—	—	—	2.0	40
100	—	—	—	1.8	36
200	25	0.79	22	1.0	22
400	—	0.56	13.5	0.75	15.5
500	10	0.40	11	0.38	8.2
800	—	0.11	4	—	—

* NTS, 1951, old shot site, scintilog TH-2, normalized from a series of ground and aircraft readings.

† Janet Island, Eniwetok Atoll, prior to Operation Castle, scintameter TH-3, P2V aircraft.

‡ Janet Island, Eniwetok Atoll, prior to Operation Castle, scintameter TH-3, helicopter.

TABLE C.2 ALTITUDE ABSORPTION MEASUREMENTS OVER LAND, FRESH FISSION PRODUCTS

All measurements made with Top Hat detector TH-10-A.

Altitude	Absorption of Radiation					
	1*		2†		3‡	
ft	mr/hr	pct	mr/hr	pct	mr/hr	pct
3	10	70§	250	100	100	100
50	6.3	49	—	—	—	—
100	4.8	34	—	—	—	—
150	4.3	30	—	—	—	—
200	3.3	23	—	—	—	—
250	2.75	19	—	—	—	—
300	2.35	17	31.7	12.7	15.9	16
350	1.85	13	—	—	—	—
400	1.7	12	—	—	—	—
450	1.52	11	—	—	—	—
500	1.7	12	21	8.4	8.6	8.6
550	1.3	9.2	—	—	—	—
600	1.0	6.2	—	—	—	—
700	—	—	13	5.2	4.8	4.8
800	0.76	5.7	—	—	—	—
900	—	—	6.9	2.8	2.7	2.7

* Operation Teapot, 1955, NTS, Shot Turk.
† Operation Plumbbob, 1957, NTS.
‡ Operation Plumbbob, 1957, NTS.
§ 10 mr/hr, based on single surface reading at 3 feet.

TABLE C.3 ALTITUDE ABSORPTION MEASUREMENTS OVER WATER, FRESH FISSION PRODUCTS

Altitude	Absorption of Radiation			
	1*		2†	
ft	mr/hr	pct	mr/hr	pct
50	83	83	—	—
100	72	72	—	—
200	60	60	17	52
300	40	40	—	—
400	35	35	15	32
600	20	20	10	18
800	10	10	6.1	10
1,000	5	5	—	—

* Operation Wigwam, 1955, scintameter TH-3, helicopter.
† Operation Wigwam, 1955, Top Hat detector TH-10-A, AD-5N aircraft.

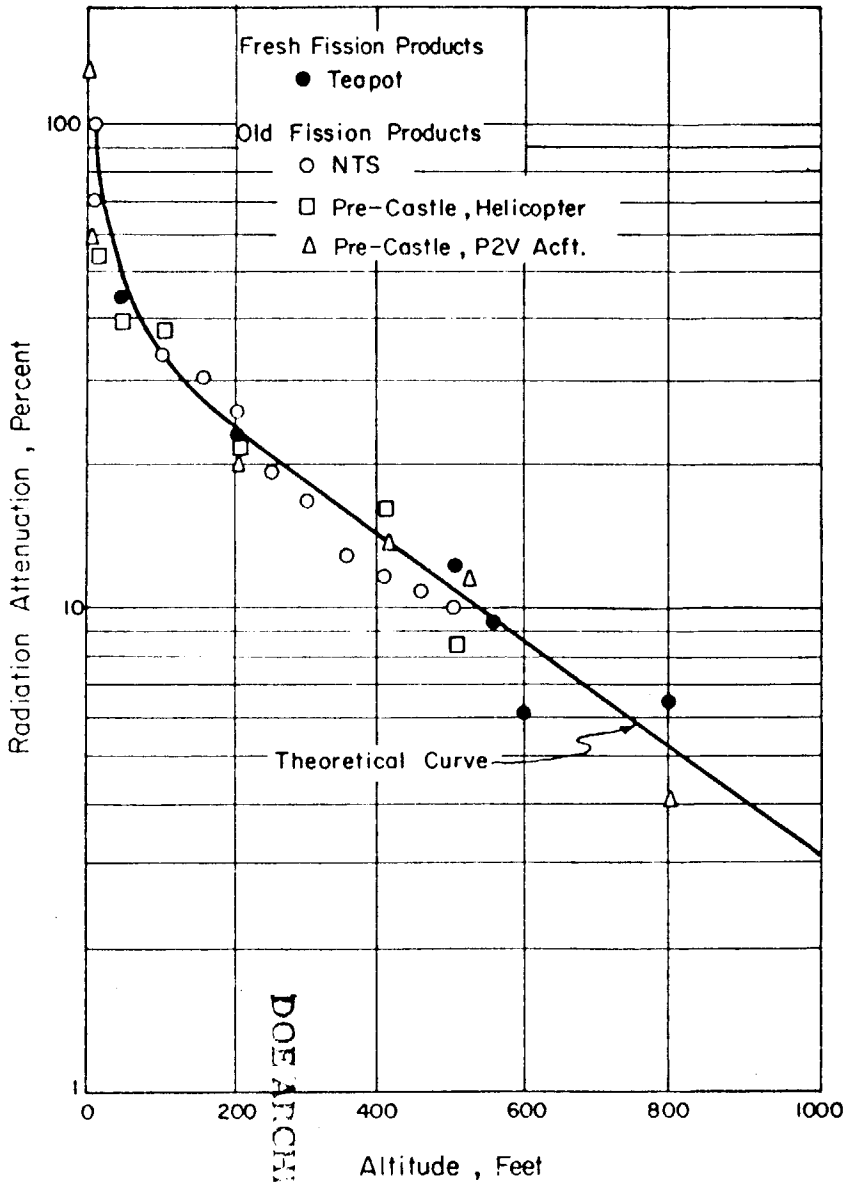

Figure C.1 Radiation attenuation over land.

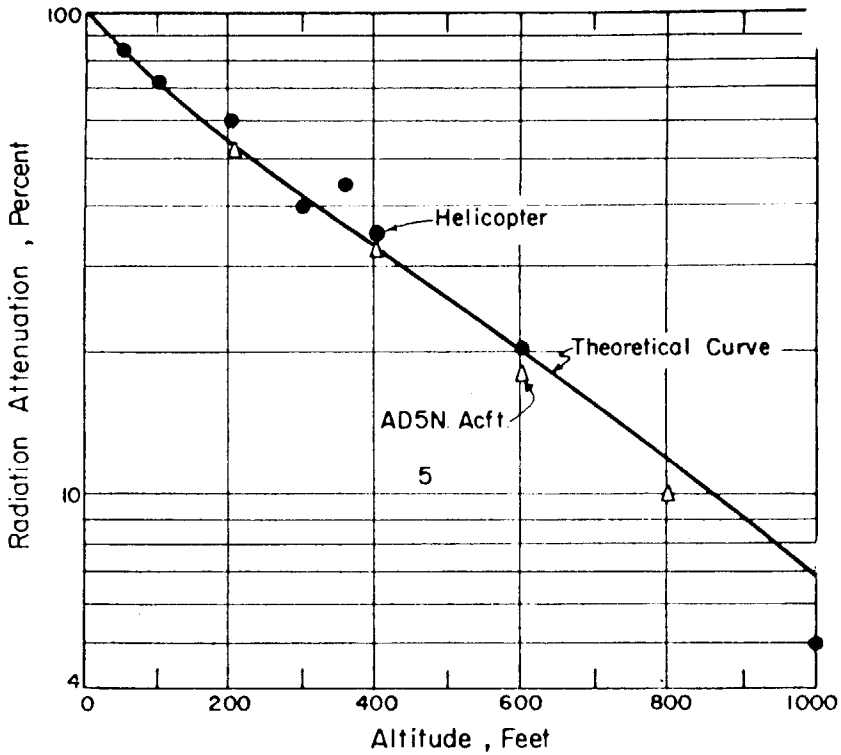

Figure C.2 Radiation attenuation over water.

Appendix D
ANALYTICAL DATA from SAMPLES of SEAWATER

Duplicate samples of sea water were furnished by the NRDL and the SIO. At the HASL, each sample was filtered and the remainder evaporated. The beta activities for both particulate and salt fractions were determined by counting. These data were corrected for radioactive decay on the basis of the decay curves in Reference 7.

D.1 SURFACE SAMPLES

The beta analysis, corrected to H + 24 hours, is summarized in Tables D.1, D.2, D.3, and D.4, for Shots Zuni, Flathead, Navajo, and Tewa. The sampling locations were plotted on the aerial-survey isodose charts and the gamma intensity at each station was estimated by extrapolation between the isodose contours. Because the gamma dose-rate values are estimated, further extrapolation may contain errors. The time of gamma survey and the time of sampling do not necessarily coincide, so the interviewing horizontal translation of the water mass can introduce displacement errors.

The surface activity, as beta disintegration per minute per liter, has been plotted against estimated gamma dose rate in Figure D.1. With the large variation of the observed data, it is not possible to confirm the calculated value of 4.43×10^6 (dis/min)/liter for 1 mr/hr gamma at 3 feet. However, the results do indicate that the general magnitude of this assumption is correct.

D.2 DEPTH SAMPLES

Particulate salt separation and beta analysis were performed on a group of depth samples supplied by Project 2.62 (SIO). The count-time corrections for radioactive decay were made to the mean of the counting period for all samples within a group. The data from Shots Flathead and Navajo are summarized in Table D.5, and from Shot Tewa in Table D.6.

These values are plotted in Figures D.2 and D.3. Activities below 10 dis/min are not particularly valid, because they correspond to counting rates below the statistically reliable level. The surface activity for samples from Shots Flathead and Tewa are based on the average of several identical samples. The surface activity for Station N-17, after Shot Navajo, is based on a single sample and may not represent the actual surface conditions. A mixing depth of 60 meters is indicated by this data (Figure 3.26).

[redacted]

TABLE D.1 ANALYSIS OF SEA WATER SAMPLES, SHOT ZUNI

Station				Beta							Gamma	
				Particulate			Salt			Total	Intensity	Chart
Number	Latitude	Longitude	Time	10^3	Time	10^6	10^3	Time	10^6	10^6		
				(dis/min)/liter	hr	(dis/min)/liter at 24 hrs	(dis/min)/liter	hr	(dis/min)/liter at 24 hrs	(dis/min)/liter at 24 hrs	mr/hr at 24 hrs	day
Y4-1	12-25	165-26	5/28-2200	20	161	0.19	264	272	3.96	4.15	1.0	D + 1
Y4-2	12-22	165-27	5/28-2300	46	162	0.43	604	272	9.06	9.49	1.0	
Z-1	12-06.5	165-39	5/28-1430	1	161	0.01	ND*				0.5	
Z-2				ND*			ND*					
Z-3	12-19	165-17	5/29-0100	69	456	1.75	137	308	2.47	4.22	1.5	
Z-4	13-00	165-12	5/29-0800	57	163	0.54	36	274	0.54	1.08	0.05	
Z-5	13-00	165-12	5/29-1430	49	162	0.46	ND*				0.05	
Z-6	13-04	165-12.5	5/29-1900	2	161	0.02	6	308	0.11	0.13	0.05	
Z-7	13-04.7	165-12.5	5/29-2345	31	163	0.29	4	308	0.07	0.36	0.05	
Zu-1	11-27	165-08.2	5/28-1300	0.7	209	0.01	ND*				0.025	
Zu-2	11-45.1	165-08.2	5/28-1650	5	210	0.05	9	309	0.16	0.21	0.2	
Zu-3	12-10	165-27.8	5/28-1950	43	210	0.43	52	309	0.94	1.37	1.0	
Zu-4	12-13.8	165-53	5/29-0015	5	210	0.05	133	309	2.39	2.44	0.12	
Zu-5	12-46.1	166-01.3	5/29-1310	41	210	0.41	8	309	0.14	0.55	0.12	
1-Z	11-40.3	165-35.2	5/28-1250	0.06	220	0.001	1.3	309	0.03	0.03	0.5	
2-Z,3-Z	11-59	165-04	5/28-1720	39	234	0.41	72	310	1.30	1.71	1.5	
Z-8	13-06	165-04.5	5/30-1100	2	161	0.02	2	309	0.04	0.06	0.08	D + 2
Z-9	13-06.4	165-02	5/30-1450	2	161	0.02	3	309	0.05	0.07	0.08	
Z-10	13-08.5	164-59	5/30-2200	4	165	0.04	4	309	0.07	0.11	0.08	
Zu-6	13-37	163-40.2	5/30-0725	6	210		ND*				Low	
6-Z	13-46	164-33	5/30-1430	15	235		15	381			Low	
7-Z	13-47	163-47	5/30-1900	ND*			ND*				Low	
Z-11	13-09	164-58.5	5/31-0200	21.5	165	0.19	3.8	309	0.07	0.26	0.15	D + 3
Z-12	13-11.5	164-55	5/31-0815	3.1	165	0.03	ND*				0.15	
Z-13	13-11.5	164-55	5/31-1000	1.9	200	0.02	3.9	309	0.07	0.09	0.15	
Z-14	13-12.5	164-56	5/31-1415	1.3	200	0.01	ND*				0.15	
Z-15	13-13	164-52	5/31-1830	4.1	209	0.04	4.8	309	0.09	0.13	0.15	
Zu-7	12-52.7	165-45.2	5/31-0100	5.3	210	0.05	14	378	0.31	0.36	0.50	
Zu-8	12-37.8	165-49.5	5/31-0300	20	211	0.20	24	309	0.43	0.63	0.25	
Zu-9	12-43.9	165-30.2	5/31-0610	24	211	0.25	9	309	0.20	0.45	0.75	
Zu-10	12-33	165-09.4	5/31-0830	36	211	0.39	15	375	0.27	0.64	3	
Zu-11	12-33	164-40	5/31-1110	13	211	0.13	21	310	0.46	0.59	0.6	
Zu-12	12-20	164-59.3	5/31-1320	60	212	0.61	130	374	2.86	3.47	4	
Zu-13	12-10.3	164-50.8	5/31-1435	4.1	212	0.04	2.5	379	0.06	0.10	0.30	
Zu-14	12-39.7	163-38	5/31-2045	1.8	210	0.02	ND*				0.15	
8-Z	12-44	165-59	6/1-0015	17.8	235	0.18	29	382	0.64	0.82	0.25	
9-Z	12-33	165-57	6/1-0130	11.5	235	0.12	30	382	0.66	0.78	0.2	

* No data.

TABLE D.2 ANALYSIS OF SEA WATER SAMPLES, SHOT FLATHEAD

Station				Beta							Gamma	
				Particulate			Salt			Total	Intensity	Chart
Number	Latitude	Longitude	Time	10^3	Time	10^6	10^3	Time	10^6	10^6		
				(dis/min)/liter	hr	(dis/min)/liter at 24 hrs	(dis/min)/liter	hr	(dis/min)/liter at 24 hrs	(dis/min)/liter at 24 hrs	mr/hr at 24 hrs	day
F-1	11-30	165-11.3	6/12-2400	9.7	369	0.20	21.7	370	0.46	0.51	0.03	D+1
F-2	12-10	165-31.3	6/13-1200	14.8	185	0.15	7.8	190	0.08	0.19	0.04	
F-2				6.4	185	0.07	13.3	190	0.13			
F-2				21.6	185	0.19	11	186	0.11			
F-2				4.7	185	0.05	7.8	188	0.08			
F-3	12-10.2	165-31	6/13-2300	148	185	1.50	55	187	0.56	0.32	0.04	
F-3				9	185	0.09	23	188	0.23			
F-3				8.1	185	0.08	18	188	0.18			
M-1	11-30.5	164-53.8	6/12-1730	ND*							0.15	
M-2	12-30	165-14.2	6/13-1220	ND*							0.07	
M-3	12-44	165-31.2	6/13-1700	ND*							0.05	
S-1	11-36	165-11	6/12-2310	9.9	368	0.21	11	368	0.23	0.43	0.15	
S-1				3.7	368	0.08	16	368	0.34			
S-2	11-52	165-23	6/13-0130	23.7	369	0.5	49	369	1.03	1.53	0.15	
S-3	11-52	165-19	6/13-1400	ND*							0.23	
S-4	11-51	165-20	6/13-1700	ND*							0.2	
S-5	11-53	164-56	6/13-1930	ND*							0.05	
Y3-1	12-04	165-26	6/12-2015	22.5	91	0.12	132	91	0.69	0.81	0.22	
Y3-2	12-08	165-28	6/13-0115	25	93	0.14	222	93	1.24	1.38	0.18	
Y4-2	12-45	166-01	6/13-0730	25	92	0.14	157	93	0.88	1.02	0.03	
Y4-3	12-41	166-05	6/13-0919	49	91	0.26	222	92	1.20	1.46	0.025	

* No data.

TABLE D.3 ANALYSIS OF SEA WATER SAMPLES, SHOT NAVAJO

Station				Beta							Gamma	
				Particulate			Salt			Total	Intensity	Chart
Number	Latitude	Longitude	Time	10^3	Time	10^6	10^3	Time	10^6	10^6		
				(dis/min)/liter	hr	(dis/min)/liter at 24 hrs	(dis/min)/liter	hr	(dis/min)/liter at 24 hrs	(dis/min)/liter at 24 hrs	mr/hr at 24 hrs	day
Y3-1	12-10	165-19	7/11-1615	218	82	1.03	1,125	82	5.29	6.32	0.125	D+1
Y3-2	11-59.5	165-15.5	7/11-2330	585	78	2.46	506	78	2.13	4.59	0.8	
Y3-3	11-59.5	165-15.5	7/12-0005	498	79	2.14	383	79	1.65	3.79	0.8	
Y3-4	11-58	165-15	7/12-1421	506	83	2.43	383	83	1.84	4.27	0.8	
Y3-5	11-56	165-15.5	7/12-1750	487	80	2.19	298	80	1.34	3.53	0.8	
Y3-6	12-00	165-15	7/12-2150	328	81	1.51	259	81	1.19	2.70	0.8	
N-1	11-21.3	165-14	7/11-1341								Low	
N-2	11-34.5	165-09	7/11-1920								0.025	
N-3	11-47.2	165-07.3	7/11-2130	102	203	1.04	213	203	2.17	3.21	1.0	
N-4	11-57	165-17.5	7/12-0030								0.5	
N-5	11-58.5	165-13	7/12-0315								0.3	
N-6	11-58.3	165-12.3	7/12-0800								0.3	
N-7	11-59	165-08	7/12-1330	18.4	203	0.19	45.3	203	0.46	0.65	0.15	
N-8	11-59.5	165-09	7/12-1700								0.15	
M-1	11-38.5	164-53.4	7/11-2000	92	206	0.94	94	206	0.96	1.90	0.8	
M-2	11-38	164-43.6	7/11-2130	77	206	0.79	123	206	1.25	2.04	0.6	
M-3	11-37.5	164-37.5	7/12-0018	105	206	1.07	81	206	0.33	1.90	0.8	
M-4	12-03	163-18.2	7/12-1830								0.01	
N-9	11-44.8	165-16.2	7/13-000								0.5	
N-10	11-50	165-14.4	7/13-0810								1.0	
N-11	11-46.5	165-14	7/13-1035	32	196	0.32	84	196	0.85	1.17	1.5	
N-12	11-43.2	165-17.2	7/13-1330								1.0	
N-13	11-34.0	165-11	7/13-2110	46	204	0.47	90	204	0.92	1.39	0.25	
M-5	12-44.3	162-40	7/13-0100								0.03	
M-6	12-23.1	164-41.4	7/13-0900								0.1	

TABLE D.4 ANALYSIS OF SEA WATER SAMPLES, SHOT TEWA

Station				Beta							Gamma	
				Particulate			Salt			Total	Intensity	Chart
Number	Latitude	Longitude	Time, Mike	10^3	Time	10^6	10^3	Time	10^6	10^6		
				(dis/min)/liter	hr	(dis/min)/liter at 24 hrs	(dis/min)/liter	hr	(dis/min)/liter at 24 hrs	(dis/min)/liter at 24 hrs	mr/hr at 24 hrs	day
Y3-2	12-03	165-16	7/21-2200	160	264	2.4	444	816	20.9	23.3	4.0	D + 1
Y3-3	12-04	165-15	7/22-0215	110	264	1.65	502	816	23.6	25.2	4.5	
Y3-4	12-04	165-13.5	7/22-1310	238	264	3.57	402	816	18.9	22.5	5.0	
Y3-5	12-09	165-07	7/22-1845	430	264	6.45	416	816	19.6	26.0	5.0	
Y3-6	12-12	165-10.5	7/22-2054	72	264	1.08	740	624	26.6	27.7	4.0	
T-1	11-53.6	165-26.2	7/22-0100	42	456	1.09	158	622	5.7	6.4	1	
				16	473	0.43	153	622	5.5			
T-2	12-06.9	165-13.2	7/22-0330	247	334	4.69	319	838	15.6	23.8	4	
				52	334	0.99	771	598	26.2			
T-3	12-06.9	165-13.2	7/22-0900	157	334	2.98	782	742	33.6	36.0	4	
				177	334	3.36	746	742	32.1			
T-4	12-06.6	165-12	7/22-1245	197	334	3.74	411	838	20.1	22.9	4.5	
				173	334	3.29	381	838	18.7			
T-5	12-11	165-10.5	7/22-2255	123	334	2.34	531	790	24.4	30.6	4.0	
				95	334	1.81	925	622	33.3			
				154	334	2.93	484	790	22.3			
				135	334	2.57	987	574	32.6			
M-1	11-31.5	165-06.2	7/21-1930	9	264	0.14	16	816	0.8	0.9	0.2	
M-2	11-35.7	164-40.0	7/22-0015	98	264	1.47	ND*				0.5	
M-3	11-36.0	164-07.2	7/22-0647	123	264	1.85	54	816	2.5	4.4	1.25	
M-4	11-43.7	163-05.7	7/22-1510	2.8	264	0.04	5.8	744	0.25	0.3	0.12	
M-5	11-51.4	163-43.6	7/22-2000	13	264	0.20	22	816	1.03	1.2	0.5	
T-6	12-13.2	165-08.7	7/23-0410	182	334	3.46	560	742	24.1	29.4	2.5	D + 2
				270	334	5.13	608	742	26.1			
T-7	12-30.5	164-57.1	7/23-0940	20	334	0.38	263	622	9.5	10.1	1.25	
				44	334	0.84	314	622	11.3			
				39	334	0.74	215	646	7.95			
				34	334	0.65	254	622	9.1			
T-8	11-53.2	165-15	7/23-1645	4.1	358	0.08	121	478	3.4	3.6	5.0	
				10.5	358	0.32	133	478	3.7			
				14.1	358	0.28	110	478	3.1			
M-6	11-57	164-32.8	7/23-0005	250	264	3.75	190	816	8.9	12.7	2.8	
M-7	12-02.5	165-13.8	7/23-0325	44	264	0.66	ND*					
M-8	11-24.2	165-24	7/23-0910	3.2	264	0.045	7	744	0.3	0.35	2.5	
M-9	13-08.7	164-51.2	7/23-2027	15.3	264	0.225	9.6	744	0.4	0.64	0.03	

* No data.

TABLE D.5 ANALYSIS OF DEPTH SAMPLES OF SEA WATER, SHOTS FLATHEAD AND NAVAJO

Count time corrected to 200 hours.

Station	Latitude	Longitude	Depth	Particulate	Salt	Total
	N	E	m	10^3 (dis/min)/liter	10^3 (dis/min)/liter	10^3 (dis/min)/liter
F-2	12-10	165-31.3	0	13	7.6	21
			0	5.8	13	19
			0	18.5	10	29
			0	4.1	7.5	12
			Aver			20
			25	0.7	7	8
			50	3.0	4.4	7
			75	3.0	15	18
			90	0	0	0
			105	0	0	0
			125	0	7.3	7
			150	0	0	0
			250	0	6	6
			300	0	3	3
			500	0	0	0
F-5	12-07	164-52.3	0	5.3	22.5	28
			11	11.5	24	35
			Aver			32
			25	3.8	20	24
			50	4.2	19	23
			75	4.0	15	19
			91	0.3	1.2	1.5
			106	0	0	0
			126	0	0	0
			151	0.1	1.2	1
			251	0.1	2.2	2
			351	0.1	5.0	5
			501	0	0	0
N-17	11-46.2	165-15.6	0	45	185	230
			10	22.2	101	123
			20	2.6	15.4	18
			30	1.1	8.8	10
			40	8.6	50	59
			50	33.5	110	144
			60	18.6	120	139
			70	11	30	41
			80	0.6	2	2.6
			90	0.4	7	7.4
			100	0.4	2	2.4

TABLE D.6 ANALYSIS OF DEPTH SAMPLES OF SEA WATER, SHOT TEWA

Count time corrected to 1,000 hours.

Station	Latitude	Longitude	Depth	Particulate	Salt	Total
	N	E	m	10^3 dis/min/liter	10^3 dis/min/liter	10^3 dis/min/liter
T-5	12-11	165-10.5	0	42.0	170	212
			0	25.0	240	265
			0	40.0	240	280
			0	36.6	270	306
			AV	35.8	230	266
			8	15.0	250	265
			16	24.0	250	275
			24	15.0	250	265
			32	24.0	250	274
			39	2.5	250	253
			51	18.0	195	213
			63	10.0	58	68
			79	1.3	12	13
			118	2.6	2.5	5.1
			158	2.5	3	5.5
T-7	12-30.5	164.57.1	0	7.5	110	118
			0	5.7	125	131
			0	3.7	125	129
			0	7.1	110	117
			AV	6.0	117.5	124
			10	15.1	130	145
			20	7.9	128	136
			30	2.5	130	133
			40	1.6	52.5	54
			50	0.1	5.1	5.2
			60	0.04	3.5	3.5
			70	0.02	1.1	1.1
			80	0.07	2.0	2.1
			90	0.13	2.0	2.1
			100	7.0	2.4	9.4
T-8	11-53.2	165-15	0	1.0	47	48
			0	2.0	58	60
			0	3.6	46	50
			0	3.3	44	47
			AV	2.5	49	51
			10	1.7	33	35
			25	0.2	30	30
			40	4.7	67	72
			45	5.4	56	61
			50	15	105	120
			55	10.2	23.7	34
			60	12.6	113	131
			70	5.7	16.5	22
			85	7.0	13.5	21
			100	3.0	9.7	13

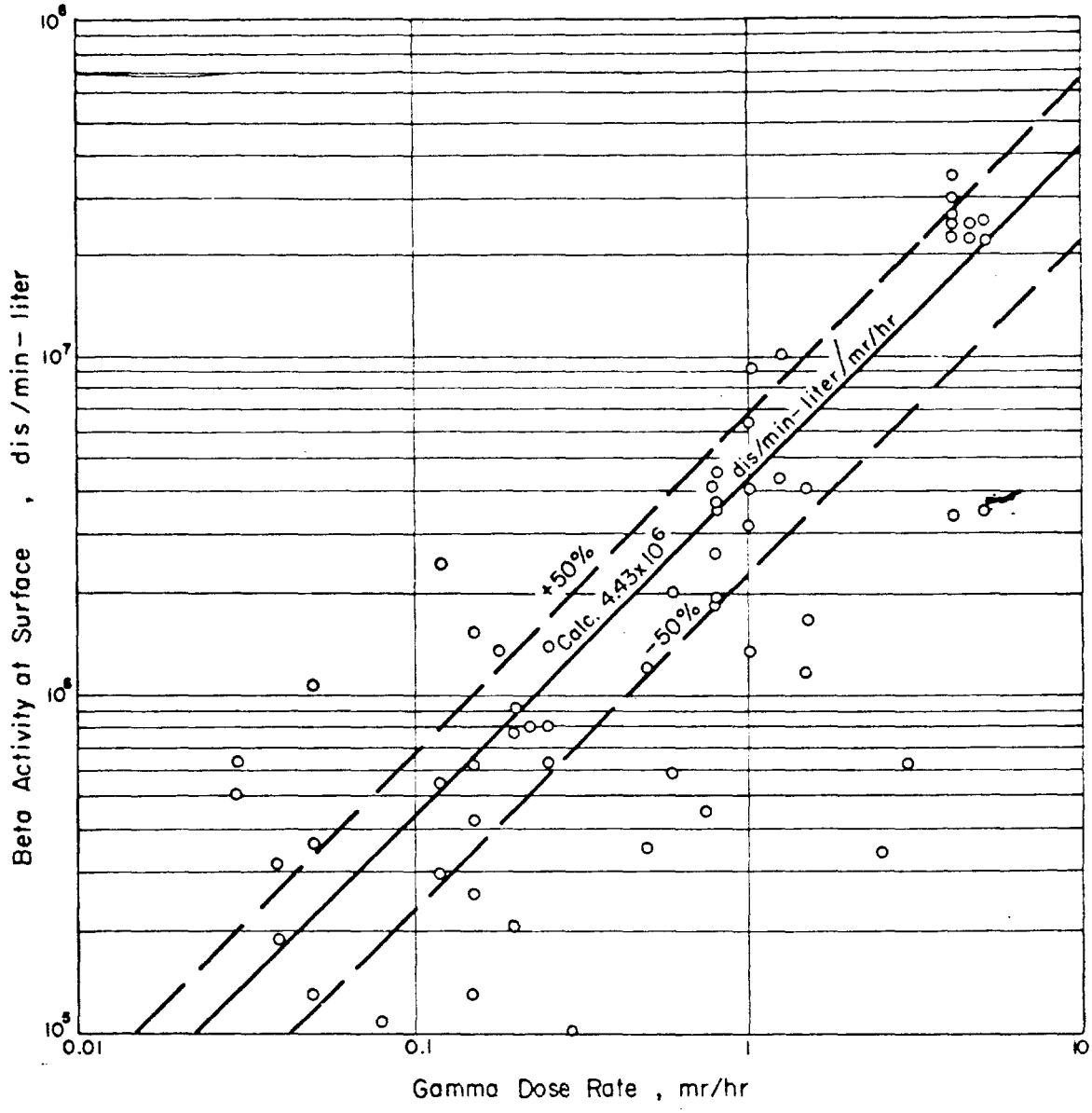

Figure D.1 Gamma dose rate at 3 feet related to surface beta activity.

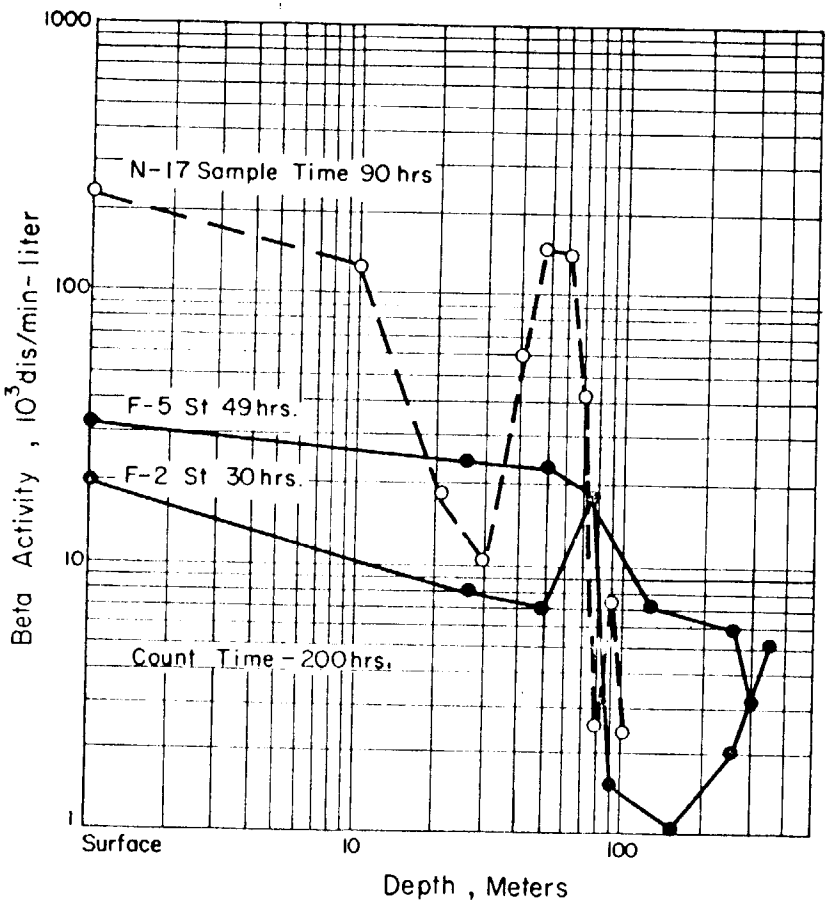

Figure D.2 Depth of mixing from sea water samples, Shots Flathead and Navajo.

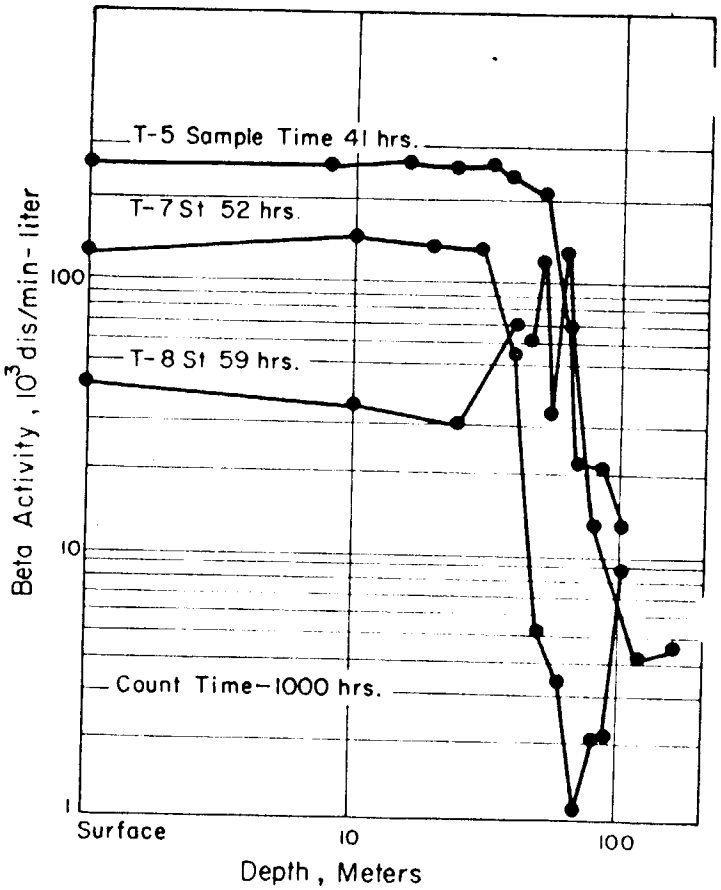

Figure D.3 Depth of mixing from sea water samples, Shot Tewa.

REFERENCES

1. Merril Eisenbud and others; "Radioactive Debris from Operation Ivy"; NYO-4522, April 1953; Health and Safety Laboratory, U.S. Atomic Energy Commission, New York Operations Office; Secret Restricted Data.

2. A. Breslin and M.E. Cassidy; "Radioactive Debris from Operation Castle, Islands of the Mid-Pacific"; NYO-4623, January 1955; Health and Safety Laboratory, U.S. Atomic Energy Commission, New York Operations Office; Secret Restricted Data.

3. H.D. LeVine and R.T. Graveson; "Radioactive Debris from Operation Castle—Aerial Surveys Following Yankee-Nectar; NYO-4613; Health and Safety Laboratory, U.S. Atomic Energy Commission, New York Operations Office; Secret Restricted Data.

4. R.T. Graveson, M.E. Cassidy and S. Watnick; "Aerial Survey Techniques, Operation Wigwam"; Internal Report; Health and Safety Laboratory, U.S. Atomic Energy Commission, New York Operations Office; Secret Restricted Data.

5. J. Harley and N. Hallden; "Method of Calculating Infinite Gamma Dose from Beta Measurements on Gummed Film"; Laboratory Report 56-2; Health and Safety Laboratory, U.S. Atomic Energy Commission, New York Operations Office; Unclassified.

6. "Capabilities of Atomic Weapons"; Department of the Army Technical Manual TM 23-200, Department of the Navy OPNAV Instruction 03400.1B, Department of the Air Force AFL 136-1, Marine Corps Publications NAVMC 1104 Rev; Revised Edition November 1957; Prepared by Armed Forces Special Weapons Project, Washington, D.C.; Confidential.

7. H.F. Hunter and N.E. Ballou; "Simultaneous Slow Neutron Fission of U^{235} Atoms. I. Individual and Total Rates of Decay of the Fission Products"; ADC-65, April 1949; U.S. Naval Radiological Laboratory, San Francisco, California; Unclassified.

8. Radiological Health Handbook, Page 250, October 1955; U.S. Department of Health, Education, and Welfare; Cincinatti, Ohio; Unclassified.

9. Feenan D. Jennings and others; "Fallout Studies by Oceanographic Methods"; Project 2.62a, Operation Redwing, ITR-1316, July 1956; University of California, Scripps Institution of Oceanography, La Jolla, California; Secret Restricted Data.

10. K. O'Brien, W.M. Lowder and L.R. Solon; "A Semi-Empirical Method of Calculating the Energy-Absorption Build-Up Factor with an Application to a Uniformly Contaminated Space Having Spherical Boundaries"; HASL-2, October 1957; Health and Safety Laboratory, U.S. Atomic Energy Commission, New York Operations Office; Unclassified.

11. M.E. Cassidy, R.T. Graveson and H.D. LeVine; "HASL Aerial Survey System"; NYO-2071, June 1957; Health and Safety Laboratory, U.S. Atomic Energy Commission, New York Operations Office; Unclassified.

12. H.D. LeVine and S. Watnick; "Portable Airborne Radiological Monitoring System"; Project 32.2, Operation Plumbbob, WT-1463 (draft manuscript); Health and Safety Laboratory, U.S. Atomic Energy Commission, New York Operations Office; Unclassified.

90 Director, U.S. Naval Research Laboratory, Washington 25, D.C. ATTN: Mrs. Katherine E. Cass
91-92 Commander, U.S. Naval Ordnance Laboratory, White Oak, Silver Spring 19, Md.
93 Director, Material Lab. (Code 900), New York Naval Shipyard, Brooklyn 1, N.Y.
94 Commanding Officer and Director, Navy Electronics Laboratory, San Diego 52, Calif.
95-98 Commanding Officer, U.S. Naval Radiological Defense Laboratory, San Francisco, Calif. ATTN: Tech. Info. Div.
99 Commanding Officer and Director, U.S. Naval Civil Engineering Laboratory, Port Hueneme, Calif. ATTN: Code L31
100 Superintendent, U.S. Naval Academy, Annapolis, Md. Commanding Officer, U.S. Naval Schools Command, U.S. Naval Station, Treasure Island, San Francisco, Calif.
101 President, U.S. Naval War College, Newport, Rhode Island
102 Superintendent, U.S. Naval Postgraduate School, Monterey, Calif.
103 Officer-in-Charge, U.S. Naval School, CEC Officers, U.S. Naval Construction Bn. Center, Port Hueneme, Calif.
104 Commanding Officer, Nuclear Weapons Training Center, Atlantic, U.S. Naval Base, Norfolk 11, Va. ATTN: Nuclear Warfare Dept.
105 Commanding Officer, Nuclear Weapons Training Center, Pacific, Naval Station, San Diego, Calif.
106 Commanding Officer, U.S. Naval Damage Control Tng. Center, Naval Base, Philadelphia 12, Pa. ATTN: ABC Defense Course
107 Commanding Officer, Air Development Squadron 5, VX-5, China Lake, Calif.
108 Commanding Officer, U.S. Naval Medical Research Institute, National Naval Medical Center, Bethesda, Md.
109 Commander, U.S. Naval Ordnance Test Station, China Lake, Calif.
110 Officer-in-Charge, U.S. Naval Supply Research and Development Facility, Naval Supply Center, Bayonne, N.J.
111 Commander-in-Chief, U.S. Atlantic Fleet, U.S. Naval Base, Norfolk 11, Va.
112 Commandant, U.S. Marine Corps, Washington 25, D.C. ATTN: Code AO3H
113 Director, Marine Corps Landing Force, Development Center, MCS, Quantico, Va.
114 Chief, Bureau of Ships, D/N, Washington 25, D.C. ATTN: Code 372
115 Commanding Officer, U.S. Naval CIC School, U.S. Naval Air Station, Glynco, Brunswick, Ga.
116 Chief of Naval Operations, Department of the Navy, Washington 25, D.C. ATTN: OP-03E5
117-119 Chief, Bureau of Naval Weapons, Navy Department, Washington 25, D.C. ATTN: RR12
120 Commander-in-Chief, U.S. Pacific Fleet, Fleet Post Office, San Francisco, Calif.

AIR FORCE ACTIVITIES

121 Deputy Chief of Staff, Operations, HQ. USAF, Washington 25, D.C. ATTN: AFOOP
122 Hq. USAF, ATTN: Operations Analysis Office, Office, Vice Chief of Staff, Washington 25, D. C.
123 Director of Civil Engineering, HQ. USAF, Washington 25, D.C. ATTN: AFOCE-ES
124-134 Air Force Intelligence Center, HQ. USAF, ACS/I (AFCIN-3V1) Washington 25, D.C.
135 Director of Research and Development, DCS/D, HQ. USAF, Washington 25, D.C. ATTN: Guidance and Weapons Div.
136 The Surgeon General, HQ. USAF, Washington 25, D.C. ATTN: Bio.-Def. Pre. Med. Division
137 Commander, Tactical Air Command, Langley AFB, Va. ATTN: Doc. Security Branch
138 Commander, Air Defense Command, Ent AFB, Colorado. ATTN: Assistant for Atomic Energy, ADLDC-A
139 Commander, Hq. Air Research and Development Command, Andrews AFB, Washington 25, D.C. ATTN: RDRWA
140 Commander, Air Force Ballistic Missile Div. HQ. ARDC Force Unit Post Office, Los Angeles 45, Calif. ATT
141-142 Commander, AF Cambridge Research Center, L. G. Hanso Field, Bedford, Mass. ATTN: CRQST-2
143-147 Commander, Air Force Special Weapons Center, Kirtlan Albuquerque, N. Mex. ATTN: Tech. Info. & Intel. Di
148-149 Director, Air University Library, Maxwell AFB, Ala.
150 Commander, Lowry Technical Training Center (TW), Lowry AFB, Denver, Colorado.
151 Commandant, School of Aviation Medicine, USAF, Aero Medical Center (ATC), Brooks Air Force Base, Tex. ATTN: Col. Gerritt L. Beekuis
152 Commander, 1009th Sp. Wpns. Squadron, HQ. USAF, Wash 25, D.C.
153-154 Commander, Wright Air Development Center, Wright-Pat AFB, Dayton, Ohio. ATTN: WCACT (For WCOSI)
155-156 Director, USAF Project RAND, VIA: USAF Liaison Offic The RAND Corp., 1700 Main St., Santa Monica, Calif
Commander, 3535th Navigator Wing, Mather AFB, Calif.
157 Commander, Air Defense Systems Integration Div., L. Hanscom AFB, Bedford, Mass. ATTN: SIDS-S
158 Commander, Air Technical Intelligence Center, USAF, Wright-Patterson AFB, Ohio. ATTN: AFCIN-4Bla, Lib
159 Assistant Chief of Staff, Intelligence, Hq. USAFE, APO 633, New York, N.Y. ATTN: Directorate of Air Targ
160 Commander, Alaskan Air Command, APO 942, Seattle, Washington. ATTN: AAATN
161 Commander-in-Chief, Pacific Air Forces, APO 953, San Francisco, Calif. ATTN: PFCLE-MB, Base Recovery

OTHER DEPARTMENT OF DEFENSE ACTIVITIES

162 Director of Defense Research and Engineering, Washi D.C. ATTN: Tech. Library
163 Executive Secretary, Military Liaison Committee, Dept. of Defense, Washington 25, D. C.
164 Director, Weapons Systems Evaluation Group, Room 1E The Pentagon, Washington 25, D.C.
165 Commandant, The Industrial College of The Armed For Ft. McNair, Washington 25, D.C.
166 Commandant, Armed Forces Staff College, Norfolk 11, Va. ATTN: Library
167-170 Chief, Defense Atomic Support Agency, Washington 25 ATTN: Document Library
171 Commander, Field Command, DASA, Sandia Base, Albuqu N. Mex.
172 Commander, Field Command, DASA, Sandia Base, Albuqu N. Mex. ATTN: FOTG
173-174 Commander, Field Command, DASA, Sandia Base, Albuqu N. Mex. ATTN: FCWT
175 Commander, JTF-7, Arlington Hall Station, Arlington
176 Commander-in-Chief, Strategic Air Command, Offutt A Neb. ATTN: OAWS
177 Commandant, US Coast Guard, 1300 E. St., N.W., Wash 25, D.C. ATTN: Cdr R. E. Kollmorgen
178 Commander-in-Chief, EUCOM, APO 128, New York, N.Y.
179 Commander-in-Chief, Pacific, c/o Fleet Post Office, Francisco, Calif.
180 U.S. Documents Officer, Office of the United States National Military Representative - SHAPE, APO 55, New York, N.Y.

ATOMIC ENERGY COMMISSION ACTIVITIES

181-183 U.S. Atomic Energy Commission, Technical Library, ton 25, D.C. ATTN: For DMA
184-185 Los Alamos Scientific Laboratory, Report Library, Box 1663, Los Alamos, N. Mex. ATTN: Helen Redman
186-190 Sandia Corporation, Classified Document Division, Base, Albuquerque, N. Mex. ATTN: E. J. Smyth, Jr
191-200 University of California Lawrence Radiation Labora P.O. Box 808, Livermore, Calif. ATTN: Clovis G.
201 Weapon Data Section, Office of Technical Informati Extension, Oak Ridge, Tenn.
202-235 Office of Technical Information Extension, Oak Rid Tenn. (Surplus)

DISTRIBUTION

Military Distribution Category 26

ARMY ACTIVITIES

1 Deputy Chief of Staff for Military Operations, D/A, Washington 25, D.C. ATTN: Dir. of SW&R
2 Chief of Research and Development, D/A, Washington 25, D.C. ATTN: Atomic Div.
3 Assistant Chief of Staff, Intelligence, D/A, Washington 25, D.C.
4- 5 Chief Chemical Officer, D/A, Washington 25, D.C.
6 Chief of Engineers, D/A, Washington 25, D.C. ATTN: ENGNB
7 Chief of Engineers, D/A, Washington 25, D.C. ATTN: ENGEB
8 Chief of Engineers, D/A, Washington 25, D.C. ATTN: ENGTB
9- 10 Office, Chief of Ordnance, D/A, Washington 25, D.C. ATTN: ORDTN
11 Chief Signal Officer, D/A, Research and Development Div., Washington 25, D.C. ATTN: SIGRD-4
12 Chief of Transportation, D/A, Office of Planning and Int., Washington 25, D.C.
13- 14 The Surgeon General, D/A, Washington 25, D.C. ATTN: MEDNE
15- 17 Commanding General, U.S. Continental Army Command, Ft. Monroe, Va.
18 Director of Special Weapons Development Office, Headquarters CONARC, Ft. Bliss, Tex. ATTN: Capt. Chester I. Peterson
19 President, U.S. Army Artillery Board, Ft. Sill, Okla.
20 President, U.S. Army Air Defense Board, Ft. Bliss, Tex.
21 President, U.S. Army Aviation Board, Ft. Rucker, Ala. ATTN: ATBG-DO
22 Commanding General, First United States Army, Governor's Island, New York 4, N.Y.
23 Commanding General, Second U.S. Army, Ft. George G. Meade, Md.
24 Commanding General, Third United States Army, Ft. McPherson, Ga. ATTN: ACofS G-3
25 Commanding General, Fourth United States Army, Ft. Sam Houston, Tex. ATTN: G-3 Section
26 Commanding General, Fifth United States Army, 1660 E. Hyde Park Blvd., Chicago 15, Ill.
27 Commanding General, Sixth United States Army, Presidio of San Francisco, San Francisco, Calif. ATTN: AMGCT-4
28 Commandant, Army War College, Carlisle Barracks, Pa. ATTN: Library
29 Commandant, U.S. Army Command & General Staff College, Ft. Leavenworth, Kansas. ATTN: ARCHIVES
30 Commandant, U.S. Army Air Defense School, Ft. Bliss, Tex. ATTN: Command & Staff Dept.
31 Commandant, U.S. Army Armored School, Ft. Knox, Ky.
32 Commandant, U.S. Army Artillery and Missile School, Ft. Sill, Okla. ATTN: Combat Development Department
33 Commandant, U.S. Army Aviation School, Ft. Rucker, Ala.
34 Commandant, U.S. Army Infantry School, Ft. Benning, Ga. ATTN: C.D.S.
35 The Superintendent, U.S. Military Academy, West Point, N.Y. ATTN: Prof. of Ordnance
36 Commandant, The Quartermaster School, U.S. Army, Ft. Lee, Va. ATTN: Chief, QM Library
37 Commandant, U.S. Army Ordnance School, Aberdeen Proving Ground, Md.
38 Commandant, U.S. Army Ordnance and Guided Missile School, Redstone Arsenal, Ala.
39 Commanding General, Chemical Corps Training Comd., Ft. McClellan, Ala.
40 Commandant, USA Signal School, Ft. Monmouth, N.J.
41 Commandant, USA Transport School, Ft. Eustis, Va. ATTN: Security and Info. Off.
42 Commanding General, The Engineer Center, Ft. Belvoir, Va. ATTN: Asst. Cmdt, Engr. School
43 Commanding General, Army Medical Service School, Brooke Army Medical Center, Ft. Sam Houston, Tex.
44 Director, Armed Forces Institute of Pathology, Walter Reed Army Med. Center, 625 16th St., NW, Washington 25, D.C.
45 Commanding Officer, U. S. Army Research Lab., Ft. Knox, Ky.
46 Commandant, Walter Reed Army Inst. of Res., Walter Reed Army Medical Center, Washington 25, D.C.
47- 48 Commanding General, Qm R&D Comd., QM R&D Cntr., Natick, Mass. ATTN: CBR Liaison Officer
49- 50 Commanding General, Qm. Research and Engr. Comd., USA, Natick, Mass.
51- 52 Commanding General, U.S. Army Chemical Corps, Research and Development Comd., Washington 25, D.C.
53- 54 Commanding Officer, Chemical Warfare Lab., Army Chemical Center, Md. ATTN: Tech. Library
55 Commanding General, Engineer Research and Dev. Lab., Ft. Belvoir, Va. ATTN: Chief, Tech. Support Branch
56 Director, Waterways Experiment Station, P.O. Box 631, Vicksburg, Miss. ATTN: Library
57 Commanding Officer, Diamond Ord. Fuze Labs., Washington 25, D.C. ATTN: Chief, Nuclear Vulnerability Br. (830)
58- 59 Commanding General, Aberdeen Proving Grounds, Md. ATTN: Director, Ballistics Research Laboratory
60 Commanding Officer, Ord. Materials Research Off., Watertown Arsenal, Watertown 72, Mass. ATTN: Dr. Foster
61 Commanding General, Ordnance Ammunition Command, Joliet, Ill.
62 Commanding Officer, USA Signal R&D Laboratory, Ft. Monmouth, N.J.
63 Commanding General, U.S. Army Electronic Proving Ground, Ft. Huachuca, Ariz. ATTN: Tech. Library
64 Commanding General, USA Combat Surveillance Agency, 1124 N. Highland St., Arlington, Va.
65 Commanding Officer, USA, Signal R&D Laboratory, Ft. Monmouth, N.J. ATTN: Tech. Doc. Ctr., Evans Area
66 Director, Operations Research Office, Johns Hopkins University, 6935 Arlington Rd., Bethesda 14, Md.
67 Commandant, U.S. Army Chemical Corps, CBR Weapons School, Dugway Proving Ground, Dugway, Utah.
68 Commander-in-Chief, U.S. Army Europe, APO 403, New York, N.Y. ATTN: Opot. Div., Weapons Br.
69 Commanding General, Southern European Task Force, APO 168, New York, N.Y. ATTN: ACofS G-3
70 Commanding General, Eighth U.S. Army, APO 301, San Francisco, Calif. ATTN: ACofS G-3
71 Commanding General, U.S. Army Alaska, APO 949, Seattle, Washington
72 Commanding General, U.S. Army Caribbean, Ft. Amador, Canal Zone. ATTN: Cml Office
73 Commander-in-Chief, U.S. Army Pacific, APO 958, San Francisco, Calif. ATTN: Ordnance Officer
74 Commanding General, USARFANT & MDPR, Ft. Brooke, Puerto Rico
75 Commanding Officer, 9th Hospital Center, APO 180, New York, N.Y. ATTN: CO, US Army Nuclear Medicine Research Detachment, Europe

NAVY ACTIVITIES

76- 77 Chief of Naval Operations, D/N, Washington 25, D.C. ATTN: OP-03EG
78 Chief of Naval Operations, D/N, Washington 25, D.C. ATTN: OP-75
79 Chief of Naval Operations, D/N, Washington 25, D.C. ATTN: OP-32P2
80 Chief of Naval Personnel, D/N, Washington 25, D.C.
81- 82 Chief of Naval Research, D/N, Washington 25, D.C. ATTN: Code 811
83- 85 Chief, Bureau of Naval Weapons, D/N, Washington 25, D.C. ATTN: DLI-3
86 Chief, Bureau of Medicine and Surgery, D/N, Washington 25, D.C. ATTN: Special Wpns. Def. Div.
87 Chief, Bureau of Ordnance, D/N, Washington 25, D.C.
88 Chief, Bureau of Ships, D/N, Washington 25, D.C. ATTN: Code 423
89 Chief, Bureau of Yards and Docks, D/N, Washington 25, D.C. ATTN: D-440